EN G 436 (Project 06/512)

Bounds on the distribution of amplitudes in ground motion prediction models

John Zhao & Jian Zhang – GNS Science
Jeff Fisher & Paul Somerville – Risk Frontiers

ENG 346

GNS SCIENCE
TE PŪ AO

ENG 346

Bounds on the distribution of amplitudes in ground motion prediction models

John Zhao	GNS Science
Jian Zhang	GNS Science
Jeff Fisher	Risk Frontiers
Paul Somerville	Risk Frontiers

GNS Science Consultancy Report 2007/98
May 2007

CONFIDENTIAL

This report has been prepared by the Institute of Geological and Nuclear Sciences Limited (GNS Science) exclusively for and under contract to Earthquake Commission (EQC). Unless otherwise agreed in writing, all liability of GNS Science to any other party other than Earthquake Commission (EQC) in respect of the report is expressly excluded.

The data presented in this Report are available to GNS Science for other use from May 2007

Project Number: 430W1197

CONTENTS

FIGURES

TABLES

APPENDIX

EXECUTIVE SUMMARY

In a probabilistic seismic hazard study, the imprecise prediction of ground motion parameters by empirical attenuation models is usually taken into account by assuming a lognormal distribution for the prediction imprecision. For some important engineering structures, such as hydro-power stations in New Zealand and nuclear power plants and nuclear waste storage overseas, their critical importance requires ground-motion estimates that have very low annual probability (very long return period). For such a level of ground motions, an assumption of lognormal distribution leads to an almost monotonic increase in the estimated ground motion parameters with increasing return period, without a limit. These properties of the estimated ground motions cause a major difficulty in the ground-motion assessment – are these estimates realistic? If not, what would be the upper limits?

In the present study, we examine the root of the problem – to estimate the upper limit of the range within which the prediction imprecision has a lognormal distribution. We use a sub-dataset from a very large dataset used for developing Japanese attenuation models. Because of data ownership and the quality of data from analogue and early versions of digital instruments, the sub-dataset consists of records from the K-net and Kik-net arrays only. We employ two methods to tackle the problem.

The first method uses graphical inspection of the probability plots and formal statistical tests. We plot the theoretical values derived from a lognormal distribution against the actual values computed from data and the attenuation models. Using visual inspection, we can identify where the upper tails of the distribution depart from the lognormal distribution for a number of spectral periods. Using formal statistical tests, we can also identify the upper tail departures from the lognormal distribution for a number of spectral periods, but they do not all correspond to those periods identified by the probability plots. This method produces mixed results.

The second method is to compare two important parameters of the data and the attenuation models. The first parameter is the expected number of records in a dataset that have a value larger than a specified spectral acceleration. The second parameter is the actual number of records exceeding this specified value. We find that the actual number of exceedances at moderately strong and strong ground shaking is much smaller than the expected number of exceedances for all spectral periods. At very high spectral accelerations (the level of design ground motion for important structures such as hydro-power stations), the actual numbers of exceedances are only 5-10% of the expected numbers of exceedances. Although we cannot put an upper limit to the ground motion parameters using this method, our results strongly suggest that there are some physical constraints that limit the maximum spectral ground accelerations in the sub-dataset used in the present study.

If these results are considered in a probabilistic seismic hazard study, the continuing increase in the estimated ground-motion parameters with increasing return period may not occur.

TECHNICAL SUMMARY

In current ground-motion models, the uncertainty in predicted ground motion is modelled with a lognormal distribution. One consequence of this is that predicted ground motions do not have an upper limit. In reality, there probably exist physical conditions that limit the ground motion. Use of unbounded models in probabilistic seismic hazard analysis leads to ground motion estimates that may be unrealistically large, especially at the low annual probabilities considered for important structures, such as dams or nuclear reactors. Attempts to estimate the upper limits have been made by others by using ground-motion records from a single event, but it is not clear if the conclusions derived are applicable to attenuation models which are derived from a large number of records generated by a large number of earthquakes. We have analysed very large strong-motion data sets from the K-net and Kik-net strong-motion networks in Japan and determined the total residuals from the ground-motion model developed for Japan. These residuals are then used to construct normal probability plots, and the departures of the residuals from lognormal distributions are quantified by visual inspection and statistical tests. For some periods, departure from a lognormal distribution at about 2.5-3 standard deviations can be identified, with the departure suggesting a shortening of the upper tail. For other periods, departure from a lognormal distribution can be identified if the largest one or two residuals are disregarded. At a few spectral periods, the distribution of the upper tail suggests long tails. Statistical tests suggest that, at a few periods, the distribution at the upper tail differs from lognormal distribution at a significance level of 5%. We have also used a statistical procedure to examine the actual and expected numbers of predicted spectral accelerations exceeding a given spectral acceleration. Our results show that, for moderate, large and very large spectral accelerations, the actual number of exceedances is much less than the expected number of exceedances. Our results from the statistical procedure do not put any limits on the upper tail, but suggest that physical constraints may limit the maximum spectral accelerations.

1.0 INTRODUCTION

Due to the limited size of strong-motion data sets, statistical analysis of the distribution of earthquake ground-motion amplitudes has, to date, been unable to provide a clear indication that the distribution has an upper limit. Recently, very large data sets of strong-motion recordings have become available, making statistical analysis more viable (Bommer et al., 2004). The three crustal earthquake data sets analyzed by these authors, using normal probability plots, all show departures from lognormal behaviour at about 2 standard deviations above the median, tending toward shorter upper tails. However, the Japanese K-net data sets that were analyzed contain ground motion values up to 5 standard deviations above the median. We anticipate that these very high values may be due to data errors or to extreme site effects. Strasser and Bommer (2005) also investigate the distribution of the upper tail of the error distribution for K-net and Kik-net data. Their basic procedure is: (1) select a number of records from a single event, (2) derive attenuation models using different functional forms with/without some of the parameters such as site terms, but allowing all the parameters to be derived by regression analyses, and (3) investigate the residuals separately for each earthquake. While their study shows clearly that a good fit to the normal distribution is limited to about 1.5-2.0σ (the standard deviation of the residuals), it is not clear whether the limits they derived can be used for existing attenuation models in a probabilistic seismic study due to the following reasons.

(1) Because they used the dataset from a single event, the variability from one earthquake to another (inter-event variability) cannot be included.

(2) Allowing all parameters, including those associated with attenuation and site effects, to be derived from records of a particular event may reduce the scatter compared with that of existing attenuation models derived from multiple events.

Because both aspects may lead to reductions in residuals and the estimated standard deviation, it is possible that the upper limits of departure from the normal distribution may not be affected. However a systematic investigation to confirm this possibility needs to be carried out. In an attenuation model, magnitude scaling, path and site parameters are usually identical for all events that have the same tectonic category, and this property of attenuation models will lead to a sizeable increase in both residuals and standard deviation compared with those derived using records of each individual earthquake. The effect of the increased residuals on the limits of departure from the normal distribution is not known.

2.0 DATA ANALYSIS

Strasser and Bommer (2005) analysed the intra-event variability of ground-motion amplitudes in sets of K-net and some Kik-net recordings of individual crustal earthquakes in Japan. They noted data quality issues in the strong-motion recordings, but did not attempt to correct them. They used site corrections derived from extrapolation of shallow shear-wave velocity measurements to 20 metre depth, but found them not to have a large impact on their measurements of ground-motion variability. They concluded that the distribution of ground-motion amplitudes overall is consistent with the lognormal distribution within ± 2.5σ level. Departure from the normal distribution occurs at 1.5σ at the upper tail for some of the events they investigated.

The methods used by Zhao et al. (2006a, b) in deriving their ground motion model may provide a more reliable basis for the evaluation of ground-motion variability, because of the approaches taken for strong-motion data processing and the classification of recording sites. In Zhao et al. (2006 a, b), strong-motion recordings from Japanese earthquakes recorded on strong-motion stations of the K-net and Kik-net networks were gathered and processed using a high-pass filter to eliminate the long-period ground motions with frequency less than the corner frequency of the filter determined for each record. Among the total of 4518 Japanese records from 249 earthquakes, 1285 are from crustal events, 1508 are from interface events and 1725 are from slab events.

Figure 1 shows the magnitude and source distance and magnitude and focal depth distribution for earthquakes with focal depths of up to 124 km for the Japanese K-net and Kik-net strong-motion data set selected from the full dataset of Zhao et al. (2006a). In order to eliminate the possible bias introduced by untriggered instruments, data for the modelling by Zhao et al (2006a) were selected from a much larger data set by exclusion of data at distances larger than a specified value for a given magnitude. For subduction slab events, the maximum source distance was set to 300km. Earthquake locations, especially focal depths, determined by JMA were not consistent with those determined by other seismological organizations, and so the relocated ISC locations and depths were used in the Zhao et al (2006a) model. The moment magnitudes from the Harvard catalogue were used unless moment magnitude from a special study was available.

The residuals used are computed from the Zhao et al. (2006a) models, in which the estimated standard deviation was assumed independent of magnitude. For subduction and slab events, these standard deviations are much lower than those of the widely used subduction zone model of Youngs et al. (1997), especially for periods longer than 0.2 seconds. This is an important feature of the Zhao et al. (2006a) model, because in probabilistic seismic hazard analysis, the variability of ground motion about the median value is often just as important as the median value itself.

Since many of the K-net stations have shear-wave velocity measurements that extend to depths of only 10 to 20 metres, Zhao et al. (2006b) devised an alternative method for categorising their site conditions, based on response spectral ratios of horizontal to vertical ground motions. They used H/V ratios for records from K-net sites having adequate shear-wave velocity measurements to establish a site classification index using the mean spectral ratios over a wide range of spectral period, to assign sites to the long-established Japanese classes (Molas and Yamazaki 1995) that correlate approximately with the US NEHRP classes as indicated in Table 1. Using the index, they were able to classify both K-net stations with soil layers thicker than 20m and other strong-motion stations in Japan. The peak period of the H/V spectral ratio was also used to identify soft soil sites.

In addition to the crustal earthquake category analysed by Strasser and Bommer (2005), our analysis includes subduction interface earthquakes and intra-slab earthquakes, which extend to larger magnitudes and have much larger numbers of recordings than the crustal earthquakes. Our analysis also looks at the full variability in the ground shaking, both the intra-event variability and the inter-event variability.

Out of concerns for data quality and the ownership of some strong-motion records, we used only a subset of the full dataset of Zhao et al (2006a). The sub-dataset includes only those records from K-net and Kik-net and consists of 3575 records of the 4518 used for PGA analysis in the complete dataset. We used the standard deviation calculated from the total residuals of the sub-set data to normalize the data used in the present study to have a zero mean and a standard deviation of 1.0. Note that the total standard deviation derived from the sub-set data are all considerably larger than those reported by Zhao et al (2006a) and this is presumably a result of the data selection. The value for each data point of the normalized residuals is referred to as the computed score (the location of the data in terms of standard deviation) and the data are arranged in an ascending order. The theoretical distribution is calculated in the following manner. The cumulative probability for a data set is computed from

$$\alpha_1 = 1 - 0.5^{1/n} \qquad \alpha_i = \frac{i - 0.3175}{n + 0.365} \qquad \alpha_n = 0.5^{1/n} \tag{1a,b,c}$$

where n is the total number of data and i varies from 2 to n-1. The theoretical score of a data set is computed by $\gamma = \Psi^{-1}(\alpha_i, 0, 1)$ - the inversion of the cumulative normal probability function with a zero mean and a standard deviation of 1.0 (see http://www.itl.nist.gov /div898/handbook/eda/section3/normprpl.htm). The computed score and the theoretical score are then plotted together in a probability plot. If the data falls on the straight diagonal line, the data distribution is close to the theoretical normal distribution, and the residuals can be well approximated by the normal distribution. Any deviation from the straight line suggests a departure from the normal distribution. The use of a probability plot is an equivalent non-parametric test.

The probability P_m that, for n trials, each with a probability of success p, we obtain m successful trials is computed by

$$P_m = \frac{n!}{(n-m)!\,m!} p^m (1-p)^{n-m} \tag{2}$$

where p=1-$\Psi(\gamma, 0, 1)$ is the probability of success of a single trial being at or beyond a given theoretical score γ. The total probability of having m or less successful trials can be estimated by

$$P_r = \sum_{i=1}^{m} P_i \tag{3}$$

In the present study, we use Equations (2) and (3) to estimate the probability of having m or fewer data over a given score γ.

The median smallest and median largest theoretical scores are defined by $\gamma_S = \Psi^{-1}(\alpha_1, 0, 1)$ and $\gamma_L = \Psi^{-1}(\alpha_n, 0, 1)$, respectively. Note that there is an equal probability of 0.5 for the largest of n values falling above or below γ_L if the residuals have a normal distribution.

3.0 RESULTS

Our basic approach is to calculate the total residuals (logarithm of observed spectral accelerations minus that of the model prediction) of the recorded data from the ground motion model of Zhao et al. (2006a) using the site classifications developed by Zhao et al. (2006b).

Table 2 shows the statistics of the data set. The total number of data for periods up to 0.7s is 3575 and decreases to 2318 at 5.0s period because the usable maximum period for many records is less than 5.0s period. The standard deviation of the total residuals varies between 0.81 and 0.94 on the natural logarithm scale. Note that the standard deviation is computed from the data used in the present study (only K-net and Kik-net data) and differs from those reported by Zhao et al (2006a). The largest maximum normalized residual (residuals divided by standard deviation) is just over 4.0, significantly larger than the median largest theoretical scores. The maximum scores larger than the median largest theoretical scores are in bold in Table 2 and they are also presented in Figure 2. Note that data at only 4 spectral periods out of 21 exceed the median largest theoretical values, while the expected number of exceedances is 10 out of 21 spectral periods, if the residuals are normally distributed. The small number of actual exceedances suggests that total residuals may not have a normal distribution at the upper tail for all spectral periods, with a possible shortening upper tail. The number of data with scores beyond a given value (between 2.5 and 3.75) is also presented in Table 2, and for 6 periods there is one point over 3.5 times the standard deviation while 10 or 11 exceedances are expected if the data is normally distributed.

We assign ranks for the 10 largest residuals for each period in the upper tail with the largest residual having rank 10 and the second largest having rank 9 etc. We examine the data distribution with respect to events and recording sites, to seek indications of the relative importance of site effects and earthquake source effects. For example, if a particular site has a large number of records in the top few ranks, site effect may be the main cause. If a particular earthquake generates a significant number of data in the top few ranks, the variability from one earthquake to another may have a relatively large effect. Table 3 presents site names, earthquake identification number and the number of periods and number of records in rank 10. All multiple periods in rank 10 are from the same record and they tend to be among the adjacent spectral periods. This tendency decreases with decreasing ranks. The total number of periods is 21 for the Zhao et al 2006a model. Event 208 has 5 periods from 2 records and 2 sites, and event 246 also has 5 periods from 2 records and 2 sites. The total number of periods for each site and event and the data ratio (the number of periods/105 in percentage) in ranks 6-10 are presented in Table 4 for all events and for those sites that have 3 or more periods. The divisor 105 corresponds to product of 5 ranks with 21 periods in each rank. About 2/3 of the data in ranks 6-10 are from 4 events while none of the sites has more than 10% of the periods. These results suggest that variability from one earthquake to another may contribute more than the site effect variability. It is important to examine the distribution of total residuals.

Figure 3 shows the frequency of the residuals for PGA, 0.4s and 1.0s periods. The left panel suggests that the data can be approximated very well by a normal distribution, especially for the descending branch of the density distribution. The right panel shows the distribution at the upper tail. It is quite difficult to judge the goodness of the fit between the theoretical density distribution and the data from the graphs alone.

Figure 4 shows the probability plots for PGA and the other spectral periods. In these figures, a lognormal probability distribution is indicated by a straight diagonal line. The change of the slope of the data points for theoretical scores between 2.5 and 4 above the median indicates departure from the normal distribution. The two red crosses indicate the median smallest and largest theoretical scores. At the upper tail, there is a probability of 0.5 to have a score falling above or below the median largest score $y_{L,}$ but the values are exceeded only 4 out of 21 spectral periods.

Figure 4a shows that the normal distribution fits the data very well within about ±2.5 standard deviation. Beyond ±2.5 standard deviation, the data appears to deviate from the normal distribution for 0.05s and 0.1s periods, suggesting a shortening upper tail, consistent with the idea that physical bounds do indeed limit the upper tail of the distribution. One data point appears outside of the theoretical limits at 0.15s, 0.25s, and 0.4s (also see Figure 2). However, apart from these records at rank 10, the data generally suggest shortening tails (with the largest few data points being below the straight line). For PGA, the data at the upper tail appears to depart from normal distribution at about 2.5 standard deviations but the two data of highest rank fall back to the normal distribution. The normal distribution fits the data for 0.2s and 0.3s spectral periods quite well at the upper tail without obvious departure.

Figure 4b shows similar mixed results. At spectral periods of 0.6s, 0.7s, 0.8s, departure from the normal distribution occurs beyond about 2.5 – 3.0 standard deviations and the distribution suggests a shortening tail. Figure 4b also suggests long tails (with the largest a few data points being above the straight line) for 0.5s and 1.5s period while the normal distribution fits the upper tail distribution quite well at the other periods. At 0.9, 1.0 and 1.25s spectral periods, a lognormal distribution fits the upper tail very well. For periods up to 1.25s in Figure 4a and 4b, the distribution suggests a shortening tail at the lower tail end.

Figure 4c shows that, at the upper tail, departure from the normal distribution can be identified for 3.0s 4.0s and 5.0s periods while it is difficult to clearly identify any departure from the normal distribution at the upper tail at 2.0s period from the probability plot alone. However, at periods between 2.0s and 4.0s, the probability plots (Figure 4c) suggest a long tail at the lower tail end.

At PGA, 0.15s, 0.2s, 0.25s, 0.3s, 0.4s, 0.5s, 0.9s, 1.0s, 1.25s, 1.5s and 2.0s periods (12 of 21 periods), there are either data that lie outside the median largest theoretical score (4 periods) or data with the largest score close to the diagonal line for the normal distribution.

In addition, departure from the normal distribution at or beyond 2.5 standard deviations can be visually identified in the probability plots for 8 spectral periods, 0.05s, 0.1s, 0.6s, 0.7s, 0.8s, 3.0s 4.0s and 5.0s. Most probability plots for PGA reported by Strasser and Bommer (2005) suggest departure at about 1.5-2 standard deviation. The larger value in the present study is likely a result of using total residuals while only intra-event residuals were used in their study. Another source of the difference is likely to be in the modelling of geometric and anelastic attenuation rates between the present study and the Strasser and Bommer (2005) study. The geometric and anelastic attenuation rates are identical for all events in the same tectonic category of earthquakes in the Zhao et al (2006a) model and but were derived separately for each of the earthquakes in the Strasser and Bommer (2005) study.

Table 5 presents the probability of having n_{exc} (the actual number of records exceeding a given score) or fewer records over a given score. At PGA, 0.05s, 0.1s, 0.15s, 0.7s, 0.8s and 2.5s spectral period, the results suggest the lognormal distribution does not fit the data above 2.75 standard deviations at the upper tail at 5% significance level, but these spectral periods do not all correspond to the periods at which the probability plots suggest a departure from the normal distribution.

The overall results are mixed and it is not possible to identify the upper limits of the data distribution for all periods. A possible reason for the mixed results is the "small" number of data, e.g., not large enough to identify the limits beyond which the normal distribution does not fit and the residuals have a shortening tail. We resort to an alternative statistical analysis suggested by Dr. David Rhoades (GNS Science). The results are presented in Figure 5 and the theoretical description of the method is given in the Appendix. The method is to examine (1) $N(z)$ - the expected number of predicted spectral accelerations (by the attenuation model) that exceed a given acceleration z, and (2) $k(z)$ - the actual number of records that have accelerations larger than z. For a given period, if $k(z)$ is much smaller than $N(z)$, there is probably a physical constraint that limits spectral acceleration. Figure 5 shows the variation of $N(z)$ and $k(z)$ with spectral acceleration z (the horizontal axis of the plots), together with mean $\pm 2\sigma(z)$ of the expected number of exceedances ($\sigma(z)=\sqrt{N(z)}$). At the lower spectral accelerations, the actual number of exceedances $k(z)$ is close to the expected number of exceedances. At moderately strong level of spectral accelerations for all periods, the actual number of exceedances is much smaller than the expected value. The differences between $N(z)$ and $k(z)$ for most spectral periods monotonically increase with increasing spectral accelerations of exceedance. For spectral periods over 0.4s, the actual number of exceedances is considerably less than $N(z)-2\sigma(z)$ at moderately strong and strong spectral accelerations.

Figure 6 shows the ratio between the actual and the expected number of exceedances at different level of spectral accelerations for 6 spectral periods. The actual numbers of exceedances are generally less than 20% of the expected numbers of exceedances at moderately large spectral accelerations and 10% at large and very large spectral accelerations.

There are some other factors that may contribute to the results presented in Figure 5. It is possible that, when the residuals decrease with increasing magnitude in the attenuation model while a magnitude-independent standard deviation is used, the actual number of exceedances may appear to be less than the expected number of exceedance because of this factor alone. In the Zhao et al (2006a) model, both inter- and intra-event residuals were found not to be magnitude dependent. The other factor is the use of a sub-dataset. The data excluded mainly come from a number of organizations that use analogue and the early versions of digital instruments (pre 1990). It is not clear if the use of standard deviation of the sub-dataset in the computation of expected number of exceedance can completely offset the possible effect due to the change of data numbers and data magnitude-distance distributions.

Although formal statistical tests were not performed, it is very unlikely that, by chance, the actual numbers of exceedances at strong ground shaking are smaller than the median-2σ of the expected numbers of exceedances. Though, in the present study, we are not able to quantify an upper limit, the results presented in Figure 5 strongly suggest that there are physical constraints that limit the response spectral accelerations in the sub-dataset used in the present study.

4.0 CONCLUSIONS

Current ground motion prediction models assume an unbounded lognormal distribution of random variability in ground motion level. In reality, there probably exist physical conditions that limit the ground motion distribution. Use of unbounded models in probabilistic seismic hazard analysis leads to ground motion estimates that may be unrealistically large, especially at low annual probabilities.

Using probability plots, significant departure from the normal distribution at the upper tail can be identified for 8 spectral periods (out of 21 in total) and the departure usually starts at 2.5-3 standard deviations and the tail distribution suggests shortening tails. At some other spectral periods, departure from the normal distribution can also be identified and a shortening tail is suggested if the largest residual is excluded. For a few spectral periods, the probability plots suggest a departure from normal distribution but a long tail. Formal statistical tests showed that at 7 spectral periods- PGA, 0.05s, 0.1s, 0.15s, 0.7s, 0.8s and 2.5s, the residuals over 2.75 standard deviations do not fit the lognormal distribution at a significance level of 5%. The periods identified by the statistical tests do not all correspond to the periods identified from the probability plots.

We examined the characteristics of the upper tails of the total residuals (intra-event and inter-event). We found that the departure from the normal distribution tends to occur at a considerably larger value of total residuals (2.5-3 standard deviation) than that reported by Strasser and Bommer (2005) (1.5-2.0 standard deviation). The lower values from Strasser and Bommer (2005) are likely the result of their use of intra-event residuals derived from a data set generated by a single event. We expect that the results from Strasser and Bommer (2005) may not be directly applicable without modification to the intra-event residuals from an attenuation model, because the intra-event residuals derived from single events do not necessarily have similar distributions at the upper tail to those of attenuation models.

We have also taken an alternative approach to investigate the possible upper limits for the predicted spectral acceleration by the Zhao et al (2006b) model. The results show that, for a moderately strong and strong spectral acceleration at a particular spectral period, the actual numbers of records that have spectral accelerations exceeding the specified value are much lower than the expected numbers of exceedances for many spectral periods, and are even lower than the expected numbers of exceedances minus two standard deviations at spectral periods beyond 1.0s. The actual number of exceedances is typically smaller than 20% of the expected number of exceedances at moderate/large spectral accelerations for all spectral periods and is less than 10% of the expected number of exceedances at very large spectral accelerations. These results strongly suggest that there are physical constraints that limit the response spectral accelerations in the sub-dataset, selected from that in the attenuation model (Zhao 2006a).

5.0 ACKNOWLEDGEMENTS

We acknowledge the research grant from the Earthquake Commission of New Zealand. We also wish to thank Dr. David Rhoades for allowing us to use his method. We wish to thank Dr. Graeme McVerry for his invaluable comments, suggestions, interpretation of parameters and the review of this report.

6.0 REFERENCES

Bommer, J.J., Abrahamson, N.A., Strasser, F.O., Pecker, A., Bard, P.Y., Bungun, H., Cotton, F., Fäh, D., Sabetta, F., Scherbaum, F. and Studer, J. (2004). The challenge of determining upper limits on earthquake ground motions *Seismological Research Letters*, 75: 82-95.

Molas, G.L. and Yamazaki, F. (1995), Attenuation of earthquake ground motion in Japan including deep focus events, *Bulletin of the Seismological Society of America*, Vol. 85, No. 5, pp. 1343-1358

Strasser, F.O., and J.J. Bommer (2005), Analysis of intra-event ground-motion residuals from K-NET and KiK-NET data, *Research Report No. 05-003-SM*, Imperial College, London, U.K.

Youngs, R.R., Chiou, S.-J., Silva, W.J. and Humphrey, J.R. (1997), Strong ground motion attenuation relationships for subduction zone earthquakes, *Seismological Research Letters*, Vol. 68, pp. 94-127

Zhao, J.X., J. Zhang, A. Asano, Y. Ohno, T. Oouchi, T. Takahashi, H. Ogawa, K. Irikura, H.K. Thio, P.G. Somerville, Yasuhiro Fukushima, and Yoshimitsu Fukushima (2006a), Attenuation relations of strong ground motion in Japan using site classification based on predominant period. *Bulletin of the Seismological Society of America*, 96, 898-913.

Zhao, J.X., Irikura, K., Zhang, J., Fukushima, Y., Somerville, P.G., Asano, A., Ohno, Y., Oouchi, T., Takahashi, T. and Ogawa, H. (2006b), An empirical site classification method for strong motion stations in Japan using H/V response spectrum ratio. *Bulletin of the Seismological Society of America*, 96, 914-925.

APPENDIX — PHYSICAL CONSTRAINT ON HIGH SPECTRAL ACCELERATIONS USING AN ATTENUATION MODEL

By David Rhoades, GNS Science

For each strong motion record, we have an observed value y_i, and a value $\hat{y}_i$, which is the strong motion predicted by the attenuation model.

$$\hat{y}_i = f(x_i, \theta)$$

where f is the attenuation model, x_i represents the relevant input data for the model corresponding to the conditions under which the record y_i was obtained, and θ represents the parameters of the model.

For a given high value of strong motion, z, we wish to evaluate whether there is a physical constraint, imposed by the nature of the earthquake source, wave propagation, or site effects on motions exceeding z. Therefore, for each strong motion record and with z fixed, we compute the probability

$$P(Y_i > z \mid x_i, \theta, f) \qquad \text{(A1)}$$

The sum (over i) of all such probabilities is the expected number of exceedances of the strong-motion level z in the whole data set, given the attenuation model and the conditions under which the strong motion records ($y_i, i = 1,...,n$) were obtained. That is

$$N(z) = \sum_{i=1}^{n} P(Y_i > z \mid x_i, \theta, f) \qquad \text{(A2)}$$

Let us denote the actual number of exceedances by k(z), i.e.

$$k(z) = \sum_{i=1}^{n} I(y_i > z) \qquad \text{(A3)}$$

where $I(e) = 1$ if e is true, and 0 otherwise.

There is evidence of some physical constraint on strong motion at level z if $k(z)$ is significantly less than $N(z)$. We could use the Poisson distribution to evaluate the probability that the number of exceedances of z would exceed $k(z)$, given the model.

Table 1 Site class definitions used by Zhao et al. (2006a; 2006b) and the approximately corresponding NEHRP site classes (BSSC 2000)

Site class	Description	Natural period	V_{30} calculated from site period	NEHRP site classes
SC I	Rock	$T < 0.2s$	$V_{30} > 600$	A+B
SC II	Hard soil	$0.2 \leq T < 0.4s$	$300 < V_{30} \leq 600$	C
SC III	Medium soil	$0.4 \leq T < 0.6s$	$200 < V_{30} \leq 300$	D
SC IV	Soft soil	$T \geq 0.6s$	$V_{30} \leq 200$	E+F

Table 2 Statistics of the dataset

Spectral period	Total number of records	Standard deviation	Max. score	γ_L	Number of records with scores ≥					
					2.5	2.75	3	3.25	3.5	3.75
PGA	3575	0.8139	3.423	3.548	12	3	2	1	0	0
0.05s	3575	0.8749	3.022	3.548	10	4	1	0	0	0
0.1s	3575	0.9379	2.898	3.548	11	5	0	0	0	0
0.15s	3575	0.9289	**3.632**	3.548	14	5	3	1	1	0
0.2s	3575	0.8925	3.454	3.548	25	11	5	2	0	0
0.25s	3575	0.8713	**3.695**	3.548	25	14	7	1	1	0
0.3s	3575	0.8530	3.467	3.548	23	10	4	2	0	0
0.4s	3575	0.8261	**4.019**	3.548	22	9	2	1	1	1
0.5s	3575	0.8139	3.422	3.548	16	8	8	4	0	0
0.6s	3575	0.8093	3.115	3.548	18	7	2	0	0	0
0.7s	3575	0.8083	3.024	3.548	18	4	1	0	0	0
0.8s	3574	0.8106	3.133	3.548	14	5	2	0	0	0
0.9s	3573	0.8150	3.396	3.548	15	8	3	2	0	0
1.0s	3569	0.8193	3.521	3.548	20	7	5	2	1	0
1.25s	3566	0.8340	**3.586**	3.548	18	9	5	2	1	0
1.5s	3564	0.8413	3.516	3.548	15	9	5	3	1	0
2.0s	3500	0.8437	3.473	3.543	19	8	3	2	0	0
2.5s	3379	0.8440	3.247	3.533	14	4	2	0	0	0
3.0s	3314	0.8535	3.023	3.528	16	8	1	0	0	0
4.0s	2920	0.8420	3.191	3.495	18	8	4	0	0	0
5.0s	2318	0.8132	3.121	3.433	22	8	2	0	0	0

Table 3 Number of periods, records, sites and earthquakes in rank 10

No of data for rank 10		Earthquake identification number							Total no. of periods / event	Total no. of records / event
		208	246	217	228	206	237	193		
Site name	bIBUH03		3						3	1
	kISK006	3							3	1
	bIWTH01						2		2	1
	kHKD067					2			2	1
	kHKD098		2						2	1
	kIBR005			2					2	1
	kISK002	2							2	1
	kOSK003				2				2	1
	kIWT011							1	1	1
	kKOC003				1				1	1
	kTCG014			1					1	1
Total no. of periods/event		5	5	3	3	2	2	1	No. of periods =21	
Total no. of records/event		2	2	2	2	1	1	1		No. of records =11

Table 4 The numbers of periods among ranks 6-10

Earthquake identification number	Number of periods	Data ratio (%)		Site name	Number of periods	Data ratio (%)
228	21	20.0		bIBUH03	10	9.5
237	18	17.1		kHKD067	8	7.6
246	16	15.2		kHKD098	7	6.7
208	15	14.3		kISK006	5	4.8
217	5	4.8		kKOC003	5	4.8
230	4	3.8		kAOM007	4	3.8
240	3	2.9		kIBR004	4	3.8
236	2	1.9		kIBR005	4	3.8
241	1	1.0		kISK002	4	3.8
243	1	1.0		bIWTH01	3	2.9
				kHKD091	3	2.9
				kISK011	3	2.9
				kOSK003	3	2.9

Table 5 Probability for having the number of data equal to or less than a given value

Spectral period	n-scores											
	2.5		2.75		3		3.25		3.5		4	
	n_{exc}	P_r	n_{exc}	P_r	n_{exc}	P_r	n_{exc}	P_r	n_{exc}	P_r	n_{exc}	P_r
PGA	12	**0.013**	3	**0.006**	2	0.140	1	0.389	0	0.435	0	0.893
0.05s	10	**0.003**	4	**0.019**	1	**0.047**	0	0.127	0	0.435	0	0.893
0.1s	11	**0.007**	5	**0.046**	0	**0.008**	0	0.127	0	0.435	0	0.893
0.15s	14	**0.043**	5	**0.046**	3	0.290	1	0.389	1	0.797	0	0.893
0.2s	25	0.764	11	0.621	5	0.646	2	0.660	0	0.435	0	0.893
0.25s	25	0.764	14	0.781	7	0.884	1	0.389	1	0.797	0	0.893
0.3s	23	0.621	10	0.405	4	0.471	2	0.660	0	0.435	0	0.893
0.4s	22	0.539	9	0.282	2	0.140	1	0.389	1	0.797	1	0.994
0.5s	16	0.109	8	0.167	8	0.943	4	0.942	0	0.435	0	0.893
0.6s	18	0.219	7	0.167	2	0.140	0	0.127	0	0.435	0	0.893
0.7s	18	0.219	4	**0.019**	1	**0.047**	0	0.127	0	0.435	0	0.893
0.8s	14	**0.044**	5	**0.046**	2	0.140	0	0.127	0	0.435	0	0.893
0.9s	15	0.071	8	0.167	3	0.290	2	0.660	0	0.435	0	0.893
1.0s	20	0.373	7	0.168	5	0.648	2	0.661	1	0.798	0	0.893
1.25s	18	0.223	9	0.285	5	0.649	2	0.576	1	0.798	0	0.893
1.5s	15	0.073	9	0.289	5	0.649	3	0.847	1	0.798	0	0.893
2.0s	19	0.325	8	0.184	3	0.306	2	0.671	0	0.443	0	0.895
2.5s	14	0.071	4	**0.028**	2	0.167	0	0.420	0	0.456	0	0.898
3.0s	16	0.163	8	0.235	1	0.062	0	0.148	0	0.462	0	0.900
4.0s	18	0.550	8	0.385	4	0.640	0	0.185	0	0.507	0	0.912
5.0s	22	0.978	8	0.613	2	0.395	0	0.262	0	0.583	0	0.929

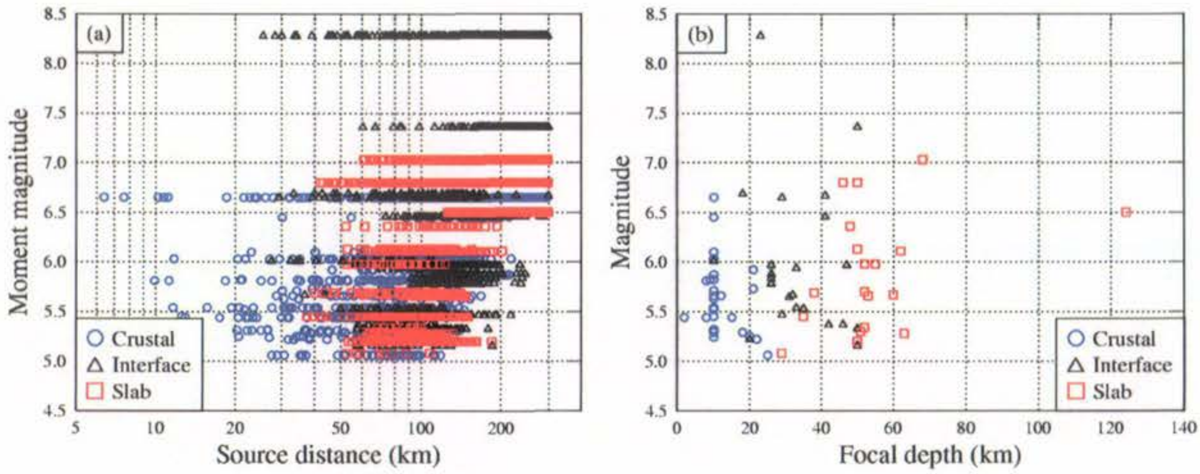

Figure 1 Data distribution with respect to magnitude, source distance and focal depth

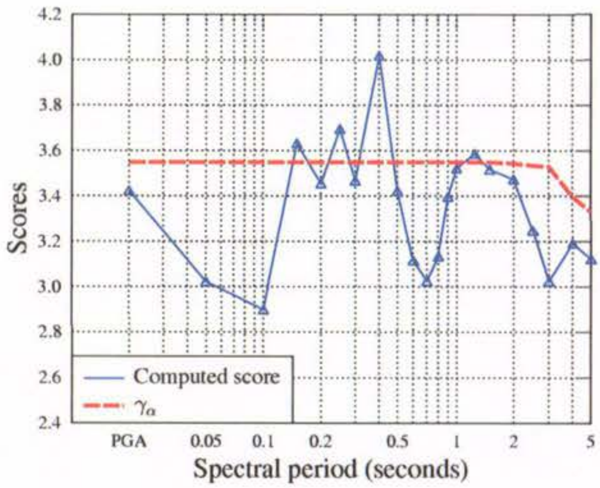

Figure 2 The computed maximum scores of the data set and the median largest theoretical scores.

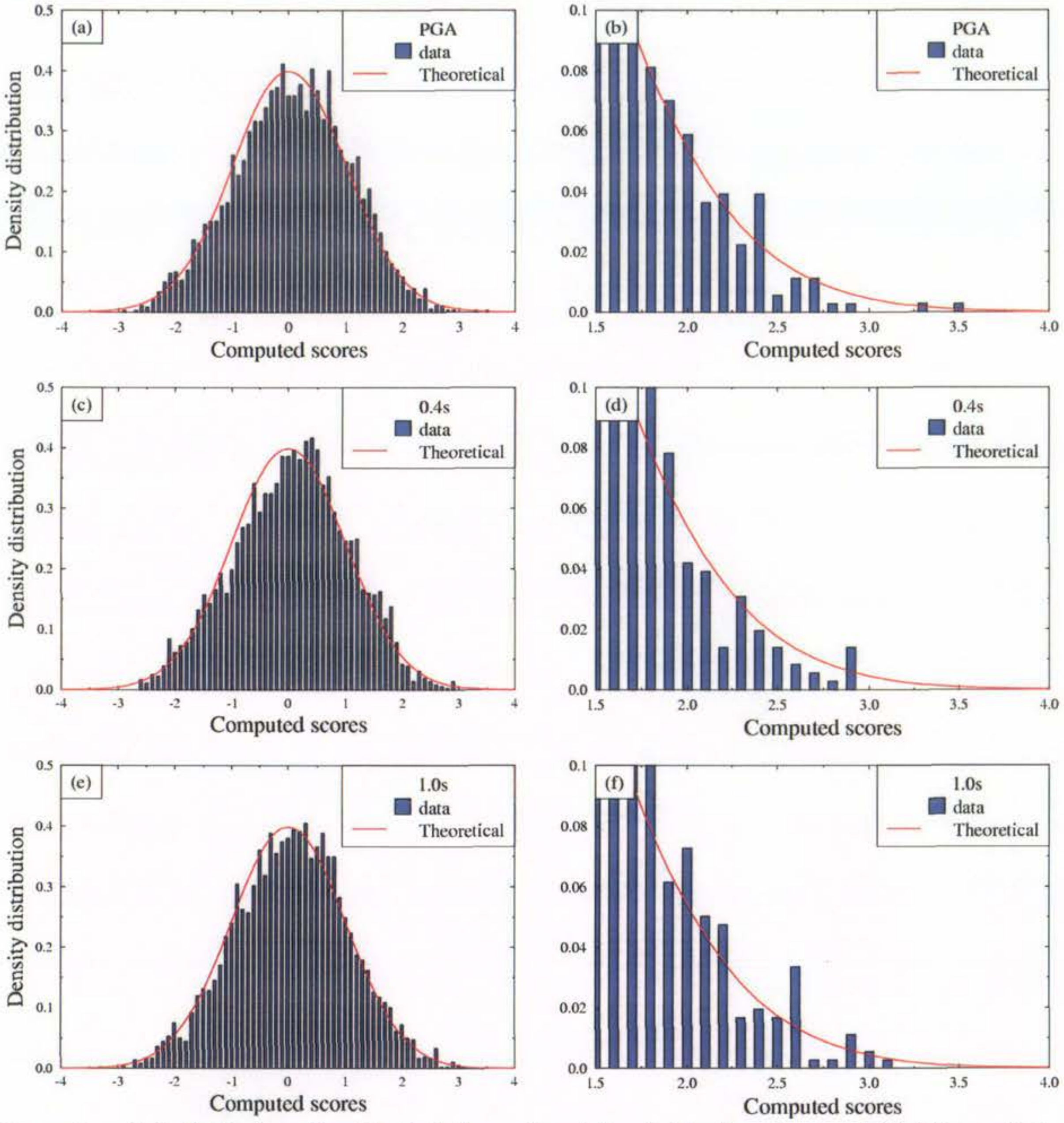

Figure 3 Full distribution of residuals (left panel) and the distribution of upper tail (right panel), for PGA, 0.4s and 1.0s spectral periods

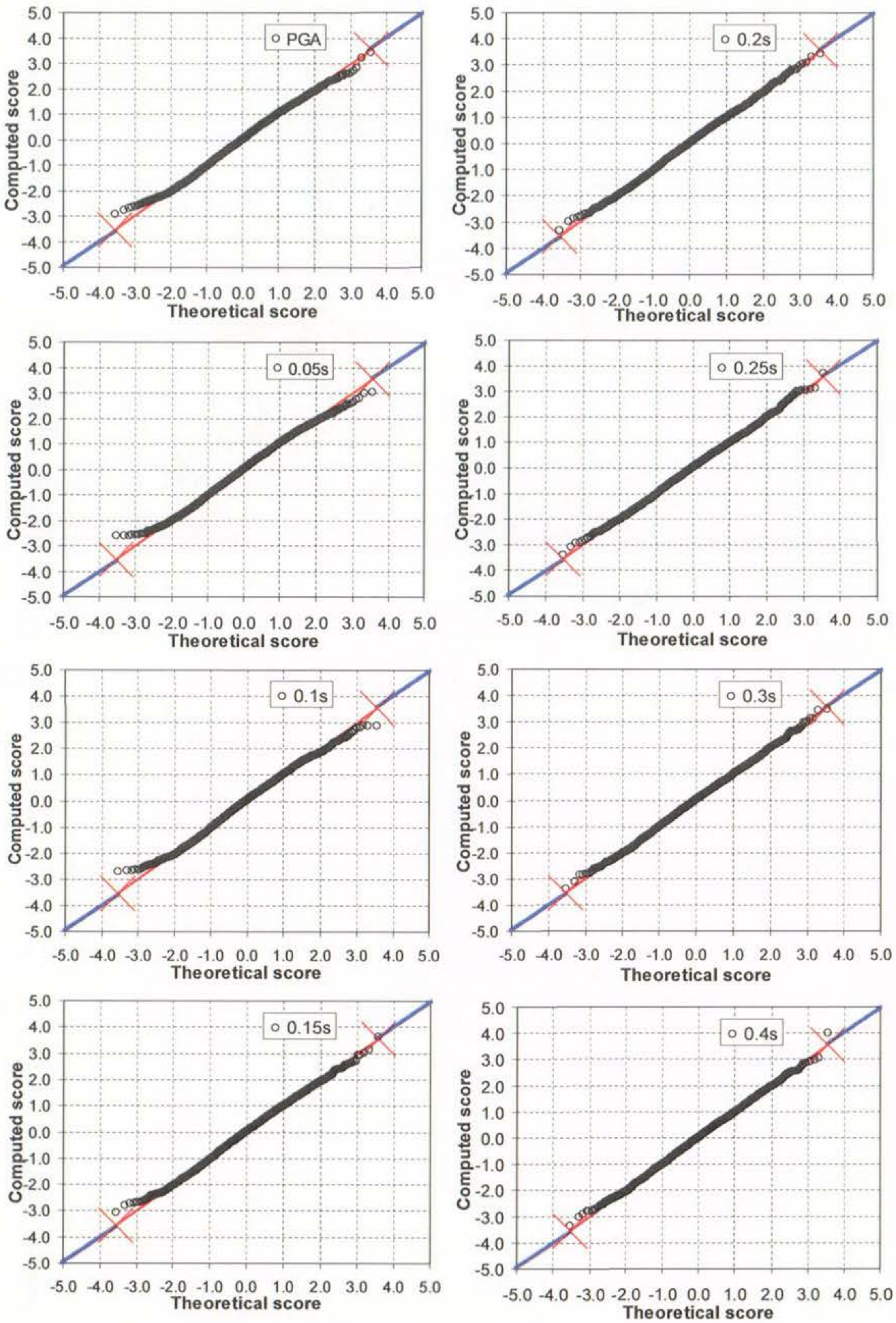

Figure 4a Probability plots for PGA and 0.05-0.4 s period

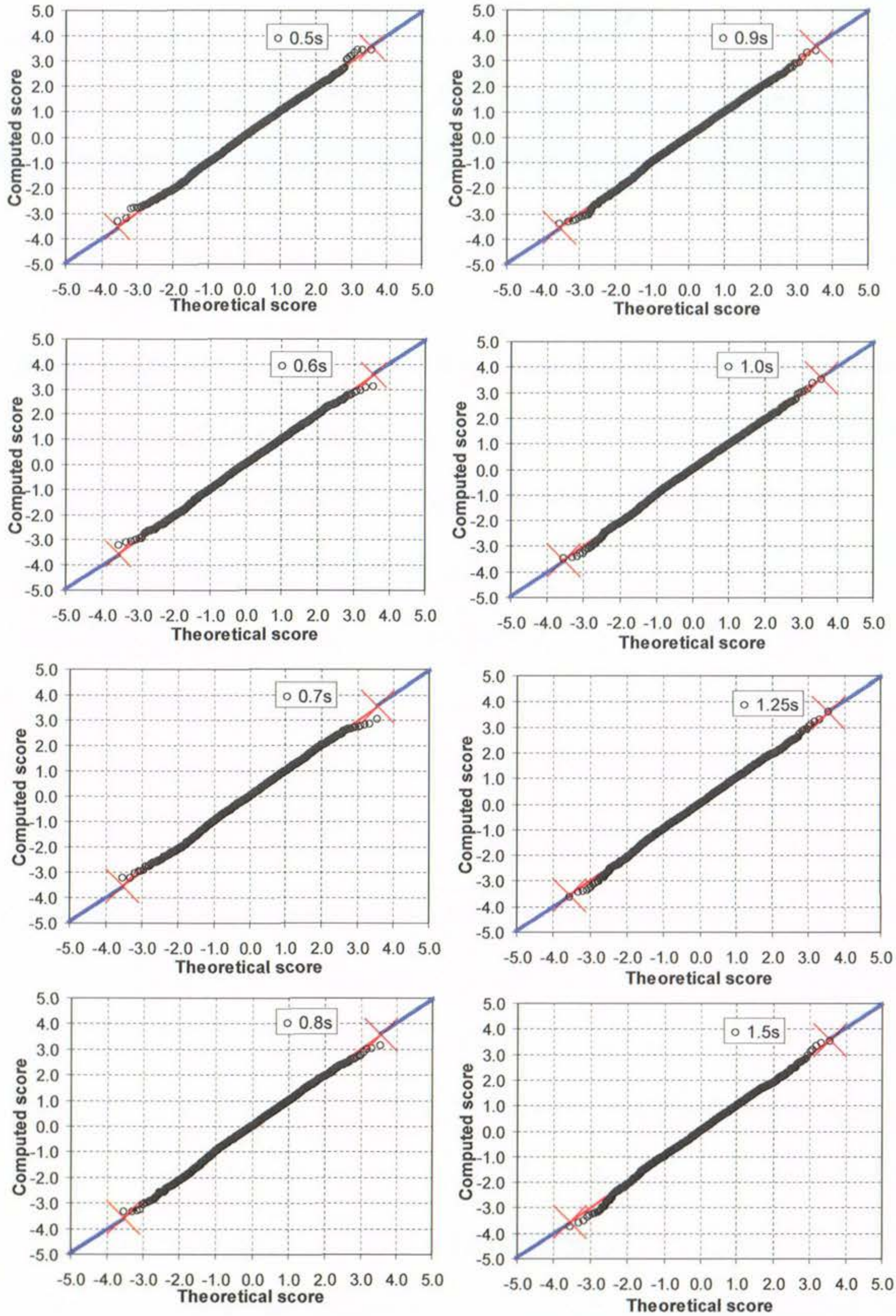

Figure 4b Probability plots for spectral periods of 0.5-1.5s

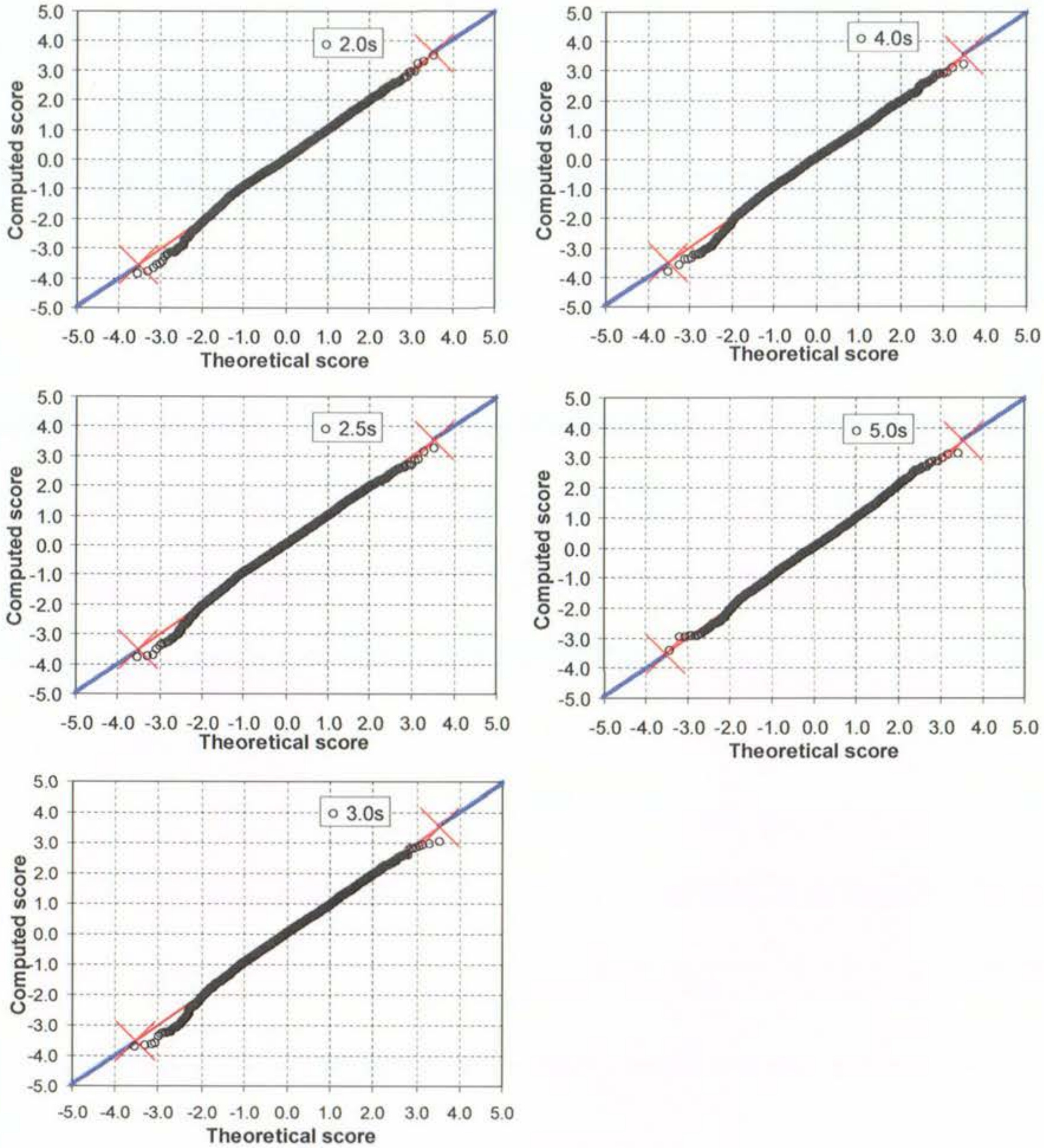

Figure 4c Probability plots for spectral periods of 2.0-5.0s

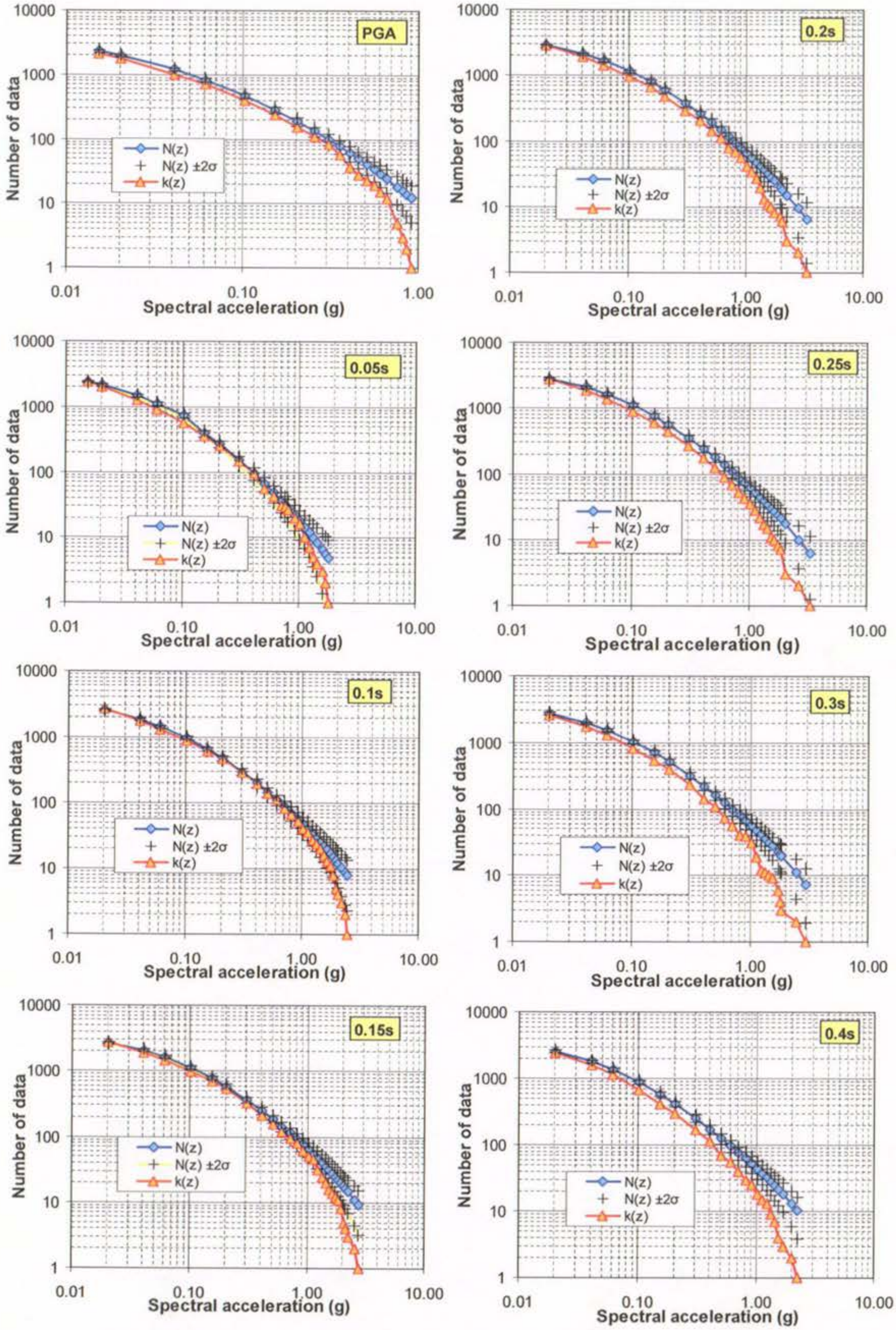

Figure 5a The expected and the actual numbers of records exceeding a given spectral acceleration for PGA, 0.05s, 0.1s, 0.15s, 0.2s, 0.25s, 0.3s and 0.4s spectral periods

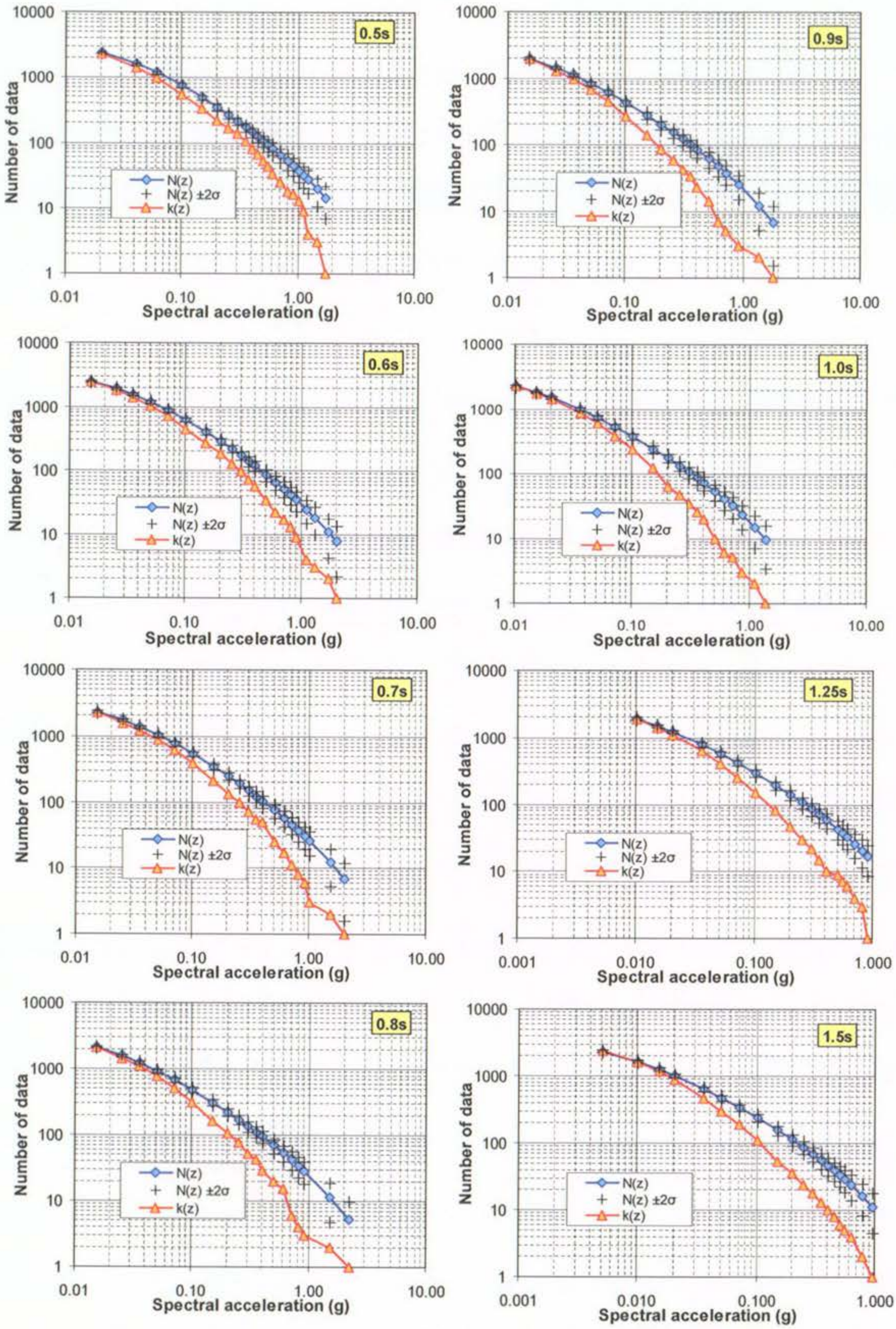

Figure 5b The expected and the actual numbers of records exceeding a given spectral acceleration for 0.5s, 0.6s, 0.7s, 0.8s, 0.9s, 1.0s, 1.25 and 1.5s spectral periods

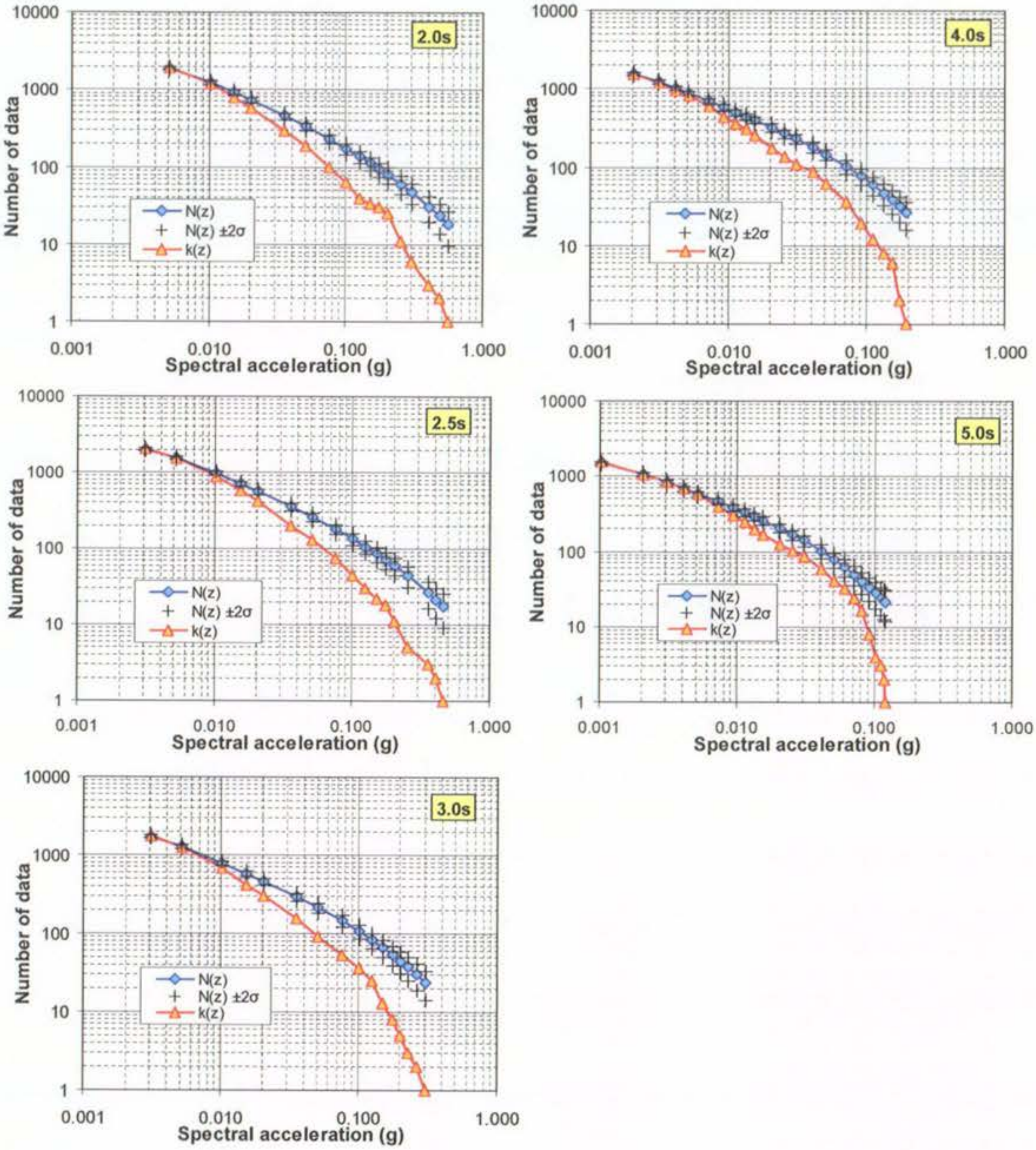

Figure 5c The expected and the actual numbers of records exceeding a given spectral acceleration for 2.0s, 2.5s, 3.0s, 4.0s, and 5.0s spectral periods

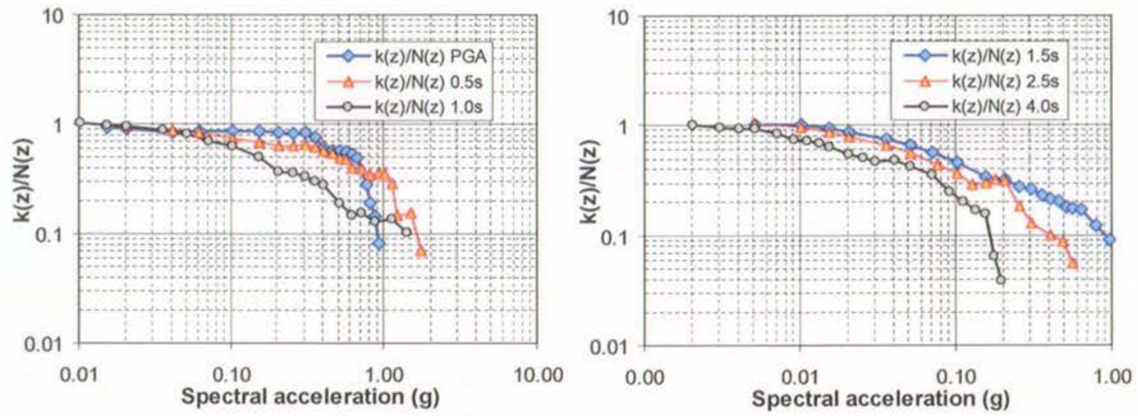

Figure 6 The ratio of the actual number and the expected number of exceedances

GNS SCIENCE
TE PŪ AO

www.gns.cri.nz

Principal Location

1 Fairway Drive
Avalon
Lower Hutt 5010
PO Box 30368
Lower Hutt 5040
New Zealand
T +64-4-570 1444
F +64-4-570 4600

Other Locations

Dunedin Research Centre
764 Cumberland Street
Dunedin 9016
Private Bag 1930
Dunedin 9054
New Zealand
T +64-3-477 4050
F +64-3-477 5232

Wairakei Research Centre
114 Karetoto Road, Wairakei
Taupo 3377
Private Bag 2000
Taupo 3352
New Zealand
T +64-7-374 8211
F +64-7-374 8199

National Isotope Centre
30 Gracefield Road, Gracefie
Lower Hutt 5010
PO Box 31312
Lower Hutt 5040
New Zealand
T +64-4-570 1444
F +64-4-570 4657

ENC 346

06/312

Bulletin of the Seismological Society of America, Vol. 98, No. 1, pp. 448–453, February 2008, doi: 10.1785/0120070133

Short Note

A Simple Test for Inhibition of Very Strong Shaking in Ground-Motion Models

by David A. Rhoades, John X. Zhao, and Graeme H. McVerry

Abstract There is considerable interest in the credibility of probabilities of exceedance estimated by ground-motion models for very high accelerations. A common statistical approach to this problem has been to examine the upper-tail shape of the distribution of residuals between recorded data and the model for evidence of suppression of high residuals. In this study, a more direct method is suggested, in which the actual number of times given accelerations are exceeded is compared to the expected numbers in strong-motion data sets. The method is illustrated by application to New Zealand and Japan models for peak ground acceleration (PGA). For the Japan model, which is based on a particularly large data set, the ratio of actual to expected number declines in a statistically significant and regular fashion from about 1 at 0.3g to about 0.15 at 1.0g. If these results are indicative of ground-motion models in general, the implications for probabilistic seismic hazard analyses may be far reaching. The method and results have particular importance for the analysis of seismic hazard at sites of critical facilities where strong ground motions with very long return periods may be of interest.

Introduction

Defining upper bounds on earthquake ground motions is recognized to be an important problem in engineering seismology (Bommer *et al.*, 2004). In probabilistic seismic hazard analysis (PSHA), a ground-motion model is applied to an earthquake-source model, and the probability of the motion exceeding a given level at a site of interest is calculated from the probability distribution associated with the ground-motion model, integrating over all earthquake sources (Cornell, 1968). The nature of the assumed probability distribution is usually such that for any level of ground motion, however large, there is a nonzero probability of it being exceeded. This type of analysis can be questioned on both physical and statistical grounds. For example, it is argued that there is a physical limit on the strongest motion that can be transmitted to the surface by shallow geological materials (Dowrick, 1987, pp. 79–81; Pecker, 2005). Also, there is clearly no solid statistical basis for attaching probabilities to ground motions that are much stronger than any ever observed. The latter argument has led to detailed studies of the distribution of residuals in ground-motion models.

Typically, the residuals of the logarithms of the acceleration are assumed to be normally distributed, and the normal distribution fits the data well out to two or three standard deviations (Bommer and Abrahamson, 2006). Any apparent departures from the normal distribution are usually associated with the more extreme residuals in the tails of the probability distribution. The tails of the distribution are important for estimation of the probability of very strong ground motions, but often not much statistical significance can be attached to the apparent departures from normality in the tails because of the small number of observations involved. In other words, the extreme-tail probabilities are often not well constrained by the data.

In studies of seismic hazard at the sites of critical facilities, it is sometimes necessary to consider very low annual probabilities of exceedance (e.g., Swissnuclear, 2004) or even probabilities of exceedance over very long time periods. In the case of long-term repositories of radioactive waste, the time period of interest is related to the half-life of the radioactive materials to be contained and can be of the order of 10^6 yr. Such analyses are inherently more sensitive to the shape of the extreme upper tail of the distribution of ground-motion-model residuals than standard PSHA modeling where the time period of interest is related to the design life of structures and is therefore much shorter, say, 50 to 100 yr, with probabilities of exceedance of a few percent in the design life resulting in consideration of return periods from about 500 up to about 2500 yr.

In reality, it is not the tail shape of this distribution *per se* that is important, but how the tail shape, in interaction with the expected strong motion, affects the likelihood of occurrence of very strong ground motion. Not every high residual corresponds to a high acceleration, as it may be associated with a modest median estimate. In an approach using analysis of residuals, a peak ground acceleration value of 0.1g associated with a median prediction of 0.01g produces a much more extreme residual than a value of 1.5g associated with a median prediction of 0.5g, while it is the latter that is an extreme motion in absolute terms.

If the condition of the ground inhibits strong ground motions from occurring, the tail shape of the distribution of residuals would be modified, but only for the stronger ground motions. The most direct way to check whether such an effect is present is not to examine the shape of the upper tail of the total distribution of residuals (Restrepo-Velez and Bommer, 2003; Bragato, 2005), which includes both very strong and less strong ground motions, but to compare the expected and actual number of exceedances of a given level of strong ground motion under the model. Such a comparison is useful when the expected number of exceedances is large enough for a meaningful statistical comparison.

Method

Consider a set of strong-motion records, indexed by the numbers $1, \ldots, n$. For the ith record, let y_i denote the observed value fitted by a ground-motion model f, and let $\hat{y}_i$ denote the value predicted by the model. That is,

$$\hat{y}_i = f(x_i, \theta), \tag{1}$$

where x_i represents the relevant input data for the model corresponding to the conditions under which the observation y_i was obtained, and θ represents the parameters of the model. For a given value of strong motion, y, we wish to test whether the model is consistent with the number of exceedances of y in the data set. Because the model is fitted to the data, it should be consistent with the bulk of the data (i.e., at moderate values of y). But if there is some physical constraint inhibiting very strong motions, the model may become progressively less consistent with the data as y increases to very high values.

Under the model, y_i is the value taken by a random variable Y_i with mean $\hat{y}_i$ and some standard deviation σ_i. When y_i represents the logarithm of acceleration, Y_i is usually assumed to be normally distributed. Then

$$P(Y_i > y) = 1 - \Phi\left(\frac{y - \hat{y}_i}{\sigma_i}\right), \tag{2}$$

where Φ is the standard normal cumulative density function. The sum (over i) of all such probabilities is the expected number $N(y)$ of exceedances of the strong-motion level y in the whole data set, given the ground-motion model and the conditions under which the strong-motion records (y_i, $i = 1, \ldots, n$) were obtained. That is

$$N(y) = \sum_{i=1}^{n} P(Y_i > y). \tag{3}$$

Let us denote the actual number of exceedances by $k(y)$; that is,

$$k(y) = \sum_{i=1}^{n} I(y_i > y), \tag{4}$$

where $I(e) = 1$ if e is true, and 0 otherwise. If $k(y)$ is found to be significantly less than $N(y)$, then the model overestimates the number of exceedances of y in the data. If such inconsistency between model and data cannot be firmly attributed to some bias of data selection, it is possible evidence of inhibition of strong motion at level y. Under the model, $k(y)$ is distributed as a mixture of binomial random variables. When $N(y)$ is much less than n (as is always true for the stronger ground motions), $k(y)$ is distributed approximately as a Poisson random variable with mean (and variance) $N(y)$. This is likely to be a good approximation, even in random effects models in which the residuals are mildly correlated through the earthquake events, because the near-source records dominate the summations in equations (4) and (5), and there are usually no more than a few of these in any earthquake. For sufficiently large $N(y)$, the normal approximation to the Poisson distribution, justified by the central limit theorem, can be used to compute tolerance limits for $k(y)$. However, for the cases of most interest here, where y is large, $N(y)$ is likely to be small, so that the normal approximation is invalid and the exact Poisson limits must be computed.

Suppose there is some physical constraint not accounted for in the model that restricts the occurrence of very strong ground motion. Then the ratio $r(y) = k(y)/N(y)$ would be expected to become progressively smaller as y increases towards the physical upper limit. Because $k(y)$ approximately follows a Poisson distribution, an upper $100(1 - \alpha)\%$ confidence limit, u, for $r(y)$ can be calculated by solving

$$\sum_{j=k(y)+1}^{\infty} \frac{e^{-\lambda}\lambda^j}{j!} = \alpha, \tag{5}$$

where $\lambda = uN(y)$.

The ratio $r(y)$—or a functional approximation $\hat{r}(y)$ to it that remains nonzero beyond the largest value in the data set—could in principle be used to correct the results of a seismic hazard analysis based on a straightforward application of the ground-motion model. A satisfactory functional approximation might be obtained from an appropriate generalized linear model (McCullagh and Nelder, 1989), such as a suitably adapted logistic regression analysis. Suppose that a seismic hazard analysis yields a curve of return period $T(y)$ against y. Then a first-order correction to the curve would be to replace $T(y)$ by $T(y)/\hat{r}(y)$. But in a rigorous analysis, it would be necessary to carefully consider the uncertainty in

$\hat{r}(y)$, along with other uncertainties in the analysis. In any case, the function $\hat{r}(y)$ would be specific to the particular ground-motion model and its associated data set; in logic-tree formulations, including several ground-motion models (Bommer *et al.*, 2005), a separate function would be needed for each model. Making the desired correction is therefore unlikely to be straightforward in practice. The details of the required analysis remain to be worked out. However, it seems an easier option than attempting to obviate the need for any such correction by modifying or augmenting the terms in each ground-motion model until no significant discrepancy between the expected and actual number of exceedances remains.

Results

As an illustration of the method, we compare actual and expected number of exceedances as functions of acceleration in the ground-motion models of McVerry *et al.* (2006) based primarily on New Zealand earthquakes (the New Zealand model), and of Zhao *et al.* (2006) based primarily on earthquakes in Japan (the Japan model). Both models include random earthquake effects (Abrahamson and Youngs, 1992) and have separate estimated variances τ^2 and σ^2 for the between-earthquake and within-earthquake components, respectively. The total residual standard deviation is calculated as the square root of $(\tau^2 + \sigma^2)$. Both sets of models include attenuation relations for PGA and spectral accelerations at a range of periods. Here we consider the PGA relations only.

The New Zealand model is based on records from 48 New Zealand earthquakes supplemented by near-source records from overseas earthquakes. In all, 526 New Zealand records and 64 overseas records contributed to the ground-motion relation for PGA. A point to note is that the overseas records in the PGA data set were those associated with most of the strongest PGA values because they were selected on the basis of having source distances of less than 10 km, a distance range lacking in the New Zealand data.

The Japan model used here is that of Zhao *et al.* (2006) corresponding to their equations (1) and (2) and tables 4 and 5. This is their model fitted directly using the random effects methodology, without the addition of quadratic magnitude terms resulting from further regression on the interearthquake residuals. It is based on a much larger data set than the New Zealand model, comprising 4695 records from 269 earthquakes, including 208 overseas near-source data. As will be seen, the number of records has a marked impact on the precision of the comparisons.

Figure 1 gives the standard residual analysis for both the New Zealand and Japan models. In both cases, the quantile–quantile plot is close to the identity line for standardized residuals less than two, showing that the normal distribution fits the residuals well out to two standard deviations. In the New Zealand model, the divergence of points from the line in the upper right corner of Figure 1a indicates that the largest positive residuals are bigger than expected under the normal distribution. In the Japan model, the closer conformity of points to the identity line in the upper right corner of Figure 1b indicates a good fit of the upper-tail residuals to

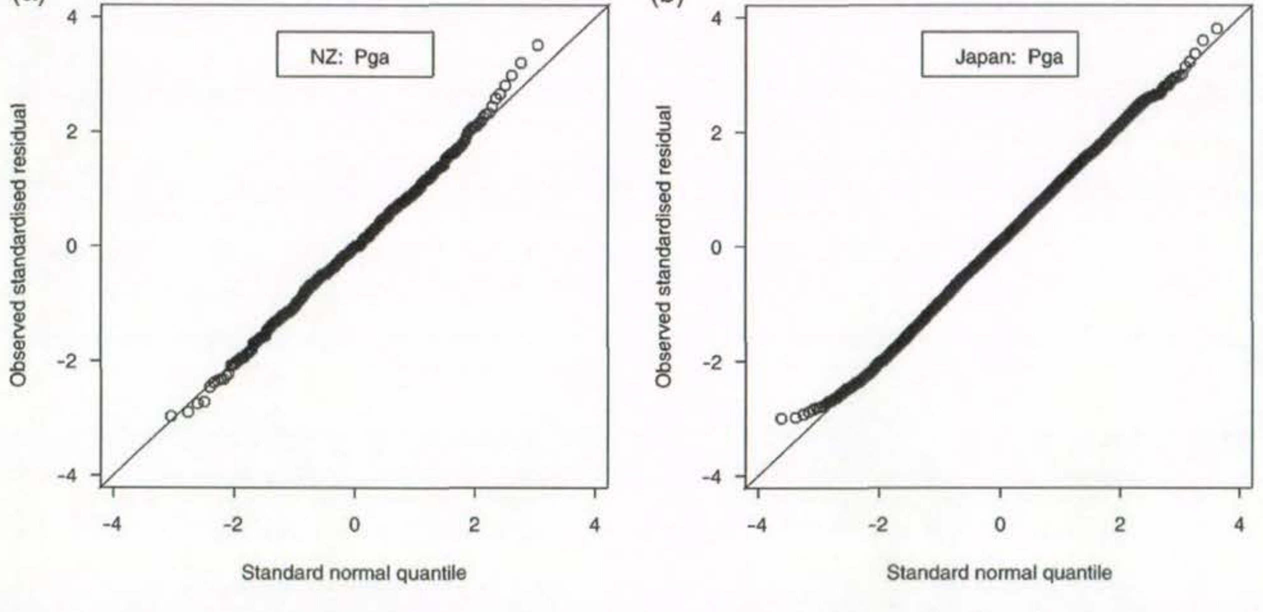

Figure 1. Examples of the standard quantile–quantile plot of residuals. Observed standardized residual versus standard normal quantile for two peak ground acceleration models. (a) New Zealand model (McVerry *et al.*, 2006); (b) Japan model (Zhao *et al.*, 2006). For normally distributed residuals, the points should fall on the identity line.

the normal distribution. Figure 1 therefore gives no indication that upper-tail residuals are suppressed in either model.

We now proceed to a comparison of actual and expected number of exceedances of a given level of acceleration. In Figure 2, the New Zealand model comparisons for PGA are plotted, including the Poisson 95% tolerance limits for the theoretical number of exceedances. In Figure 2a, there is a slight trend for the actual number of exceedances to drop below the expected number as peak ground acceleration increases, but only the value at 1.0g (which is zero when the expected number is more than four) is outside the 95% tolerance limits. In Figure 2b, the ratio of the actual to expected number of exceedances and its 95% confidence limits are shown. The ratio is well constrained where the expected number of exceedances is large, but much less so when the expected numbers are less than about 20 (i.e., for accelerations greater than about 0.7g). Consistent with Figure 2a, the entire confidence interval is less than one (i.e., the ratio is significantly less than one) only at 1.0g.

In Figure 3, the Japan model comparisons for PGA are plotted. In this larger data set, there is a strong and statistically significant trend for the actual number of exceedances to progressively decline below the expected number as the value of acceleration increases. The decline begins at about 0.4g, and the ratio of the actual number of exceedances to the expected number drops to about 0.15 at 1.0g. The expected number of exceedances is high enough that the confidence limits on the ratio are quite narrow, even at values exceeding 1g. For example, we can say with high confidence that the ratio is less than 0.5 for PGA values exceeding 0.7g (Fig. 3b). The data at high accelerations deviate markedly from the model in a manner which is consistent with the ground being inhibited in producing very strong motions. The probabilities of very strong ground motions occurring are much less than those predicted by the model.

Discussion

It is necessary to consider whether the inconsistencies found between the New Zealand and Japan PGA models and the data from which they are derived could be attributed to some bias of data selection, by which very strong ground motions were somehow excluded. Although no strong-motion data set is ever evenly distributed over the values of all the explanatory variables, we are not aware of any particular bias of data selection to exclude very strong ground motions from these data sets. Indeed, the opposite seems to be the case; both data sets were augmented by near-source records from overseas, which would have had the effect of boosting the number of very strong ground-motion records. In any case, the ratios of observed to expected number of exceedances apply to the records that are actually present in the data set, and are therefore not necessarily biased by including or excluding near-source records. Therefore, the results are interpreted as possible evidence of inhibition of very strong ground motions. This evidence can best be strengthened or negated by the application of the method

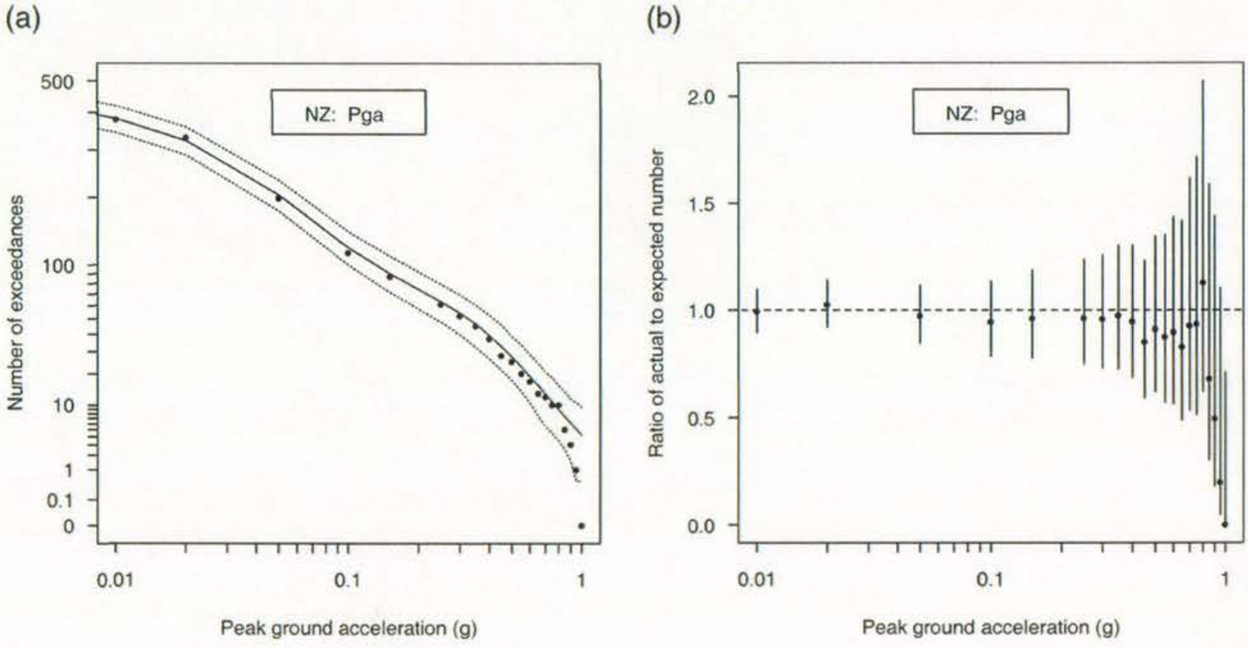

Figure 2. (a) Expected number of exceedances, that is, $N(y)$ (solid line), and actual number of exceedances, that is, $k(y)$ (points), of levels of peak ground acceleration in the New Zealand model (McVerry *et al.*, 2006). Dotted lines are 95% tolerance limits. (b) Ratio of actual to expected number of exceedances, that is, $k(y)/N(y)$ and its 95% confidence limits.

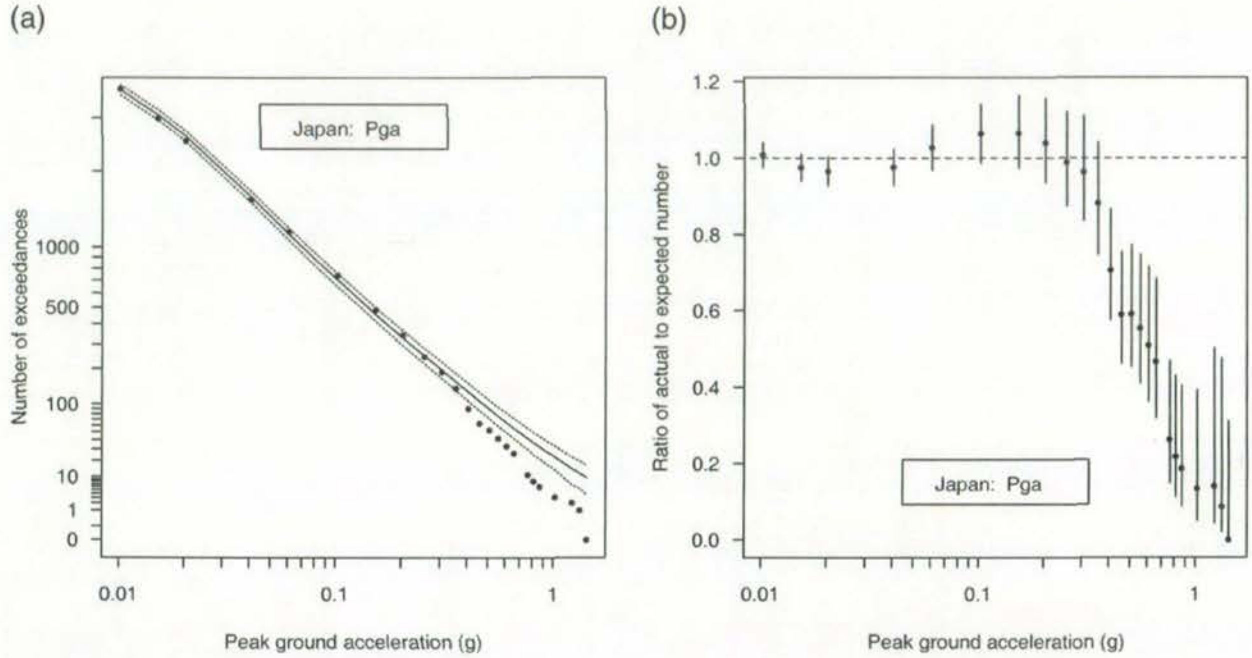

Figure 3. (a) Expected number of exceedances, that is, $N(y)$ (solid line), and actual number of exceedances, that is, $k(y)$ (points), of levels of peak ground acceleration in the Japan model (Zhao *et al.*, 2006). Dotted lines are 95% tolerance limits. (b) Ratio of actual to expected number of exceedances, that is, $k(y)/N(y)$ and its 95% confidence limits.

to a variety of data sets and ground-motion models in future studies.

The method is in principle as applicable to any model of spectral acceleration as it is to PGA. Indeed, there would be much interest in applying it to check for evidence of inhibition of strong ground motions at a variety of spectral response periods. The nonlinear behavior of surface deposits has only been observed to have limiting effects at short response periods; at longer response periods, the stronger ground-motion amplitudes are sometimes considered to be enhanced. The method would reveal any such amplification of ground motions by finding ratios of observed to expected number of exceedances significantly greater than one for the stronger ground motions. There would also be much interest in applying the method to different ground types, to determine whether the inhibition effect varies with ground conditions, as some models suggest (Dowrick, 1987).

Conclusions

The examples show that the method proposed here can be effective in identifying deviations, consistent with inhibition of very strong ground motions, from ground-motion models supported by large data sets, even where an analysis of the upper tail of the distribution of residuals shows no departure from the normal distribution. If applied to sufficiently data-rich models, the method could be used to examine how the inhibition of strong motions varies with the period of the spectral response, or with measurements of the ground condition. The details of how to adjust seismic hazard estimates for these inhibition effects remain to be worked out. But, if the results found here for the Japan PGA model are borne out in other studies, there may be important implications for probabilistic seismic hazard modelling, and, in particular, for seismic hazard studies of critical facilities, such as repositories of radioactive waste.

Acknowledgments

This research was supported by a biennial research grant from the New Zealand Earthquake Commission and by the Foundation for Research, Science and Technology under Program Number CO5X0402. Mark Stirling, Jim Cousins, and Fleur Strasser provided helpful reviews of the manuscript. Also, Norm Abrahamson made useful comments.

References

Abrahamson, N. A., and R. R. Youngs (1992). A stable algorithm for regression analyses using the random effects model, *Bull. Seismol. Soc. Am.* **82,** 505–510.

Bommer, J. J., and N. A. Abrahamson (2006). Why do modern probabilistic seismic hazard analyses often lead to increased hazard estimates?, *Bull. Seismol. Soc. Am.* **96,** 1967–1977.

Bommer, J. J., N. A. Abrahamson, F. O. Strasser, A. Pecker, P. Y. Bard, H. Bungun, F. Cotton, D. Fäh, F. Sabetta, F. Scherbaum, and J. Studer (2004). The challenge of determining upper limits on earthquake ground motions, *Seism. Res. Lett.* **75,** 82–95.

Bommer, J., F. Scherbaum, H. Buyngum, F. Cotton, F. Sabetta, and N. Abrahamson (2005). On the use of logic trees for ground-motion prediction equations in seismic hazard analysis, *Bull. Seismol. Soc. Am.* **95,** 377–389.

Bragato, P. L. (2005). Estimating an upper limit probability distribution for peak ground acceleration using the randomly clipped normal distribution, *Bull. Seismol. Soc. Am.* **95,** 2058–2065.

Cornell, C. A. (1968). Engineering seismic risk analysis, *Bull. Seismol. Soc. Am.* **58,** 1583–1606.

Dowrick, D. J. (1987). *Earthquake Resistant Design for Engineers and Architects*, Second Ed., Wiley, New York, 519 pp.

McCullagh, P., and J. A. Nelder (1989). *Generalized Linear Models*, Second Ed., Chapman and Hall, London, 511 pp.

McVerry, G. H., J. X. Zhao, N. A. Abrahamson, and P. G. Somerville (2006). New Zealand acceleration response spectrum attenuation relations for crustal and subduction zone earthquakes, *Bull. New Zealand Soc. Earthq. Eng.* **39,** no. 1, 1–58.

Pecker, A. (2005). Maximum ground surface motion in probabilistic seismic hazard analysis, *J. Earthq. Eng.* **9,** Special Issue, 187–211.

Restrepo-Velez, L. F., and J. J. Bommer (2003). An exploration of the nature of the scatter in ground-motion prediction equations and the implications for seismic hazard assessment, *J. Earthquake Eng.* **7** , Special Issue, 171–199.

Swissnuclear (2004). *Proceedings of Specialists' Meeting on State of the Art in Seismic Hazard Evaluation Methodology: Insights and Lessons from the Pegasos Project*, Baden, Switzerland, 9–10 November.

Zhao, J. X., J. Zhang, A. Asano, Y. Ohno, T. Oouchi, T. Takahashi, H. Ogawa, K. Irikura, H. K. Thio, P. G. Somerville, Fukushima Yasuhiro, and Fukushima Yoshimitsu (2006). Attenuation relations of strong ground motion in Japan using site classification based on predominant period, *Bull. Seismol. Soc. Am.* **96,** 898–913.

GNS Science
P.O. Box 30-368
Lower Hutt, New Zealand 5010

Manuscript received 23 May 2007

6/4/1 B/06/512

Bulletin of the Seismological Society of America, Vol. 99, No. 3, pp. 1487–1501, June 2009, doi: 10.1785/0120080279

Inhibition of Very Strong Ground Motion in Response Spectral Attenuation Models and Effects of Site Class and Tectonic Category

by John X. Zhao, David A. Rhoades, Graeme H. McVerry, and Paul G. Somerville

Abstract In current ground-motion models, the uncertainty in predicted ground motion is usually modeled with a lognormal distribution. One consequence of this is that predicted ground motions do not have an upper limit. In reality, however, there probably exist physical conditions that limit the ground motion. Applying the usual uncertainty distribution in probabilistic seismic hazard analysis may lead to ground-motion estimates that are unrealistically large, especially at the low annual probabilities considered for important structures, such as dams or nuclear reactors. A recently proposed statistical procedure to compare the actual and expected numbers of predicted spectral accelerations exceeding a given value gives clear results when applied to a ground-motion model developed for Japan from a very large strong-motion data set. It shows that, for increasingly large spectral accelerations, the actual number of exceedances becomes progressively less than the expected number of exceedances. The pattern of this discrepancy depends on the site class and the earthquake tectonic category. These results suggest that assuming a normal distribution for the prediction errors of an attenuation model (empirical ground-motion prediction equation) is likely to result in overestimation of the extreme values of spectral accelerations.

Introduction

Because of the limited size of strong-motion data sets, statistical analysis of the distribution of earthquake ground-motion amplitudes has so far been unable to provide a clear indication that the distribution has an upper limit. Recently, very large data sets of strong-motion recordings have become available, making statistical analysis more viable (Bommer *et al.*, 2004). The three crustal earthquake data sets analyzed by Bommer *et al.*, using normal probability plots, all show departures from a normal distribution of the residuals of log acceleration behavior at about two standard deviations above the median, tending toward shorter upper tails.

Possible upper limits of the ground motion have been investigated in a number of studies. Shi *et al.* (1996) and Anooshehpoor and Brune (2002) attempted to identify the maximum peak ground accelerations (PGAs) using precarious rocks that may have been subjected to strong ground motions from past large earthquakes. Bragato (2005) estimated the upper limit of the probability distribution using a randomly clipped normal distribution. Strasser and Bommer (2005) investigated the distribution of the upper tail of the error distribution for K-NET and KiK-NET data using probability plots. The procedure they used was to fit attenuation models to the records from each individual earthquake and then to investigate the residuals separately for each earthquake. Zhao *et al.* (2007) also used probability plots to identify the departure from the normal distribution at the upper tails, using a subset (including records obtained from the K-NET and Kik-NET only) of the data used by Zhao, Zhang, *et al.* (2006).

The Zhao, Zhang, *et al.* (2006) data and models are again the focus of the present study. Here we apply a simple statistical method proposed by Rhoades *et al.* (2008) to identify the possible inhibition of very strong ground motions by comparing the actual and expected numbers of exceedances of a given level of shaking. We then show how the inhibition effect differs between the models for different spectral periods and how it is affected by the ground class.

The method of Rhoades *et al.* (2008) can clearly identify that the distribution of extreme values of response spectra predicted by the Zhao, Zhang, *et al.* (2006) model deviates significantly from the normal distribution, and the method does not identify the largest possible extreme values of recorded ground motions. This feature makes it possible to use the data set (which does not contain the largest possible recorded spectra) from the study by Zhao, Zhang, *et al.* (2006).

Strong-Motion Data Set and Attenuation Models

In Zhao, Zhang, *et al.* (2006) and Zhao, Irikura, *et al.* (2006), strong-motion recordings from Japanese earthquakes recorded on the strong-motion stations of the K-NET and KiK-NET networks and other organizations in Japan were gathered and processed using a high-pass filter to eliminate the long-period ground motions with frequencies less than the corner frequency of the filter. The corner frequency was determined for each record so as to minimize the impact of long-period noise. Among the total of 4518 Japanese records from 249 earthquakes, 1285 are from crustal events, 1508 from interface events, and 1725 from slab events. Near-source data from California and Iran were used to complement the small number of near-source records obtained from earthquakes in Japan.

Figure 1 shows the scatter plots of magnitude against source distance and against focal depth for earthquakes with focal depths of up to 160 km for the data set of Zhao, Zhang, *et al.* (2006). In order to eliminate the possible bias introduced by untriggered instruments, data for the modeling by Zhao, Zhang, *et al.* (2006) were selected from a much larger data set by exclusion of data at distances larger than a specified value for a given magnitude. For all events, the maximum source distance was set to 300 km. Earthquake locations, especially focal depths, determined by the Japan Meterological Agency (JMA) were not consistent with those determined by other seismological organizations, and so the relocated International Seismological Centre (ISC) locations and depths were used in the Zhao, Zhang, *et al.* (2006) model. The moment magnitudes from the Harvard catalog were used unless a moment magnitude from a special study was available.

The residuals used are computed from the Zhao, Zhang, *et al.* (2006) model, in which the estimated standard deviation was assumed to be independent of magnitude. For subduction and slab events, these standard deviations are generally lower than those of the widely used subduction zone model of Youngs *et al.* (1997), especially for periods longer than 0.2 sec. This is an important feature of the Zhao, Zhang, *et al.* (2006) model because in probabilistic seismic hazard analysis the variability of ground motion about the median value is often just as important as the median value itself.

Because many of the K-NET stations have shear-wave velocity measurements that extend to depths of only 10–20 m, Zhao, Irikura, *et al.* (2006) devised an alternative method for categorizing their site conditions based on response spectral ratios of horizontal to vertical (H/V) ground motions. They used ratios of H/V response spectra for records from K-NET sites having adequate shear-wave velocity measurements to establish a site classification index, using the mean spectral ratios over a wide range of spectral periods to assign sites to the long-established Japanese classes (Molas and Yamazaki, 1995). The site classes used by Zhao, Irikura, *et al.* (2006) correlate approximately with the U.S. National Earthquake Hazards Reduction Program (NEHRP) classes as indicated in Table 1 if we assume that bedrock is reached at a depth 30 m. Using the index, they were able to classify both K-NET stations with soil layers thicker than 20 m and other strong-motion stations in Japan. The peak period of the H/V spectral ratio was also used to identify soft soil sites.

In addition to the crustal earthquake category analyzed by Strasser and Bommer (2005), our analysis includes subduction interface earthquakes and intraslab earthquakes, which extend to larger magnitudes and have much larger numbers of recordings than the crustal earthquakes. Our analysis examines the total variability in the ground shaking, that is, combing both the intraevent and interevent components (Abrahamson and Youngs, 1992).

Application of a Recently Developed Statistical Test

We apply a statistical test developed by Rhoades *et al.* (2008). The method is to examine

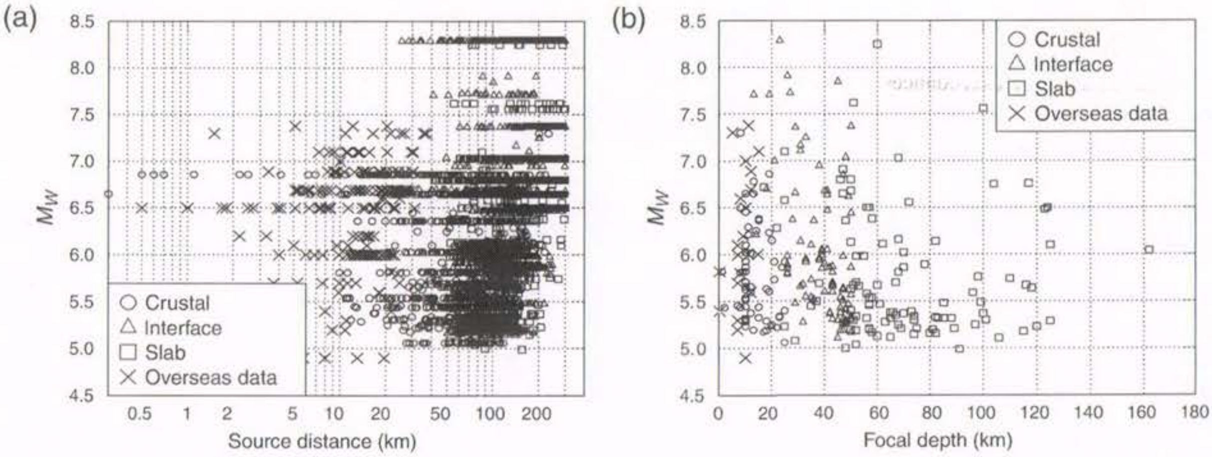

Figure 1. Data distribution with respect to magnitude, source distance, and focal depth used in the Zhao, Zhang, *et al.* (2006) model and here. The number of records in each earthquake category is about the same. Two hundred and eight near-source records from California and Iran were used to complement the small number of near-source records from earthquakes in Japan

Table 1
Site Class Definitions* and the Approximately Corresponding NEHRP Site Classes†

Site Class	Description	Natural Period	V_{30} Calculated from Site Period	NEHRP Site Classes
SC I	Rock	$T < 0.2$ sec	$V_{30} > 600$	$A + B$
SC II	Hard soil	$0.2 \le T < 0.4$ sec	$300 < V_{30} \le 600$	C
SC III	Medium soil	$0.4 \le T < 0.6$ sec	$200 < V_{30} \le 300$	D
SC IV	Soft soil	$T \ge 0.6$ sec	$V_{30} \le 200$	$E + F$

*Site class definitions used by Zhao, Zhang, *et al.* (2006) and Zhao, Irikura, *et al.* (2006).
†Building Seismic Safety Council (BSSC) (2000).

1. $N(z)$, the expected number of spectral accelerations in the given data set that are predicted by the ground-motion model to exceed a given acceleration z; and
2. $k(z)$, the actual number of records in the data set that have accelerations larger than z.

For a given period, if $k(z)$ is much smaller than $N(z)$, there may be evidence of a physical constraint that limits spectral acceleration.

Rhoades *et al.* (2008) described the statistical details of the test and applied it to PGA models. For the Zhao, Zhang, *et al.* (2006) model, they found that the ratio of actual to expected number of exceedances declined in a statistically significant and regular fashion from about 1 at $0.3g$ to about 0.15 at $1.0g$.

We computed the actual and expected numbers of exceedances from the full data set used in the Zhao, Zhang, *et al.* (2006) attenuation models but without their magnitude-squared terms and using the model parameters listed in tables 4 and 5 of their manuscript. The models applied here, unlike those involving the magnitude-squared term in the same article, were obtained directly from the random-effects methodology.

Figures 2–4 show the variation of $N(z)$ and $k(z)$ with spectral acceleration z (the horizontal axis of the plots) for a series of spectral periods ranging from zero (PGA) to 5 sec, together with the 95% tolerance limits for numbers conforming to the model. At the lower spectral accelerations, the actual number of exceedances $k(z)$ is close to the expected number of exceedances. At moderately strong levels of spectral accelerations for all periods, the actual numbers of exceedances are much smaller than the expected values. The differences between $N(z)$ and $k(z)$ for most spectral periods monotonically increase with increasing spectral accelerations of exceedance. For all spectral periods, the actual numbers of exceedances are considerably less than the lower tolerance limits at moderately strong and strong spectral accelerations. At spectral accelerations close to the largest recorded value for most periods, the actual numbers of exceedances are about 10% or less of the expected number of exceedances calculated from the acceleration spectra predicted assuming that the residuals of the attenuation models have a lognormal distribution. Figures 2–4 clearly demonstrate that the method of Rhoades *et al.* (2008) provides clearer and more powerful visual evidence of discrepancies of the distribution of extreme values from the model than do probability plots.

The difference between the expected and the actual number of exceedances is not a simple function of either prediction error or maximum score (i.e., maximum normalized residual). The values of $N(z) - 2\sigma(z)$ are close to the actual exceedances at 0.05, 1.25, and 2 sec spectral periods at the largest spectral accelerations in the data for these periods, and these periods do not all have the largest (or the smallest) model-prediction errors or the largest (or the smallest) maximum residuals of the Zhao, Zhang, *et al.* (2006) model. When the number of actual exceedance $k(z) = 1$, the expected numbers of exceedances at 0.15 and 1.0 sec are close to 20 and at 3.0, 4.0, and 5.0 sec are close to 15, considerably larger than those at the other spectral periods, and again they are not consistently from the spectral periods that have the largest (or the smallest) model-prediction errors or the largest (or the smallest) maximum scores.

The number of strong-motion records does not seem to affect the difference between the expected and the actual number of exceedances. For example, the number of records decreases from 4582 at a 2.0 sec spectral period to 2865 at 5.0 sec with the relative differences between $N(z)$ and $k(z)$ changing very little. These results indicate that the statistical procedure proposed by Rhoades *et al.* (2008) is robust.

Figure 5 shows the ratios between the actual and the expected numbers of exceedances at different values of spectral accelerations together with 95% confidence limits for six spectral periods. For PGA in Figure 5a, the ratio $k(z)/N(z)$ descends quickly from 1.0 at about $0.25g$ to zero at $1.43g$. Within this range, the spectral acceleration increases by a factor of over 5 (1.43/0.25). Figure 5b shows that, at a 0.5 sec spectral period, $k(z)/N(z)$ is close to 1.0 for spectral accelerations up to $z = 0.4g$ and then rapidly decrease to zero at about $3.0g$ within a range in which the spectral acceleration increases by a factor of 7.5. At long periods, $k(z)/N(z)$ starts to descend at much smaller spectral accelerations than for the short-period spectra and much less rapidly. At a 1.0 sec period, for example, $k(z)/N(z)$ descends from 1.0 at about a spectral acceleration of $0.02g$ to zero at about $1.5g$. In this range, the spectral acceleration increases by a factor of 75. We have no plausible explanation for the differences but the aspects of the data set described in the next section may be relevant.

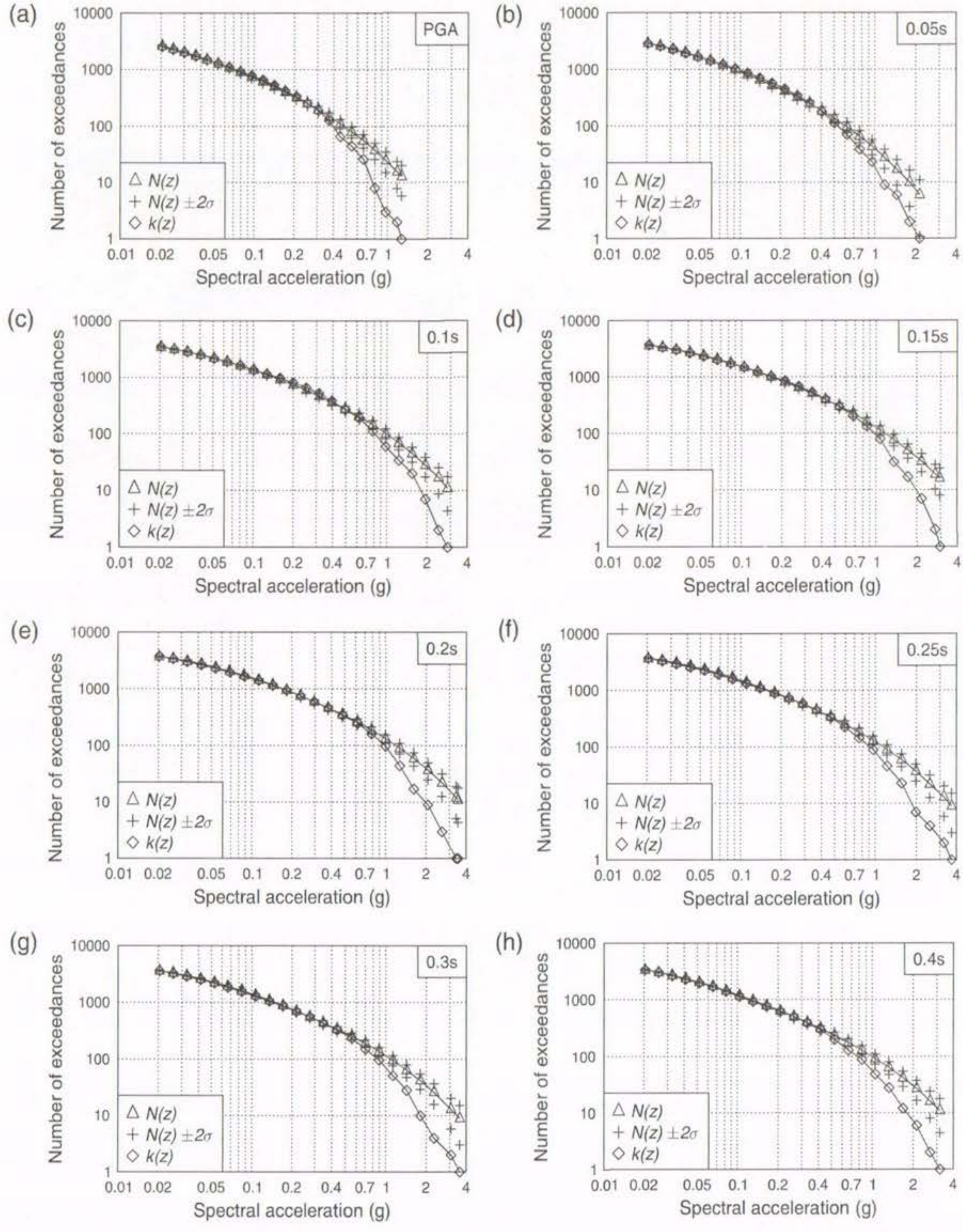

Figure 2. The expected, $N(z)$, and the actual, $k(z)$, number of records exceeding a given spectral acceleration for (a) PGA, (b) 0.05, (c) 0.1, (d) 0.15, (e) 0.2, (f) 0.25, (g) 0.3, and (h) 0.4 sec spectral periods. At all periods shown here, the difference between the actual and the expected number of exceedances increases rapidly with increasing spectral acceleration over $1.0g$, with the actual number of exceedances being well below the mean expected number minus 2 standard deviations.

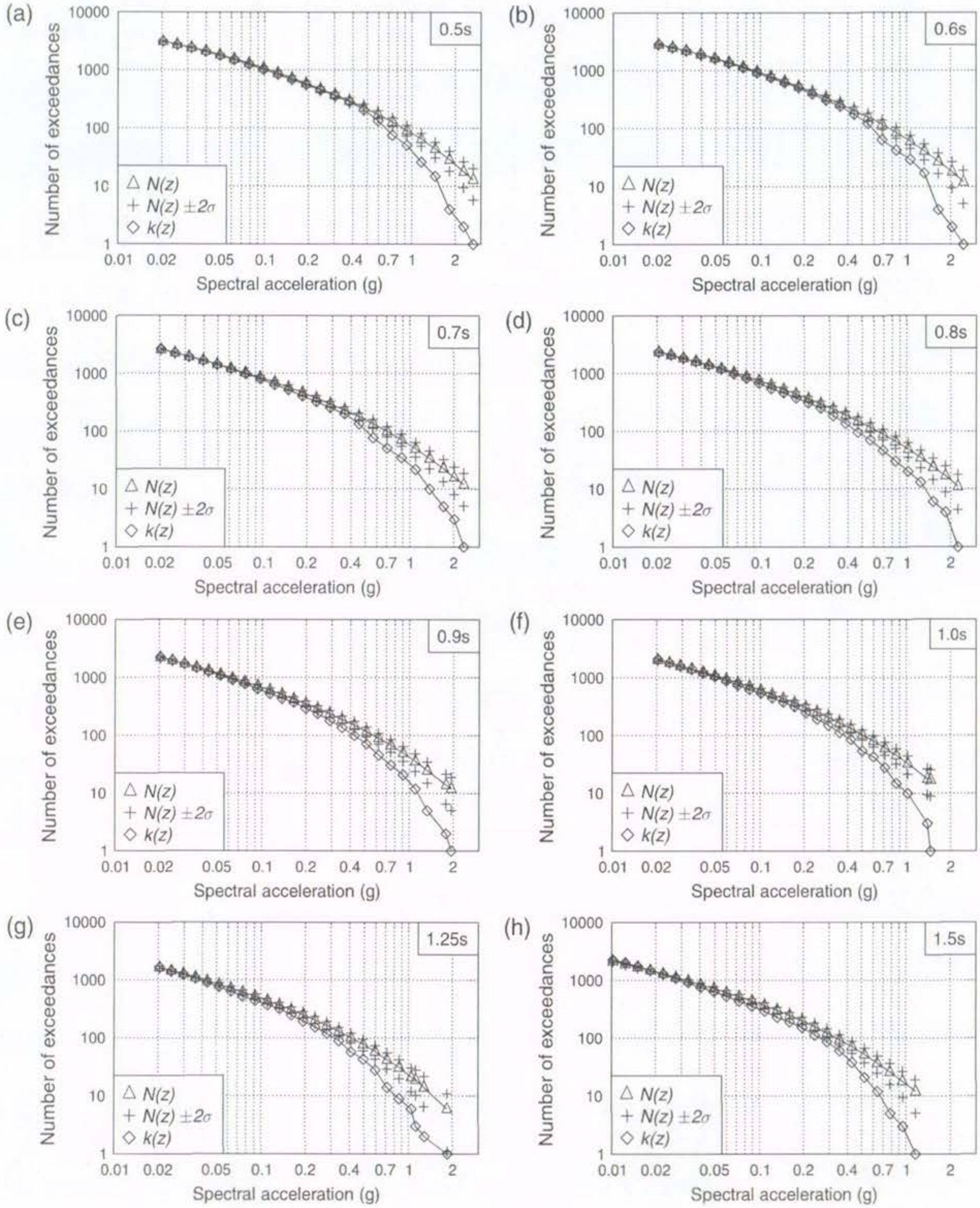

Figure 3. The expected, $N(z)$, and the actual, $k(z)$, number of records exceeding a given spectral acceleration for (a) 0.5, (b) 0.6, (c) 0.7, (d) 0.8, (e) 0.9, (f) 1.0, (g) 1.25, and (h) 1.5 sec spectral periods. At moderate and large accelerations, the actual number of exceedances is well below the mean expected number minus 2 standard deviations for most spectral periods.

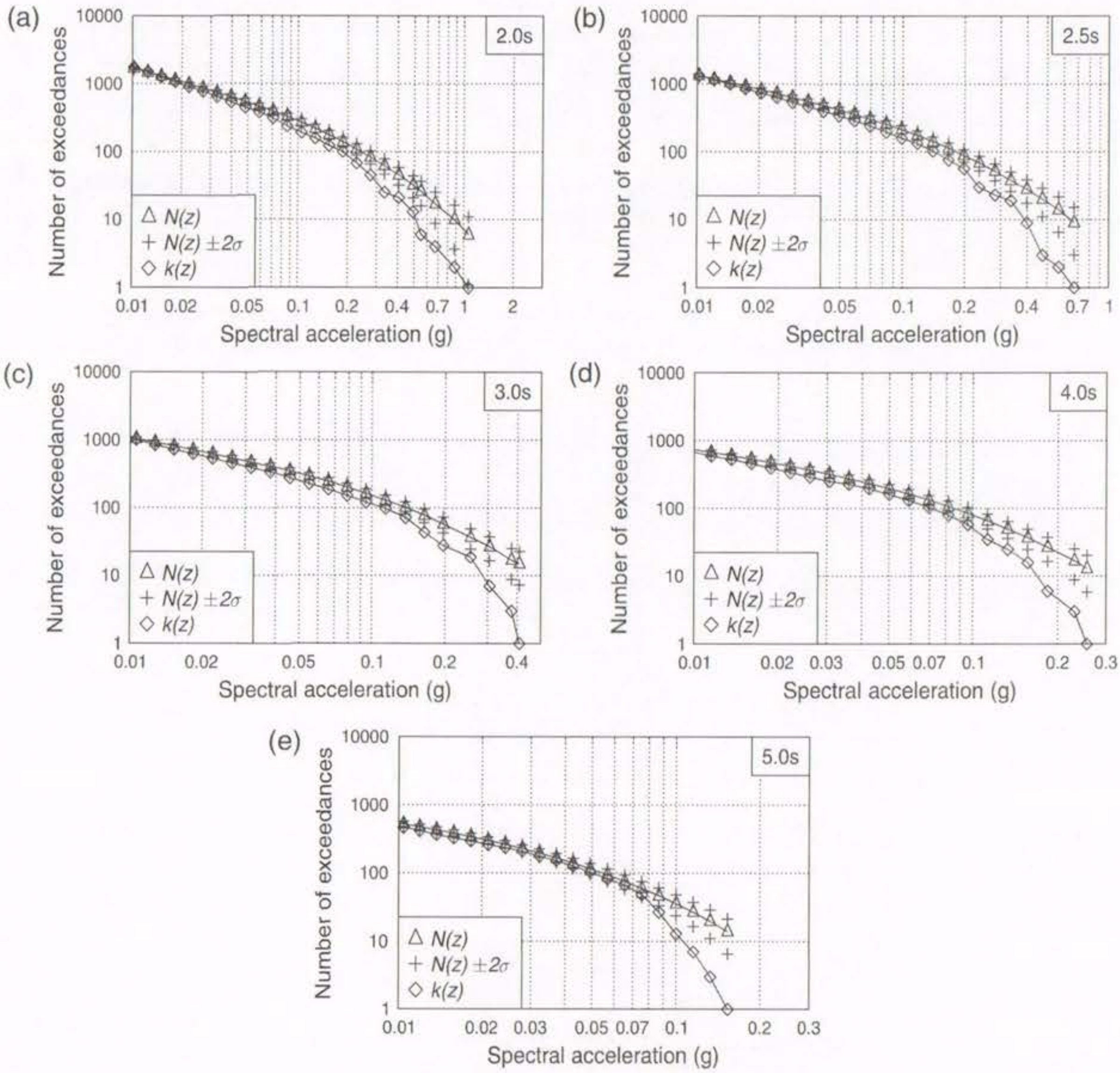

Figure 4. The expected, $N(z)$, and the actual, $k(z)$, numbers of records exceeding a given spectral acceleration for (a) 2.0, (b) 2.5, (c) 3.0, (d) 4.0, and (e) 5.0 sec spectral periods. At moderate and large accelerations, the actual number of exceedances is well below the mean expected number minus 2 standard deviations for most spectral periods.

Effects of Soil Site Classes and Earthquake Tectonic Types

In this section, we attempt to identify the effects of soil conditions at recording stations, as it is very well known that nonlinear soil response and liquefaction may limit the maximum PGA (Idriss, 1990; Pavlenko and Irikura, 2002) and short-period ground motions. We will also investigate the effect of earthquake tectonic types because the Zhao, Zhang, *et al.* (2006) models show a significant effect of earthquake tectonic types on the predicted response spectra.

In order to make a meaningful comparison we have to find a method to normalize the comparison parameters in a logical manner. One way is perhaps to compare the data composition among different spectral periods for the data range that have values of $k(z)/N(z)$ larger than a given value. We define a ground-motion threshold z_{sh} as the minimum spectral acceleration for which $k(z_{sh})/N(z_{sh})$ is less than or equal to some desired value. Table 2 shows the number of records in each site class for PGA and 1.0 and 4.0 sec spectral periods with $k(z)/N(z) \leq 0.5$. A reasonably consistent pattern of data distribution can be identified. For PGA, over 60% of the data with $k(z)/N(z) \leq 0.5$ are from site class (SC) I

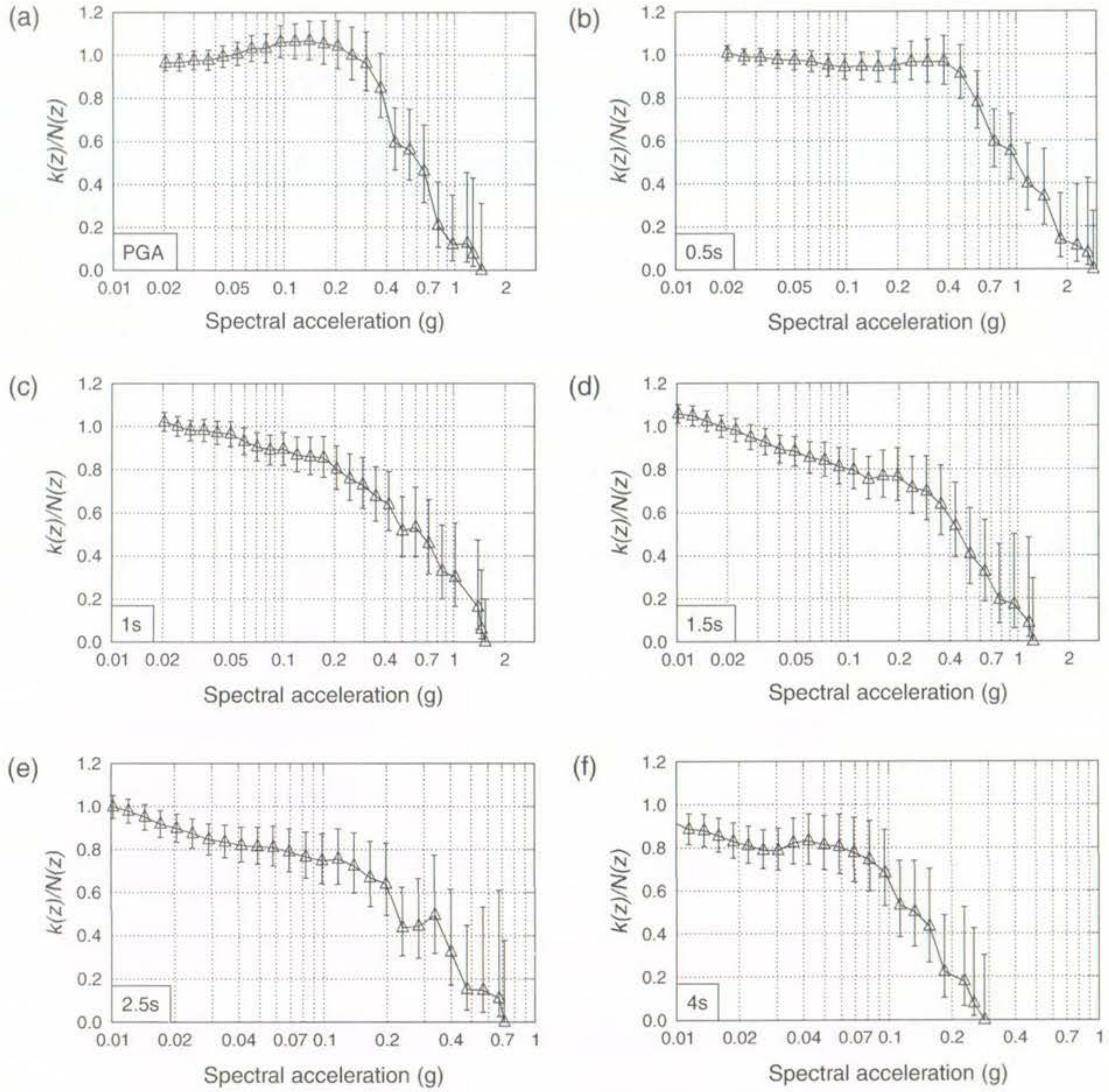

Figure 5. The ratio of the actual and the expected numbers of exceedances together with 95% confidence limits. For PGA and spectra at a 0.5 sec spectral period, $k(z)/N(z)$ is close to 1.0 at small and moderate spectral accelerations and decreases rapidly with increasing exceedance accelerations. At the other spectral periods, $k(z)/N(z)$ starts to decrease from about 1.0 at very small spectral accelerations.

and SC II sites, 90% of data are from SC I, SC II, and SC III (also see Table 3), and only 10% (three records) are from SC IV. Among the 12 records from SC III and SC IV sites of the PGA data set, 4 are from the 1995 Kobe earthquake and 3 are from the 1994 Northridge earthquake. At 1.0 and 4.0 sec periods most data with $k(z)/N(z) \leq 0.5$ are from site classes SC III and SC IV. Among the 17 records from SC IV at a 1.0 sec spectral period, 9 records are from the 1995 Kobe earthquakes, and 6 out of 9 records in SC IV at a 4.0 sec spectral period are also from this event. Strong nonlinear soil responses have been identified from recorded ground motions at some of these sites (Pavlenko and Irikura, 2002), and it is very likely that nonlinear soil responses developed at these sites limit the PGA and the short-period ground motions. Although we cannot link the data distribution, site effects, and possible nonlinear soil response in a rigorous theoretical manner to the variation of $k(z)/N(z)$ with increasing spectral acceleration, it is possible that site effects contribute to the different behavior of $k(z)/N(z)$ at different spectral periods. For example, the rapid reduction in

Table 2
Number of Records That Have a Value of $K(Z)/n(Z) \leq 0.5$ for Four Site Classes and Three Spectral Periods

	Number of Records		
Site Class	PGA	1.0 sec	4.0 sec
SC I	10	2	1
SC II	11	9	6
SC III	9	22	11
SC IV	3	17	9
Total of records	33	50	27

$k(z)/N(z)$ for PGA in Figure 5a may well be a result of the nonlinear soil response of the 12 SC III and SC IV sites, that is, PGA at these sites may be limited when soil responds nonlinearly. The Zhao, Zhang, *et al.* (2006) models do not model the effect of nonlinear soil response because the number of near-source records from soil sites is too small to derive nonlinear soil site terms.

Table 3 presents percentages of the records in each site class for PGA and 1.0 and 4.0 sec spectral periods for $k(z)/N(z) \leq 0.5$, 0.7, 0.8, and all data. The distribution of records changes little across the spectral periods, about 1/3 of the data being from SC I sites, 1/3 from SC II sites, and 1/3 from the combined SC III and SC IV classes.

Table 3
Percentage of Records in Each Site Class Selected at a Specific Value of $k(z)/N(z)$

	All Data			
Site Class	PGA	0.5 sec	1.0 sec	4.0 sec
I	33	33	33	29
II	33	33	33	34
III	14	14	13	14
IV	21	21	21	23
	$k(z)/N(z) \leq 0.8$			
Site Class	PGA	0.5 sec	1.0 sec	4.0 sec
I	26	13	9	16
II	32	29	27	30
III	25	33	29	27
IV	18	24	36	27
SA* threshold z_{sh} (g)	0.39	0.15	0.23	0.025
	$k(z)/N(z) \leq 0.7$			
Site Class	PGA	0.5 sec	1.0 sec	4.0 sec
I	26	13	5	10
II	34	30	26	20
III	23	34	35	39
IV	16	23	33	30
SA* threshold z_{sh} (g)	0.41	0.62	0.33	0.088
	$k(z)/N(z) \leq 0.5$			
Site Class	PGA	0.5 sec	1.0 sec	4.0 sec
I	30	8	4	4
II	33	38	18	22
III	27	33	44	41
IV	9	23	34	33
SA* threshold z_{sh} (g)	0.61	1.02	0.52	0.13

*SA stands for spectral acceleration.

We examined the record distribution for three nested $k(z)/N(z)$ classes, namely, larger than or equal to 0.5, 0.7, and 0.8. The resulting thresholds of the spectral accelerations corresponding to each value of $k(z)/N(z)$ for each spectral period are given in Table 3. The PGA threshold z_{sh} for $k(z)/N(z) \leq 0.5$ is $0.61g$. Under such strong ground shaking, the ground motion at these soil sites would have passed the crossover point that separates the range of amplification from that of deamplification with respect to rock site motion. Typical values for the crossover point are between 0.3 and $0.5g$ (Idriss, 1990), depending on the soil properties and site natural periods. When the PGA of a soil site is over the crossover point, a strong nonlinear response that would develop in the SC III and SC IV sites may lead to deamplification of PGA and short-period spectra. It is possible that only a few soil sites would be able to sustain a PGA of much larger than this high value of $0.61g$; and therefore very few SC IV sites are present among the records with such a large PGA. At long-spectral periods, such as 1 and 4 sec (much larger than the site natural period), soil nonlinear deformation has little effect and soils tend to amplify long-period ground motion regardless of the shaking strength (Zhao *et al.*, 1999). This is perhaps the reason why many SC III and SC IV soil sites are present at 1 and 4 sec spectral periods and relatively few rock sites at this level of ground shaking. The distribution of rock and soil sites for records with $k(z)/N(z) \leq 0.5$ is very different from those of the whole data set, suggesting that site effect may play a very important role in the variation of $k(z)/N(z)$ with respect to spectral acceleration z.

The PGA threshold z_{sh} is $0.41g$ for $k(z)/N(z) \leq 0.7$ and $0.39g$ for $k(z)/N(z) \leq 0.8$. At these values, the percentage of records from the SC IV class is significantly larger than that for $k(z)/N(z) \leq 0.5$. This may be a result of less possible extent of nonlinear soil deformation for sites with a PGA in a range between 0.39 and $0.61g$ and the sites with a PGA equal to or over $0.61g$ ($k(z)/N(z) \leq 0.5$).

On the other hand, if nonlinear soil response is indeed a significant factor that limits the maximum response spectra at short periods, the variation in $k(z)/N(z)$ for rock and soil sites needs to be examined separately. Note that the effects of nonlinear soil response were not modeled in the Zhao, Zhang, *et al.* (2006) model. The few records from soil sites where significant nonlinear response apparently developed have very little effect on the maximum likelihood and the values of regression parameters, simply because of the overwhelming effect from the low-amplitude records obtained from soil sites (Zhao, Zhang, *et al.*, 2006). However, because of the nature of empirical models, the unmodeled possible nonlinear soil response affects not only the model parameters for the soil sites but also the parameters and residuals of the other site classes. These effects cannot be clearly identified by the overall distribution of residuals but may well be captured in the distribution of the residuals for large spectral accelerations. It is possible that the expected number of exceedances for rock and soft soil classes may change at large values of short-period spectra if nonlinear site terms are incorporated in the attenuation models. This point will be addressed later in this article.

The spectral accelerations predicted by the Zhao, Zhang, *et al.* (2006) models for subduction earthquakes differ significantly from those of shallow crustal earthquakes. At short periods, the predicted spectral accelerations from subduction slab events are much larger than those from crustal events and from subduction interface events with the same magnitude and source distance. At long periods, the predicted spectral accelerations of the subduction events are much lower than those of the shallow crustal events with the same magnitude and source distance. Table 4 shows the percentage of records in each earthquake category. Over all data, about 1/3 of the records are from each type of earthquake. A striking feature is that crustal events have the largest number of records for $k(z)/N(z) \leq 0.5$ for PGA and 0.5, 1.0, and 4.0 sec spectral periods, suggesting that the records from crustal events tend to have larger spectral accelerations at these periods. At a 4 sec period, the crustal component decreases from 63% for $k(z)/N(z) \leq 0.5$ to 47% for $k(z)/N(z) \leq 0.8$. For PGA the interface component increases from about 12% for $k(z)/N(z) \leq 0.5$ to 22% for $k(z)/N(z) \leq 0.8$, with no trends evident at the other spectral periods. The slab component decreases with increasing spectral periods and tends to increase with increasing values of $k(z)/N(z)$. At a 4.0 sec period, the numbers of records from slab events are very small. Table 4 implies that records with spectral acceleration larger than the corresponding spectral acceleration threshold are mainly from crustal events, while the records with spectral accelerations less than the corresponding thresholds are mainly from subduction slab events at spectral periods of 0.5 sec or longer.

Table 4
Percentage of Records in Each Earthquake Category at Specific Values of $k(z)/N(z)$

	All Data			
Earthquake type	PGA	0.5 sec	1.0 sec	4.0 sec
Crustal	31	31	31	30
Interface	32	32	32	37
Slab	36	36	36	33
	$k(z)/N(z) \leq 0.8$			
	PGA	0.5 sec	1.0 sec	4.0 sec
Crustal	54	63	64	47
Interface	22	21	26	44
Slab	24	17	10	9
	$k(z)/N(z) \leq 0.7$			
	PGA	0.5 sec	1.0 sec	4.0 sec
Crustal	57	62	65	57
Interface	20	20	27	42
Slab	23	18	8	1
	$k(z)/N(z) \leq 0.5$			
	PGA	0.5 sec	1.0 sec	4.0 sec
Crustal	61	63	72	63
Interface	12	28	22	37
Slab	27	10	6	0

The reason for the changes in the contribution from each type of earthquake with $k(z)/N(z)$ is probably to be found in the nature of the data set. Most subduction events in Japan occur offshore at large distance and large depth. It is possible that the decrease in the $k(z)/N(z)$ ratio at large spectral acceleration is due to the reduced number of records from subduction events, though we cannot confirm or reject the possibility in a rigorous manner.

Analyses of Site-Class Subsets

The data set used by the Zhao, Zhang, *et al.* (2006) model is large, and this allows us to examine subsets of the data. We group the records according to site class, with each group having more than 1500 records for PGA. We combine SC III and SC IV sites together because the number of records from SC III sites is too small to be a group of its own. In the results presented subsequently, we assume that the standard deviation is the same as that derived from the random effect methodology for all groups. Figure 6a,b,c shows $k(z)/N(z)$ for three groups of data separated according to site class. For rock (SC I) sites, the ratio $k(z)/N(z)$ between 0.05 and $0.5g$ in Figure 6a is considerably larger than 1.0, suggesting a longer-tailed distribution than lognormal, that is, $k(z)/N(z) > 1.0$, and this is likely caused by the slab records in Figure 6f. The ratio $k(z)/N(z)$ for SC II and SC III/SC IV sites are generally similar in Figure 6b,c, suggesting that the nonlinear soil response for PGA and for 0.5 and 1.0 sec spectral periods is unlikely to be the only cause for the decrease of $k(z)/N(z)$. The rapid decrease in $k(z)/N(z)$ from about $0.02g$ for subduction interface events may be caused by the data distribution. At a 1.0 sec spectral period, the variation of $k(z)/N(z)$ for SC II, SC III/SC IV sites, and for crustal and subduction slab events are generally similar, suggesting that nonlinear soil response (which does not have a profound effect at a 1.0 sec spectral period) and data composition are unlikely to be the only reasons for the decrease in $k(z)/N(z)$ with increasing exceeding spectral accelerations.

The striking feature for rock (SC I) sites is that $k(z)/N(z)$ for PGA is much larger than 1.0 in the spectral acceleration range of 0.07–$0.4g$ and then decreases rapidly to zero at about $1.2g$. The very large values in the range of 0.07–$0.4g$ for PGA suggest that the distribution of the PGA prediction error is more long tailed than the lognormal distribution in this range. The ratio $k(z)/N(z)$ at a 0.5 sec period is close to 0.9 up to $0.7g$ and then decreases rapidly to zero. The variation of $k(z)/N(z)$ for PGA and a 0.5 sec period is in contrast to the PGA data in Figure 5a where $k(z)/N(z)$ starts to decrease sharply at about $0.25g$ for PGA and $0.4g$ for a 0.5 sec period. At 1.0 sec spectral acceleration, for the rock class, the ratio $k(z)/N(z)$ decreases almost linearly from 1.0 at about $0.02g$ to 0 at $0.8g$, while for the other site classes the decrease starts more gradually. For SC III and IV sites, $k(z)/N(z)$ decreases from 1.0 at a $0.15g$ period to 0 at about $1.5g$. The changes in the variation pattern of $k(z)/N(z)$ among the three groups of sites are the largest for PGA and the least for a 1.0 sec spectral period, and the

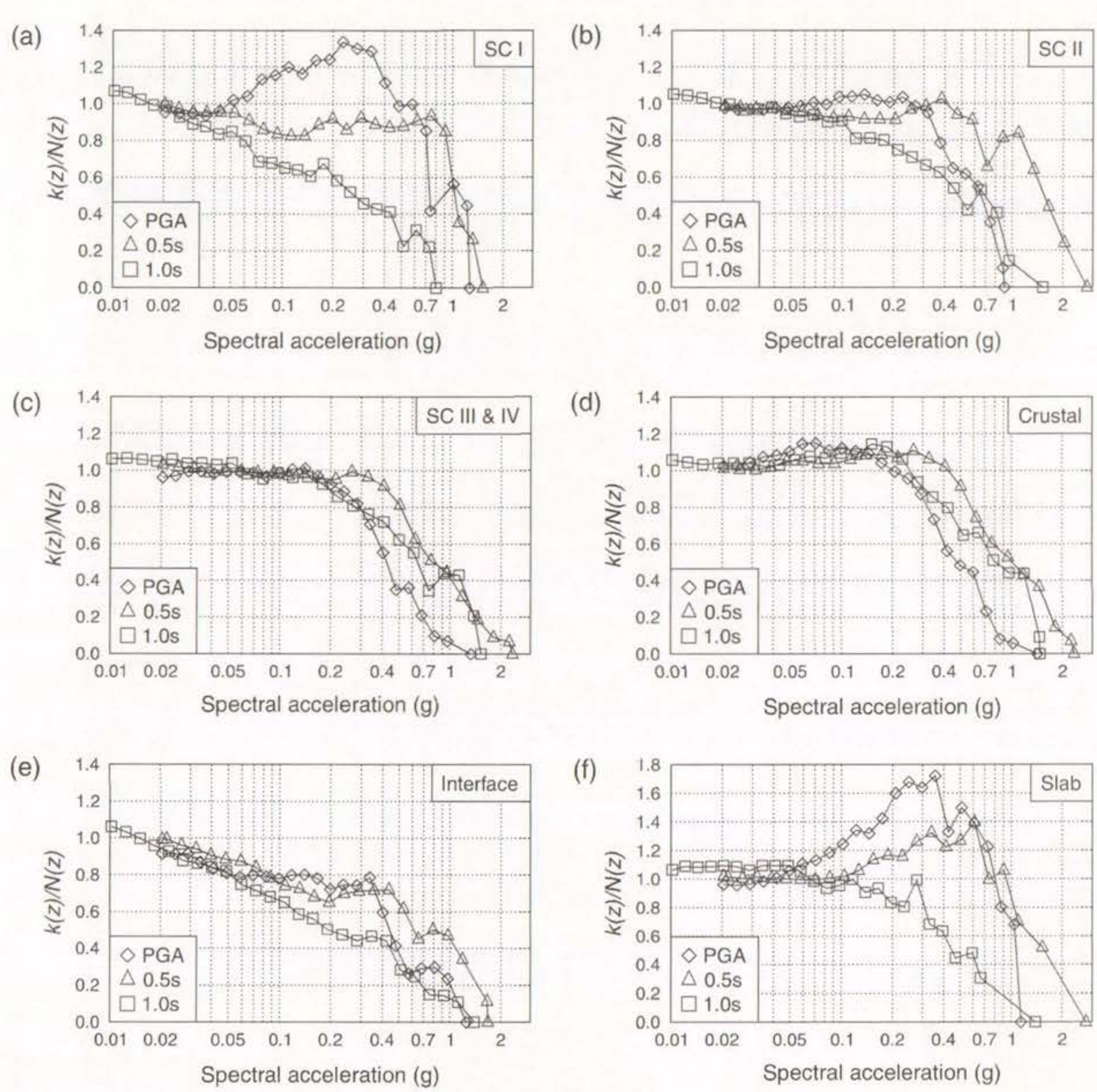

Figure 6. The ratio of the actual and the expected numbers of exceedances in each site class in (a), (b), and (c) and earthquake category in (d), (e), and (f).

variation pattern of $k(z)/N(z)$ for a 1.0 sec period is generally similar to that of Figure 5c. These results are consistent with the effect of nonlinear soil response, and the effect is large for short-period spectra and the least for long-period spectra (Zhao *et al.*, 1999).

Figure 7 shows the expected and the actual number of exceedances for rock site records for PGA and a 0.5 sec spectral period. The actual numbers of exceedances are less than the expected ones only at large spectral accelerations. For PGA the expected number of exceedances is two when the actual exceedance is one. At 0.5 sec, the expected number of exceedances for the last data is just less than four when the actual exceedance is one. The differences between the expected and the actual numbers of exceedances in Figures 2a and 3a are much larger that those in Figure 7 and the large differences in Figures 2a and 3a are likely caused by nonlinear soil response.

Analyses of Earthquake-Category Subsets

Figure 6d,e,f shows the ratio $k(z)/N(z)$ for the three earthquake categories. The pattern of variation of

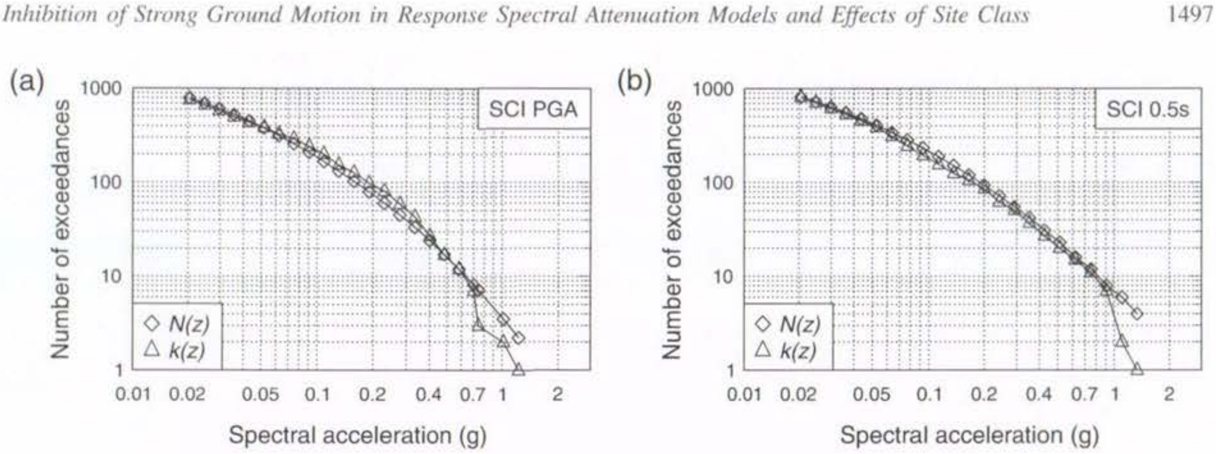

Figure 7. Number of exceedances for (a) PGA and (b) 0.5 sec spectral period of rock (SC I) sites.

$k(z)/N(z)$ for crustal events (Fig. 6d) is generally similar to the full data set as shown in the Figure 5a,b,c. Figure 6e shows that $k(z)/N(z)$ for interface events decreases quickly with increasing spectral accelerations. Figure 6f shows a strong increase in $k(z)/N(z)$ to values much greater than 1 at acceleration levels in the range 0.1–0.6g for PGA and a 0.5 sec spectral acceleration from slab events, followed by a decrease to values less than 1 at acceleration levels exceeding 1.0g.

The number of records is an important consideration when the data set is divided into different subsets, as we have done here. Some aspects of the variation of $k(z)/N(z)$ in each subset of the data may be a result of the reduced number of data.

Figure 8 shows that, for slab events, the differences between the expected and actual number of exceedances for PGA and 0.5 sec spectral acceleration $> 1.0g$ are trivial, because $N(z)$ and $k(z)$ are both small (≤ 4). However, the excess of $k(z)$ over $N(z)$ at intermediate accelerations is supported by larger values of $N(z)$ and $k(z)$ ranging from a few tens to more than a hundred, so the discrepancies are significant. There is interest in examining whether they can be reduced by improvement of the model. The Zhao, Zhang, *et al.* (2006) models selected in the present study have only linear magnitude terms, in consideration of strictly appropriate use of random-effects methodology and appropriate estimates of interevent error. Also, the anelastic attenuation rate was set to equal that of the crustal events, perhaps leading to inappropriate anelastic and geometric attenuation coefficients for the slab events. To examine the effects of these modeling choices, we consider a modified model with additional cubic-magnitude terms (as suggested for slab events by Zhao, Zhang, *et al.*, 2006) and with separate geometric and anelastic attenuation coefficients, which are derived by fitting a function of these parameters to the total residuals for the slab events from the original model. Figure 9 shows the results for the modified model. It can be noted that the ratio $k(z)/N(z)$ is significantly reduced, reaching a maximum of only 1.2 (Fig. 9a) as compared with 1.75 (Fig. 6f) for the previous model. For the modified model, the reduction of $k(z)/N(z)$ to values less than one at accelerations exceeding 0.4g is now more significant, being supported by values of $k(z)$ and $N(z)$ up to a few tens, as shown in Figure 9b. Overall, the pattern of variation of $k(z)/N(z)$ in the modified model for slab earthquakes is

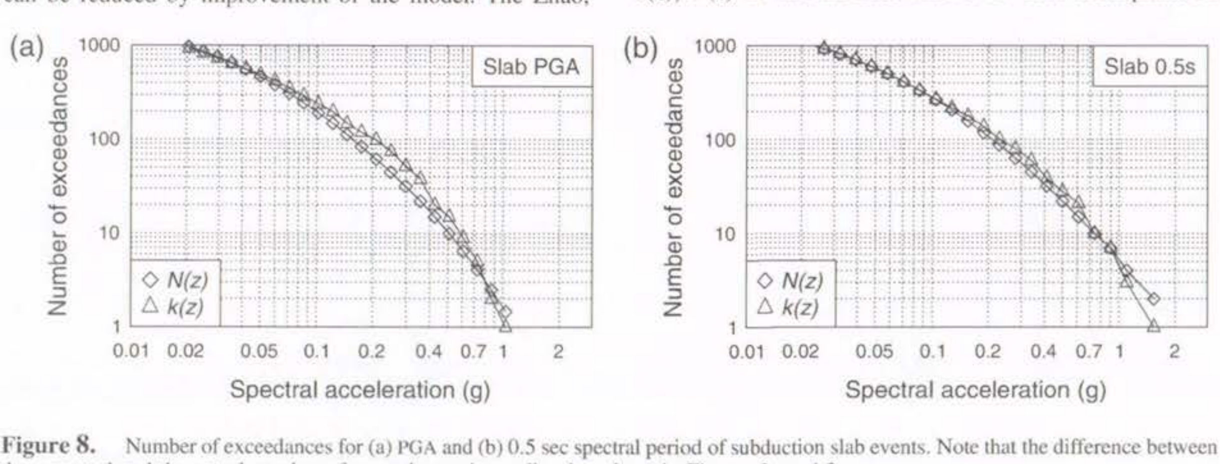

Figure 8. Number of exceedances for (a) PGA and (b) 0.5 sec spectral period of subduction slab events. Note that the difference between the expected and the actual number of exceedances is smaller than those in Figures 2a and 3a.

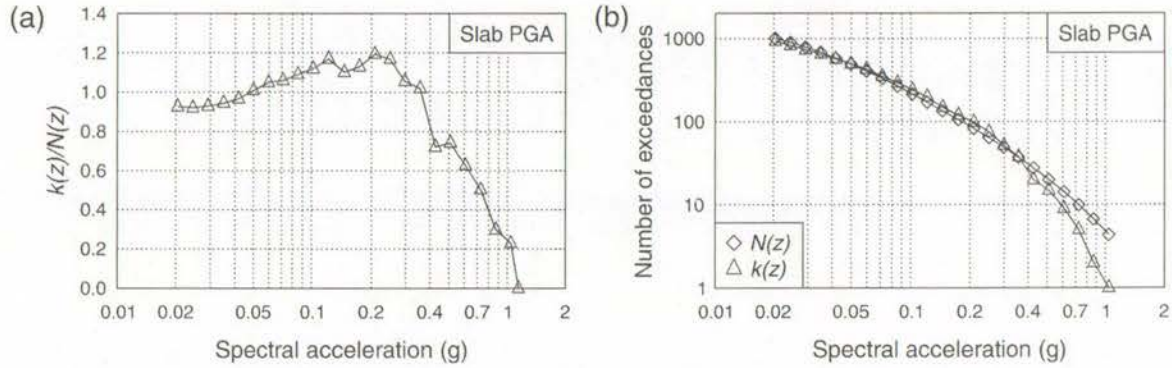

Figure 9. (a) Number of exceedances for PGA for subduction slab records using a modified model with additional parameters derived from the residual of the model in Figure 8a. (b) The expected number of exceedances at moderate-to-large accelerations is greater than in Figure 8a.

much more similar to that for the other subsets of the data, and the inhibition effect is more significant.

Discussion

The results presented in Figures 2–5 consistently show a decrease in the ratio of actual to expected number of exceedances at large spectral acceleration across a range of spectral periods. It seems possible that allowing a magnitude-dependent standard deviation, in which the standard deviation decreases with increasing magnitude, as seen in the models of Abrahamson and Silva (1997), Youngs *et al.* (1997), and McVerry *et al.* (2006), could correct this apparent misfit of the model to the data. The correlation between the response spectra, magnitude, and source distance can exacerbate or reduce the effect of magnitude-dependent prediction errors depending on the variation of standard error with magnitude. Therefore, there is interest in examining the evidence for magnitude dependence of the residuals in the present models.

In the Zhao, Zhang, *et al.* (2006) model, both interevent and intraevent residuals were found not to be strongly and systematically magnitude dependent at short- and intermediate-spectral periods. Figure 10 shows the standard deviations σ_{es} for intraevent residuals and τ_{es} for interevent residuals estimated in moving magnitude windows. Note that σ_{es} and τ_{es} are the square roots of the variance for the intraevent and interevent residuals in each magnitude window and do not equal the intraevent and the interevent errors derived from random-effects models even if all data are used in computing σ_{es} and τ_{es}. We assume that the variations of σ_{es} and τ_{es} with respect to magnitude can be used to gauge the magnitude dependency of the intraevent and interevent errors.

Figure 10 shows that σ_{es} at a 1.0 sec spectral period appears to decrease with increasing magnitude while σ_{es} for other periods appears to be constant (0.5 sec) or to increase with increasing magnitude. At 0.5 and 1.0 sec spectral periods, τ_{es} appears to decrease with increasing magnitude, while at PGA and 4.0 sec, τ_{es} appears to increase rapidly with increasing magnitude. Note that the average magnitude in each moving window for intraevent error differs from that of the interevent error. The variation of $N(z)$ in Figures 2–4 is very similar for all spectral periods even though the variation of σ_{es} and τ_{es} with respect to magnitude is very different at different spectral periods, suggesting that the possible magnitude-dependent prediction error of the attenuation models is unlikely to be the cause for the rapid decrease in $k(z)/N(z)$ as shown in Figure 5.

Conclusions

Current ground-motion prediction models assume an unbounded lognormal distribution of random variability in ground-motion level. In reality, there probably exist physical conditions that limit the ground-motion distribution. Use of unbounded models in probabilistic seismic hazard analysis leads to ground-motion estimates that may be unrealistically large, especially at low annual probabilities.

We have applied the statistical procedure of Rhoades *et al.* (2008) to compare the actual and expected number of exceedances of a given spectral acceleration in the Zhao, Zhang, *et al.* (2006) model. The results show that, for moderately strong and strong spectral accelerations, the actual numbers of records that have spectral accelerations exceeding the specified value are much lower than the expected numbers for many spectral periods and are even lower than the expected numbers of exceedances minus two standard deviations at spectral periods beyond 1.0 sec. The actual number of exceedances is typically less than 20% of the expected number of exceedances at moderate-to-large spectral accelerations for all spectral periods and is less than 10% of the expected number at very large spectral accelerations. These results strongly suggest that assuming a normal distribution for the model-prediction error would lead to an overestimate for the number of extreme values of the predicted spectral accelerations by the Zhao, Zhang, *et al.*

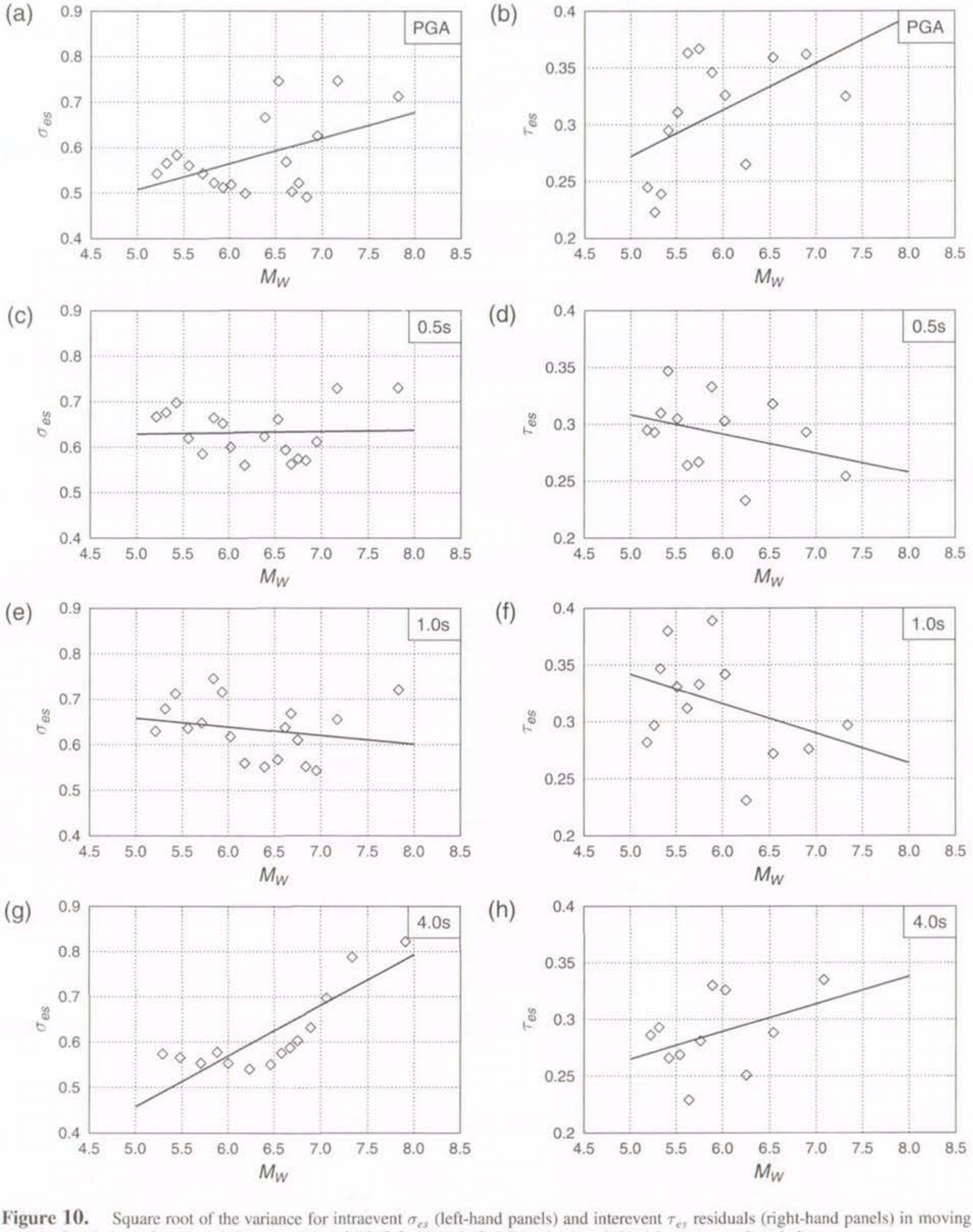

Figure 10. Square root of the variance for intraevent σ_{es} (left-hand panels) and interevent τ_{es} residuals (right-hand panels) in moving magnitude windows for (a) and (b) PGA, (c) and (d) 0.5, (e) and (f) 1.0, and (g) and (h) 4.0 sec spectral periods.

(2006) attenuation models. Similar conclusions for the NGA data set (N. A. Abrahamson, personal comm., 2008) are also reached.

For the ratio of actual to expected number of exceedances of a given value, the numbers of data from different site classes and earthquake categories vary significantly with the selected exceedance value. The variation of the numbers in each group of the records is likely to be the result of possible nonlinear soil response of soft soil sites and the different spectral acceleration values of records from different earthquake categories at a given magnitude and source distance.

Our results show that the inhibition effects for short-period acceleration spectra of rock sites differ significantly from those of the soil sites, with the numbers of expected and actual exceedances being rather similar for rock sites at large spectral accelerations. However, at very strong peak ground accelerations over $0.7g$, the actual number of exceedances is $1/2$–$2/3$ of the expected number. For soil sites, the actual number of exceedances is similar to the expected number for PGAs up to $0.2g$ and then decreases to 0 at $1.3g$. These differences are consistent with possible nonlinear soil deformation at soft soil sites subjected to strong ground shaking.

Our results also show that the ratio of the actual to expected number of exceedances varies across different earthquake categories—crustal, interface, and slab—mainly at short-spectral periods. An anomaly in the PGA model for slab earthquakes, in which the ratio is much greater than one at moderate accelerations, is greatly reduced by including additional terms in the model. All earthquake categories then show strong decreases in the ratio at large accelerations.

Whether these results are interpreted as evidence of actual physical inhibition of very strong ground motions, or as inadequacies in the present generation of ground-motion models, they clearly present a challenge to current assessments of the rate of occurrence of extreme ground motions across a range of spectral periods, site classes, and earthquake tectonic categories.

Data and Resources

The strong-motion data used in the present study were collected from the following organizations:

1. The following data sets are available from the listed web sites: California Division of Water Resources, California Strong Motion Instrumentation Program, U.S. Geological Survey (http://peer.berkeley.edu/nga/earthquakes.html, last accessed March 2009), Japan Meteorological Agency (http://www.jma.go.jp/en/quake, last accessed March 2009), National Research Institute for Earthquake Science and Disaster Prevention: K-NET and KiK-net (http://www.k-net.bosai.go.jp/k-net/index_en.shtml, last accessed March 2009), and Port and Airport Research Institute (http://www.eq.ysk.nilim.go.jp, last accessed March 2009).
2. Central Research Institute of Electric Power Industry, Hanshin Expressway Public Corporation, Honshu-Shikoku Bridge Authority, JR group, Kansai Electric Power Company, Kobe City Office, Kyoto University, Maeda Corporation, Matsumura-gumi Corporation, Ministry of Internal Affairs and Communications, National Institute for Land and Infrastructure Management, Obayashi Corporation, Osaka Gas Co., Ltd., Railway Technical Research Institute, Shiga Prefecture, The Association for Earthquake Disaster Prevention, The Committee of Earthquake Observation and Research in the Kansai Area, The University of Shiga Prefecture, Tokyo Electric Power Company, and Urban Renaissance Agency (data cannot be released to the public).

Acknowledgments

We acknowledge the research grant from the Earthquake Commission (EQC) of New Zealand. We wish to thank Warwick Smith and Jim Cousins for their review of the manuscript. We also wish to thank Jeffery Fisher for his work on the EQC project that inspires the work reported here. The results reported here are partially supported by the Foundation for Research Science and Technology of New Zealand, Contract Number C05X0402.

References

Abrahamson, N. A., and W. J. Silva (1997). Empirical response spectral attenuation relations for shallow crustal earthquakes, *Seism. Res. Lett.* **68,** 94–127.

Abrahamson, N. A., and R. R. Youngs (1992). A stable algorithm for regression analyses using the random effects model, *Bull. Seismol. Soc. Am.* **82,** 505–510.

Anooshehpoor, A., and J. N. Brune (2002). Verification of precarious rock methodology using shake table tests of rock models, *Soil Dyn. Earthq. Eng.* **22,** 917–922.

Bommer, J. J., N. A. Abrahamson, F. O. Strasser, A. Pecker, P. Y. Bard, H. Bungun, F. Cotton, D. Fäh, F. Sabetta, F. Scherbaum, and J. Studer (2004). The challenge of determining upper limits on earthquake ground motions, *Seism. Res. Lett.* **75,** 82–95.

Bragato, P. L. (2005). Estimating an upper limit probability distribution for peak ground acceleration using the randomly clipped normal distribution, *Bull. Seismol. Soc. Am.* **95,** 2058–2065.

Building Seismic Safety Council (BSSC) (2000). *The 2000 NEHRP Recommended Provisions for New Buildings and Other Structures, Part I (Provisions) and Part II (Commentary)*, FEMA **368/369,** Washington, D.C.

Idriss, I. M. (1990). Response of soft soil sites during earthquakes, in: *Proc. of the Memorial Symp. to Honor Professor Harry Bolton Seed*, Berkeley, California, Vol **2,** 273–289.

McVerry, G. H., J. X. Zhao, N. A. Abrahamson, and G. H. Somerville (2006). Crustal and subduction zone attenuation relations for New Zealand earthquakes, *Bull. N. Z. Soc. Earthq. Eng.* **39,** no. 1, 1–58.

Molas, G. L., and F. Yamazaki (1995). Attenuation of earthquake ground motion in Japan including deep focus events, *Bull. Seismol. Soc. Am.* **85,** 1343–1358.

Pavlenko, O., and K. Irikura (2002) Changes in shear moduli of liquefied and nonliquefied soils during the 1995 Kobe earthquake and its aftershocks at three vertical-array sites, *Bull. Seismol. Soc. Am.* **92,** 1952–1969.

Rhoades, D. A., J. X. Zhao, and G. H. McVerry (2008). A simple test for inhibition of very strong ground motions in attenuation models, *Bull. Seismol. Soc. Am.* **98,** 448–453.

Shi, B., A. Anooshehpoor, Y. Zeng, and J. N. Brune (1996). Rocking and overturning of precariously balanced rocks by earthquakes, *Bull. Seismol. Soc. Am.* **86,** 1364–1371.

Strasser, F. O., and J. J. Bommer (2005). Analysis of intra-event ground-motion residuals from K-NET and KiK-NET data, Research Rept. No. 05-003-SM, Imperial College, London, U.K.

Youngs, R. R., S.-J. Chiou, W. J. Silva, and J. R. Humphrey (1997). Strong ground motion attenuation relationships for subduction zone earthquakes, *Seism. Res. Lett.* **68,** 94–127.

Zhao, J. X., P. N. Davenport, and G. H. McVerry (1999). Modelling and earthquake response of Gisborne post office site, New Zealand, *Bull. N. Z. Soc. Earthq. Eng.* **32,** no. 3, 146–169.

Zhao, J. X., K. Irikura, J. Zhang, Y. Fukushima, P. G. Somerville, A. Asano, Y. Ohno, T. Oouchi, T. Takahashi, and H. Ogawa (2006). An empirical site classification method for strong motion stations in Japan using H/V response spectrum ratio, *Bull. Seismol. Soc. Am.* **96,** 914–925.

Zhao, J. X., J. Zhang, A. Asano, Y. Ohno, T. Oouchi, T. Takahashi, H. Ogawa, K. Irikura, H. K. Thio, P. G. Somerville, Y. Fukushima, and Y. Fukushima (2006). Attenuation relations of strong ground motion in Japan using site classification based on predominant period, *Bull. Seismol. Soc. Am.* **96,** 898–913.

Zhao, J. X., J. Zhang, J. Fisher, and P. G. Somerville (2007). Bounds on the distribution of amplitudes in ground motion prediction models, GNS Science Consultancy Report 2007/98 prepared for Earthquake Commission, New Zealand.

GNS Science
1 Fairway Drive, Avalon
Lower Hutt 5040, New Zealand
(J.X.Z., D.A.R., G.H.M.)

Risk Frontiers
Macquarie University
Sidney, Australia
(P.G.S.)

Manuscript received 19 September 2008

ENG
34

Bounds on the distribution of amplitudes in ground motion prediction models

John Zhao	GNS Science
Jian Zhang	GNS Science
Jeff Fisher	Risk Frontiers
Paul Somerville	Risk Frontiers

GNS Science Consultancy Report 2007/98
May 2007

CONFIDENTIAL

This report has been prepared by the Institute of Geological and Nuclear Sciences Limited (GNS Science) exclusively for and under contract to Earthquake Commission (EQC). Unless otherwise agreed in writing, all liability of GNS Science to any other party other than Earthquake Commission (EQC) in respect of the report is expressly excluded.

The data presented in this Report are available to GNS Science for other use from May 2007

CONTENTS

FIGURES

TABLES

APPENDIX

EXECUTIVE SUMMARY

In a probabilistic seismic hazard study, the imprecise prediction of ground motion parameters by empirical attenuation models is usually taken into account by assuming a lognormal distribution for the prediction imprecision. For some important engineering structures, such as hydro-power stations in New Zealand and nuclear power plants and nuclear waste storage overseas, their critical importance requires ground-motion estimates that have very low annual probability (very long return period). For such a level of ground motions, an assumption of lognormal distribution leads to an almost monotonic increase in the estimated ground motion parameters with increasing return period, without a limit. These properties of the estimated ground motions cause a major difficulty in the ground-motion assessment – are these estimates realistic? If not, what would be the upper limits?

In the present study, we examine the root of the problem – to estimate the upper limit of the range within which the prediction imprecision has a lognormal distribution. We use a sub-dataset from a very large dataset used for developing Japanese attenuation models. Because of data ownership and the quality of data from analogue and early versions of digital instruments, the sub-dataset consists of records from the K-net and Kik-net arrays only. We employ two methods to tackle the problem.

The first method uses graphical inspection of the probability plots and formal statistical tests. We plot the theoretical values derived from a lognormal distribution against the actual values computed from data and the attenuation models. Using visual inspection, we can identify where the upper tails of the distribution depart from the lognormal distribution for a number of spectral periods. Using formal statistical tests, we can also identify the upper tail departures from the lognormal distribution for a number of spectral periods, but they do not all correspond to those periods identified by the probability plots. This method produces mixed results.

The second method is to compare two important parameters of the data and the attenuation models. The first parameter is the expected number of records in a dataset that have a value larger than a specified spectral acceleration. The second parameter is the actual number of records exceeding this specified value. We find that the actual number of exceedances at moderately strong and strong ground shaking is much smaller than the expected number of exceedances for all spectral periods. At very high spectral accelerations (the level of design ground motion for important structures such as hydro-power stations), the actual numbers of exceedances are only 5-10% of the expected numbers of exceedances. Although we cannot put an upper limit to the ground motion parameters using this method, our results strongly suggest that there are some physical constraints that limit the maximum spectral ground accelerations in the sub-dataset used in the present study.

If these results are considered in a probabilistic seismic hazard study, the continuing increase in the estimated ground-motion parameters with increasing return period may not occur.

TECHNICAL SUMMARY

In current ground-motion models, the uncertainty in predicted ground motion is modelled with a lognormal distribution. One consequence of this is that predicted ground motions do not have an upper limit. In reality, there probably exist physical conditions that limit the ground motion. Use of unbounded models in probabilistic seismic hazard analysis leads to ground motion estimates that may be unrealistically large, especially at the low annual probabilities considered for important structures, such as dams or nuclear reactors. Attempts to estimate the upper limits have been made by others by using ground-motion records from a single event, but it is not clear if the conclusions derived are applicable to attenuation models which are derived from a large number of records generated by a large number of earthquakes. We have analysed very large strong-motion data sets from the K-net and Kik-net strong-motion networks in Japan and determined the total residuals from the ground-motion model developed for Japan. These residuals are then used to construct normal probability plots, and the departures of the residuals from lognormal distributions are quantified by visual inspection and statistical tests. For some periods, departure from a lognormal distribution at about 2.5-3 standard deviations can be identified, with the departure suggesting a shortening of the upper tail. For other periods, departure from a lognormal distribution can be identified if the largest one or two residuals are disregarded. At a few spectral periods, the distribution of the upper tail suggests long tails. Statistical tests suggest that, at a few periods, the distribution at the upper tail differs from lognormal distribution at a significance level of 5%. We have also used a statistical procedure to examine the actual and expected numbers of predicted spectral accelerations exceeding a given spectral acceleration. Our results show that, for moderate, large and very large spectral accelerations, the actual number of exceedances is much less than the expected number of exceedances. Our results from the statistical procedure do not put any limits on the upper tail, but suggest that physical constraints may limit the maximum spectral accelerations.

1.0 INTRODUCTION

Due to the limited size of strong-motion data sets, statistical analysis of the distribution of earthquake ground-motion amplitudes has, to date, been unable to provide a clear indication that the distribution has an upper limit. Recently, very large data sets of strong-motion recordings have become available, making statistical analysis more viable (Bommer et al., 2004). The three crustal earthquake data sets analyzed by these authors, using normal probability plots, all show departures from lognormal behaviour at about 2 standard deviations above the median, tending toward shorter upper tails. However, the Japanese K-net data sets that were analyzed contain ground motion values up to 5 standard deviations above the median. We anticipate that these very high values may be due to data errors or to extreme site effects. Strasser and Bommer (2005) also investigate the distribution of the upper tail of the error distribution for K-net and Kik-net data. Their basic procedure is: (1) select a number of records from a single event, (2) derive attenuation models using different functional forms with/without some of the parameters such as site terms, but allowing all the parameters to be derived by regression analyses, and (3) investigate the residuals separately for each earthquake. While their study shows clearly that a good fit to the normal distribution is limited to about 1.5-2.0σ (the standard deviation of the residuals), it is not clear whether the limits they derived can be used for existing attenuation models in a probabilistic seismic study due to the following reasons.

(1) Because they used the dataset from a single event, the variability from one earthquake to another (inter-event variability) cannot be included.

(2) Allowing all parameters, including those associated with attenuation and site effects, to be derived from records of a particular event may reduce the scatter compared with that of existing attenuation models derived from multiple events.

Because both aspects may lead to reductions in residuals and the estimated standard deviation, it is possible that the upper limits of departure from the normal distribution may not be affected. However a systematic investigation to confirm this possibility needs to be carried out. In an attenuation model, magnitude scaling, path and site parameters are usually identical for all events that have the same tectonic category, and this property of attenuation models will lead to a sizeable increase in both residuals and standard deviation compared with those derived using records of each individual earthquake. The effect of the increased residuals on the limits of departure from the normal distribution is not known.

2.0 DATA ANALYSIS

Strasser and Bommer (2005) analysed the intra-event variability of ground-motion amplitudes in sets of K-net and some Kik-net recordings of individual crustal earthquakes in Japan. They noted data quality issues in the strong-motion recordings, but did not attempt to correct them. They used site corrections derived from extrapolation of shallow shear-wave velocity measurements to 20 metre depth, but found them not to have a large impact on their measurements of ground-motion variability. They concluded that the distribution of ground-motion amplitudes overall is consistent with the lognormal distribution within ± 2.5σ level. Departure from the normal distribution occurs at 1.5σ at the upper tail for some of the events they investigated.

The methods used by Zhao et al. (2006a, b) in deriving their ground motion model may provide a more reliable basis for the evaluation of ground-motion variability, because of the approaches taken for strong-motion data processing and the classification of recording sites. In Zhao et al. (2006 a, b), strong-motion recordings from Japanese earthquakes recorded on strong-motion stations of the K-net and Kik-net networks were gathered and processed using a high-pass filter to eliminate the long-period ground motions with frequency less than the corner frequency of the filter determined for each record. Among the total of 4518 Japanese records from 249 earthquakes, 1285 are from crustal events, 1508 are from interface events and 1725 are from slab events.

Figure 1 shows the magnitude and source distance and magnitude and focal depth distribution for earthquakes with focal depths of up to 124 km for the Japanese K-net and Kik-net strong-motion data set selected from the full dataset of Zhao et al. (2006a). In order to eliminate the possible bias introduced by untriggered instruments, data for the modelling by Zhao et al (2006a) were selected from a much larger data set by exclusion of data at distances larger than a specified value for a given magnitude. For subduction slab events, the maximum source distance was set to 300km. Earthquake locations, especially focal depths, determined by JMA were not consistent with those determined by other seismological organizations, and so the relocated ISC locations and depths were used in the Zhao et al (2006a) model. The moment magnitudes from the Harvard catalogue were used unless moment magnitude from a special study was available.

The residuals used are computed from the Zhao et al. (2006a) models, in which the estimated standard deviation was assumed independent of magnitude. For subduction and slab events, these standard deviations are much lower than those of the widely used subduction zone model of Youngs et al. (1997), especially for periods longer than 0.2 seconds. This is an important feature of the Zhao et al. (2006a) model, because in probabilistic seismic hazard analysis, the variability of ground motion about the median value is often just as important as the median value itself.

Since many of the K-net stations have shear-wave velocity measurements that extend to depths of only 10 to 20 metres, Zhao et al. (2006b) devised an alternative method for categorising their site conditions, based on response spectral ratios of horizontal to vertical ground motions. They used H/V ratios for records from K-net sites having adequate shear-wave velocity measurements to establish a site classification index using the mean spectral ratios over a wide range of spectral period, to assign sites to the long-established Japanese classes (Molas and Yamazaki 1995) that correlate approximately with the US NEHRP classes as indicated in Table 1. Using the index, they were able to classify both K-net stations with soil layers thicker than 20m and other strong-motion stations in Japan. The peak period of the H/V spectral ratio was also used to identify soft soil sites.

In addition to the crustal earthquake category analysed by Strasser and Bommer (2005), our analysis includes subduction interface earthquakes and intra-slab earthquakes, which extend to larger magnitudes and have much larger numbers of recordings than the crustal earthquakes. Our analysis also looks at the full variability in the ground shaking, both the intra-event variability and the inter-event variability.

Out of concerns for data quality and the ownership of some strong-motion records, we used only a subset of the full dataset of Zhao et al (2006a). The sub-dataset includes only those records from K-net and Kik-net and consists of 3575 records of the 4518 used for PGA analysis in the complete dataset. We used the standard deviation calculated from the total residuals of the sub-set data to normalize the data used in the present study to have a zero mean and a standard deviation of 1.0. Note that the total standard deviation derived from the sub-set data are all considerably larger than those reported by Zhao et al (2006a) and this is presumably a result of the data selection. The value for each data point of the normalized residuals is referred to as the computed score (the location of the data in terms of standard deviation) and the data are arranged in an ascending order. The theoretical distribution is calculated in the following manner. The cumulative probability for a data set is computed from

$$\alpha_1 = 1 - 0.5^{1/n} \qquad \alpha_i = \frac{i - 0.3175}{n + 0.365} \qquad \alpha_n = 0.5^{1/n} \tag{1a,b,c}$$

where n is the total number of data and i varies from 2 to n-1. The theoretical score of a data set is computed by $\gamma = \Psi^{-1}(\alpha_i, 0, 1)$ - the inversion of the cumulative normal probability function with a zero mean and a standard deviation of 1.0 (see http://www.itl.nist.gov /div898/handbook/eda/section3/normprpl.htm). The computed score and the theoretical score are then plotted together in a probability plot. If the data falls on the straight diagonal line, the data distribution is close to the theoretical normal distribution, and the residuals can be well approximated by the normal distribution. Any deviation from the straight line suggests a departure from the normal distribution. The use of a probability plot is an equivalent non-parametric test.

The probability P_m that, for n trials, each with a probability of success p, we obtain m successful trials is computed by

$$P_m = \frac{n!}{(n-m)!\,m!} p^m (1-p)^{n-m} \tag{2}$$

where $p=1-\Psi(\gamma, 0, 1)$ is the probability of success of a single trial being at or beyond a given theoretical score γ. The total probability of having m or less successful trials can be estimated by

$$P_r = \sum_{i=1}^{m} P_i \tag{3}$$

In the present study, we use Equations (2) and (3) to estimate the probability of having m or fewer data over a given score γ.

The median smallest and median largest theoretical scores are defined by $\gamma_S=\Psi^{-1}(\alpha_1, 0, 1)$ and $\gamma_L=\Psi^{-1}(\alpha_n, 0, 1)$, respectively. Note that there is an equal probability of 0.5 for the largest of n values falling above or below γ_L if the residuals have a normal distribution.

3.0 RESULTS

Our basic approach is to calculate the total residuals (logarithm of observed spectral accelerations minus that of the model prediction) of the recorded data from the ground motion model of Zhao et al. (2006a) using the site classifications developed by Zhao et al. (2006b).

Table 2 shows the statistics of the data set. The total number of data for periods up to 0.7s is 3575 and decreases to 2318 at 5.0s period because the usable maximum period for many records is less than 5.0s period. The standard deviation of the total residuals varies between 0.81 and 0.94 on the natural logarithm scale. Note that the standard deviation is computed from the data used in the present study (only K-net and Kik-net data) and differs from those reported by Zhao et al (2006a). The largest maximum normalized residual (residuals divided by standard deviation) is just over 4.0, significantly larger than the median largest theoretical scores. The maximum scores larger than the median largest theoretical scores are in bold in Table 2 and they are also presented in Figure 2. Note that data at only 4 spectral periods out of 21 exceed the median largest theoretical values, while the expected number of exceedances is 10 out of 21 spectral periods, if the residuals are normally distributed. The small number of actual exceedances suggests that total residuals may not have a normal distribution at the upper tail for all spectral periods, with a possible shortening upper tail. The number of data with scores beyond a given value (between 2.5 and 3.75) is also presented in Table 2, and for 6 periods there is one point over 3.5 times the standard deviation while 10 or 11 exceedances are expected if the data is normally distributed.

We assign ranks for the 10 largest residuals for each period in the upper tail with the largest residual having rank 10 and the second largest having rank 9 etc. We examine the data distribution with respect to events and recording sites, to seek indications of the relative importance of site effects and earthquake source effects. For example, if a particular site has a large number of records in the top few ranks, site effect may be the main cause. If a particular earthquake generates a significant number of data in the top few ranks, the variability from one earthquake to another may have a relatively large effect. Table 3 presents site names, earthquake identification number and the number of periods and number of records in rank 10. All multiple periods in rank 10 are from the same record and they tend to be among the adjacent spectral periods. This tendency decreases with decreasing ranks. The total number of periods is 21 for the Zhao et al 2006a model. Event 208 has 5 periods from 2 records and 2 sites, and event 246 also has 5 periods from 2 records and 2 sites. The total number of periods for each site and event and the data ratio (the number of periods/105 in percentage) in ranks 6-10 are presented in Table 4 for all events and for those sites that have 3 or more periods. The divisor 105 corresponds to product of 5 ranks with 21 periods in each rank. About 2/3 of the data in ranks 6-10 are from 4 events while none of the sites has more than 10% of the periods. These results suggest that variability from one earthquake to another may contribute more than the site effect variability. It is important to examine the distribution of total residuals.

Figure 3 shows the frequency of the residuals for PGA, 0.4s and 1.0s periods. The left panel suggests that the data can be approximated very well by a normal distribution, especially for the descending branch of the density distribution. The right panel shows the distribution at the upper tail. It is quite difficult to judge the goodness of the fit between the theoretical density distribution and the data from the graphs alone.

Figure 4 shows the probability plots for PGA and the other spectral periods. In these figures, a lognormal probability distribution is indicated by a straight diagonal line. The change of the slope of the data points for theoretical scores between 2.5 and 4 above the median indicates departure from the normal distribution. The two red crosses indicate the median smallest and largest theoretical scores. At the upper tail, there is a probability of 0.5 to have a score falling above or below the median largest score $y_{L,}$ but the values are exceeded only 4 out of 21 spectral periods.

Figure 4a shows that the normal distribution fits the data very well within about ±2.5 standard deviation. Beyond ±2.5 standard deviation, the data appears to deviate from the normal distribution for 0.05s and 0.1s periods, suggesting a shortening upper tail, consistent with the idea that physical bounds do indeed limit the upper tail of the distribution. One data point appears outside of the theoretical limits at 0.15s, 0.25s, and 0.4s (also see Figure 2). However, apart from these records at rank 10, the data generally suggest shortening tails (with the largest few data points being below the straight line). For PGA, the data at the upper tail appears to depart from normal distribution at about 2.5 standard deviations but the two data of highest rank fall back to the normal distribution. The normal distribution fits the data for 0.2s and 0.3s spectral periods quite well at the upper tail without obvious departure.

Figure 4b shows similar mixed results. At spectral periods of 0.6s, 0.7s, 0.8s, departure from the normal distribution occurs beyond about 2.5 – 3.0 standard deviations and the distribution suggests a shortening tail. Figure 4b also suggests long tails (with the largest a few data points being above the straight line) for 0.5s and 1.5s period while the normal distribution fits the upper tail distribution quite well at the other periods. At 0.9, 1.0 and 1.25s spectral periods, a lognormal distribution fits the upper tail very well. For periods up to 1.25s in Figure 4a and 4b, the distribution suggests a shortening tail at the lower tail end.

Figure 4c shows that, at the upper tail, departure from the normal distribution can be identified for 3.0s 4.0s and 5.0s periods while it is difficult to clearly identify any departure from the normal distribution at the upper tail at 2.0s period from the probability plot alone. However, at periods between 2.0s and 4.0s, the probability plots (Figure 4c) suggest a long tail at the lower tail end.

At PGA, 0.15s, 0.2s, 0.25s, 0.3s, 0.4s, 0.5s, 0.9s, 1.0s, 1.25s, 1.5s and 2.0s periods (12 of 21 periods), there are either data that lie outside the median largest theoretical score (4 periods) or data with the largest score close to the diagonal line for the normal distribution.

In addition, departure from the normal distribution at or beyond 2.5 standard deviations can be visually identified in the probability plots for 8 spectral periods, 0.05s, 0.1s, 0.6s, 0.7s, 0.8s, 3.0s 4.0s and 5.0s. Most probability plots for PGA reported by Strasser and Bommer (2005) suggest departure at about 1.5-2 standard deviation. The larger value in the present study is likely a result of using total residuals while only intra-event residuals were used in their study. Another source of the difference is likely to be in the modelling of geometric and anelastic attenuation rates between the present study and the Strasser and Bommer (2005) study. The geometric and anelastic attenuation rates are identical for all events in the same tectonic category of earthquakes in the Zhao et al (2006a) model and but were derived separately for each of the earthquakes in the Strasser and Bommer (2005) study.

Table 5 presents the probability of having n_{exc} (the actual number of records exceeding a given score) or fewer records over a given score. At PGA, 0.05s, 0.1s, 0.15s, 0.7s, 0.8s and 2.5s spectral period, the results suggest the lognormal distribution does not fit the data above 2.75 standard deviations at the upper tail at 5% significance level, but these spectral periods do not all correspond to the periods at which the probability plots suggest a departure from the normal distribution.

The overall results are mixed and it is not possible to identify the upper limits of the data distribution for all periods. A possible reason for the mixed results is the "small" number of data, e.g., not large enough to identify the limits beyond which the normal distribution does not fit and the residuals have a shortening tail. We resort to an alternative statistical analysis suggested by Dr. David Rhoades (GNS Science). The results are presented in Figure 5 and the theoretical description of the method is given in the Appendix. The method is to examine (1) $N(z)$ - the expected number of predicted spectral accelerations (by the attenuation model) that exceed a given acceleration z, and (2) $k(z)$ - the actual number of records that have accelerations larger than z. For a given period, if $k(z)$ is much smaller than $N(z)$, there is probably a physical constraint that limits spectral acceleration. Figure 5 shows the variation of $N(z)$ and $k(z)$ with spectral acceleration z (the horizontal axis of the plots), together with mean $\pm 2\sigma(z)$ of the expected number of exceedances ($\sigma(z)=\sqrt{N(z)}$). At the lower spectral accelerations, the actual number of exceedances $k(z)$ is close to the expected number of exceedances. At moderately strong level of spectral accelerations for all periods, the actual number of exceedances is much smaller than the expected value. The differences between $N(z)$ and $k(z)$ for most spectral periods monotonically increase with increasing spectral accelerations of exceedance. For spectral periods over 0.4s, the actual number of exceedances is considerably less than $N(z)-2\sigma(z)$ at moderately strong and strong spectral accelerations.

Figure 6 shows the ratio between the actual and the expected number of exceedances at different level of spectral accelerations for 6 spectral periods. The actual numbers of exceedances are generally less than 20% of the expected numbers of exceedances at moderately large spectral accelerations and 10% at large and very large spectral accelerations.

There are some other factors that may contribute to the results presented in Figure 5. It is possible that, when the residuals decrease with increasing magnitude in the attenuation model while a magnitude-independent standard deviation is used, the actual number of exceedances may appear to be less than the expected number of exceedance because of this factor alone. In the Zhao et al (2006a) model, both inter- and intra-event residuals were found not to be magnitude dependent. The other factor is the use of a sub-dataset. The data excluded mainly come from a number of organizations that use analogue and the early versions of digital instruments (pre 1990). It is not clear if the use of standard deviation of the sub-dataset in the computation of expected number of exceedance can completely offset the possible effect due to the change of data numbers and data magnitude-distance distributions.

Although formal statistical tests were not performed, it is very unlikely that, by chance, the actual numbers of exceedances at strong ground shaking are smaller than the median-2σ of the expected numbers of exceedances. Though, in the present study, we are not able to quantify an upper limit, the results presented in Figure 5 strongly suggest that there are physical constraints that limit the response spectral accelerations in the sub-dataset used in the present study.

4.0 CONCLUSIONS

Current ground motion prediction models assume an unbounded lognormal distribution of random variability in ground motion level. In reality, there probably exist physical conditions that limit the ground motion distribution. Use of unbounded models in probabilistic seismic hazard analysis leads to ground motion estimates that may be unrealistically large, especially at low annual probabilities.

Using probability plots, significant departure from the normal distribution at the upper tail can be identified for 8 spectral periods (out of 21 in total) and the departure usually starts at 2.5-3 standard deviations and the tail distribution suggests shortening tails. At some other spectral periods, departure from the normal distribution can also be identified and a shortening tail is suggested if the largest residual is excluded. For a few spectral periods, the probability plots suggest a departure from normal distribution but a long tail. Formal statistical tests showed that at 7 spectral periods- PGA, 0.05s, 0.1s, 0.15s, 0.7s, 0.8s and 2.5s, the residuals over 2.75 standard deviations do not fit the lognormal distribution at a significance level of 5%. The periods identified by the statistical tests do not all correspond to the periods identified from the probability plots.

We examined the characteristics of the upper tails of the total residuals (intra-event and inter-event). We found that the departure from the normal distribution tends to occur at a considerably larger value of total residuals (2.5-3 standard deviation) than that reported by Strasser and Bommer (2005) (1.5-2.0 standard deviation). The lower values from Strasser and Bommer (2005) are likely the result of their use of intra-event residuals derived from a data set generated by a single event. We expect that the results from Strasser and Bommer (2005) may not be directly applicable without modification to the intra-event residuals from an attenuation model, because the intra-event residuals derived from single events do not necessarily have similar distributions at the upper tail to those of attenuation models.

We have also taken an alternative approach to investigate the possible upper limits for the predicted spectral acceleration by the Zhao et al (2006b) model. The results show that, for a moderately strong and strong spectral acceleration at a particular spectral period, the actual numbers of records that have spectral accelerations exceeding the specified value are much lower than the expected numbers of exceedances for many spectral periods, and are even lower than the expected numbers of exceedances minus two standard deviations at spectral periods beyond 1.0s. The actual number of exceedances is typically smaller than 20% of the expected number of exceedances at moderate/large spectral accelerations for all spectral periods and is less than 10% of the expected number of exceedances at very large spectral accelerations. These results strongly suggest that there are physical constraints that limit the response spectral accelerations in the sub-dataset, selected from that in the attenuation model (Zhao 2006a).

5.0 ACKNOWLEDGEMENTS

We acknowledge the research grant from the Earthquake Commission of New Zealand. We also wish to thank Dr. David Rhoades for allowing us to use his method. We wish to thank Dr. Graeme McVerry for his invaluable comments, suggestions, interpretation of parameters and the review of this report.

6.0 REFERENCES

Bommer, J.J., Abrahamson, N.A., Strasser, F.O., Pecker, A., Bard, P.Y., Bungun, H., Cotton, F., Fäh, D., Sabetta, F., Scherbaum, F. and Studer, J. (2004). The challenge of determining upper limits on earthquake ground motions *Seismological Research Letters*, 75: 82-95.

Molas, G.L. and Yamazaki, F. (1995), Attenuation of earthquake ground motion in Japan including deep focus events, *Bulletin of the Seismological Society of America*, Vol. 85, No. 5, pp. 1343-1358

Strasser, F.O., and J.J. Bommer (2005), Analysis of intra-event ground-motion residuals from K-NET and KiK-NET data, *Research Report No. 05-003-SM*, Imperial College, London, U.K.

Youngs, R.R., Chiou, S.-J., Silva, W.J. and Humphrey, J.R. (1997), Strong ground motion attenuation relationships for subduction zone earthquakes, *Seismological Research Letters*, Vol. 68, pp. 94-127

Zhao, J.X., J. Zhang, A. Asano, Y. Ohno, T. Oouchi, T. Takahashi, H. Ogawa, K. Irikura, H.K. Thio, P.G. Somerville, Yasuhiro Fukushima, and Yoshimitsu Fukushima (2006a), Attenuation relations of strong ground motion in Japan using site classification based on predominant period. *Bulletin of the Seismological Society of America*, 96, 898-913.

Zhao, J.X., Irikura, K., Zhang, J., Fukushima, Y., Somerville, P.G., Asano, A., Ohno, Y., Oouchi, T., Takahashi, T. and Ogawa, H. (2006b), An empirical site classification method for strong motion stations in Japan using H/V response spectrum ratio. *Bulletin of the Seismological Society of America*, 96, 914-925.

PHYSICAL CONSTRAINT ON HIGH SPECTRAL ACCELERATIONS USING AN ATTENUATION MODEL

By David Rhoades, GNS Science

For each strong motion record, we have an observed value y_i, and a value $\hat{y}_i$, which is the strong motion predicted by the attenuation model.

$$\hat{y}_i = f(x_i, \theta)$$

where f is the attenuation model, x_i represents the relevant input data for the model corresponding to the conditions under which the record y_i was obtained, and θ represents the parameters of the model.

For a given high value of strong motion, z, we wish to evaluate whether there is a physical constraint, imposed by the nature of the earthquake source, wave propagation, or site effects on motions exceeding z. Therefore, for each strong motion record and with z fixed, we compute the probability

$$P(Y_i > z \mid x_i, \theta, f) \tag{A1}$$

The sum (over i) of all such probabilities is the expected number of exceedances of the strong-motion level z in the whole data set, given the attenuation model and the conditions under which the strong motion records ($y_i, i = 1,...,n$) were obtained. That is

$$N(z) = \sum_{i=1}^{n} P(Y_i > z \mid x_i, \theta, f) \tag{A2}$$

Let us denote the actual number of exceedances by k(z), i.e.

$$k(z) = \sum_{i=1}^{n} I(y_i > z) \tag{A3}$$

where $I(e) = 1$ if e is true, and 0 otherwise.

There is evidence of some physical constraint on strong motion at level z if $k(z)$ is significantly less than $N(z)$. We could use the Poisson distribution to evaluate the probability that the number of exceedances of z would exceed $k(z)$, given the model.

Table 1 Site class definitions used by Zhao et al. (2004; 2005) and the approximately corresponding NEHRP site classes (BSSC 2000)

Site class	Description	Natural period	V_{30} calculated from site period	NEHRP site classes
SC I	Rock	$T < 0.2s$	$V_{30} > 600$	A+B
SC II	Hard soil	$0.2 \leq T < 0.4s$	$300 < V_{30} \leq 600$	C
SC III	Medium soil	$0.4 \leq T < 0.6s$	$200 < V_{30} \leq 300$	D
SC IV	Soft soil	$T \geq 0.6s$	$V_{30} \leq 200$	E+F

Table 2 Statistics of the dataset

Spectral period	Total number of records	Standard deviation	Max. score	γ_L	Number of records with scores ≥					
					2.5	2.75	3	3.25	3.5	3.75
PGA	3575	0.8139	3.423	3.548	12	3	2	1	0	0
0.05s	3575	0.8749	3.022	3.548	10	4	1	0	0	0
0.1s	3575	0.9379	2.898	3.548	11	5	0	0	0	0
0.15s	3575	0.9289	**3.632**	3.548	14	5	3	1	1	0
0.2s	3575	0.8925	3.454	3.548	25	11	5	2	0	0
0.25s	3575	0.8713	**3.695**	3.548	25	14	7	1	1	0
0.3s	3575	0.8530	3.467	3.548	23	10	4	2	0	0
0.4s	3575	0.8261	**4.019**	3.548	22	9	2	1	1	1
0.5s	3575	0.8139	3.422	3.548	16	8	8	4	0	0
0.6s	3575	0.8093	3.115	3.548	18	7	2	0	0	0
0.7s	3575	0.8083	3.024	3.548	18	4	1	0	0	0
0.8s	3574	0.8106	3.133	3.548	14	5	2	0	0	0
0.9s	3573	0.8150	3.396	3.548	15	8	3	2	0	0
1.0s	3569	0.8193	3.521	3.548	20	7	5	2	1	0
1.25s	3566	0.8340	**3.586**	3.548	18	9	5	2	1	0
1.5s	3564	0.8413	3.516	3.548	15	9	5	3	1	0
2.0s	3500	0.8437	3.473	3.543	19	8	3	2	0	0
2.5s	3379	0.8440	3.247	3.533	14	4	2	0	0	0
3.0s	3314	0.8535	3.023	3.528	16	8	1	0	0	0
4.0s	2920	0.8420	3.191	3.495	18	8	4	0	0	0
5.0s	2318	0.8132	3.121	3.433	22	8	2	0	0	0

Table 3 Number of periods, records, sites and earthquakes in rank 10

No of data for rank 10		Earthquake identification number							Total no. of periods / event	Total no. of records / event
		208	246	217	228	206	237	193		
Site name	bIBUH03		3						3	1
	kISK006	3							3	1
	bIWTH01						2		2	1
	kHKD067					2			2	1
	kHKD098		2						2	1
	kIBR005			2					2	1
	kISK002	2							2	1
	kOSK003				2				2	1
	kIWT011							1	1	1
	kKOC003				1				1	1
	kTCG014			1					1	1
Total no. of periods/event		5	5	3	3	2	2	1	No. of periods =21	
Total no. of records/event		2	2	2	2	1	1	1		No. of records =11

Table 4 The numbers of periods among ranks 6-10

Earthquake identification number	Number of periods	Data ratio (%)		Site name	Number of periods	Data ratio (%)
228	21	20.0		bIBUH03	10	9.5
237	18	17.1		kHKD067	8	7.6
246	16	15.2		kHKD098	7	6.7
208	15	14.3		kISK006	5	4.8
217	5	4.8		kKOC003	5	4.8
230	4	3.8		kAOM007	4	3.8
240	3	2.9		kIBR004	4	3.8
236	2	1.9		kIBR005	4	3.8
241	1	1.0		kISK002	4	3.8
243	1	1.0		bIWTH01	3	2.9
				kHKD091	3	2.9
				kISK011	3	2.9
				kOSK003	3	2.9

Table 5 Probability for having the number of data equal to or less than a given value

Spectral period	n-scores											
	2.5		2.75		3		3.25		3.5		4	
	n_{exc}	P_r	n_{exc}	P_r	n_{exc}	P_r	n_{exc}	P_r	n_{exc}	P_r	n_{exc}	P_r
PGA	12	**0.013**	3	**0.006**	2	0.140	1	0.389	0	0.435	0	0.893
0.05s	10	**0.003**	4	**0.019**	1	**0.047**	0	0.127	0	0.435	0	0.893
0.1s	11	**0.007**	5	**0.046**	0	**0.008**	0	0.127	0	0.435	0	0.893
0.15s	14	**0.043**	5	**0.046**	3	0.290	1	0.389	1	0.797	0	0.893
0.2s	25	0.764	11	0.621	5	0.646	2	0.660	0	0.435	0	0.893
0.25s	25	0.764	14	0.781	7	0.884	1	0.389	1	0.797	0	0.893
0.3s	23	0.621	10	0.405	4	0.471	2	0.660	0	0.435	0	0.893
0.4s	22	0.539	9	0.282	2	0.140	1	0.389	1	0.797	1	0.994
0.5s	16	0.109	8	0.167	8	0.943	4	0.942	0	0.435	0	0.893
0.6s	18	0.219	7	0.167	2	0.140	0	0.127	0	0.435	0	0.893
0.7s	18	0.219	4	**0.019**	1	**0.047**	0	0.127	0	0.435	0	0.893
0.8s	14	**0.044**	5	**0.046**	2	0.140	0	0.127	0	0.435	0	0.893
0.9s	15	0.071	8	0.167	3	0.290	2	0.660	0	0.435	0	0.893
1.0s	20	0.373	7	0.168	5	0.648	2	0.661	1	0.798	0	0.893
1.25s	18	0.223	9	0.285	5	0.649	2	0.576	1	0.798	0	0.893
1.5s	15	0.073	9	0.289	5	0.649	3	0.847	1	0.798	0	0.893
2.0s	19	0.325	8	0.184	3	0.306	2	0.671	0	0.443	0	0.895
2.5s	14	0.071	4	**0.028**	2	0.167	0	0.420	0	0.456	0	0.898
3.0s	16	0.163	8	0.235	1	0.062	0	0.148	0	0.462	0	0.900
4.0s	18	0.550	8	0.385	4	0.640	0	0.185	0	0.507	0	0.912
5.0s	22	0.978	8	0.613	2	0.395	0	0.262	0	0.583	0	0.929

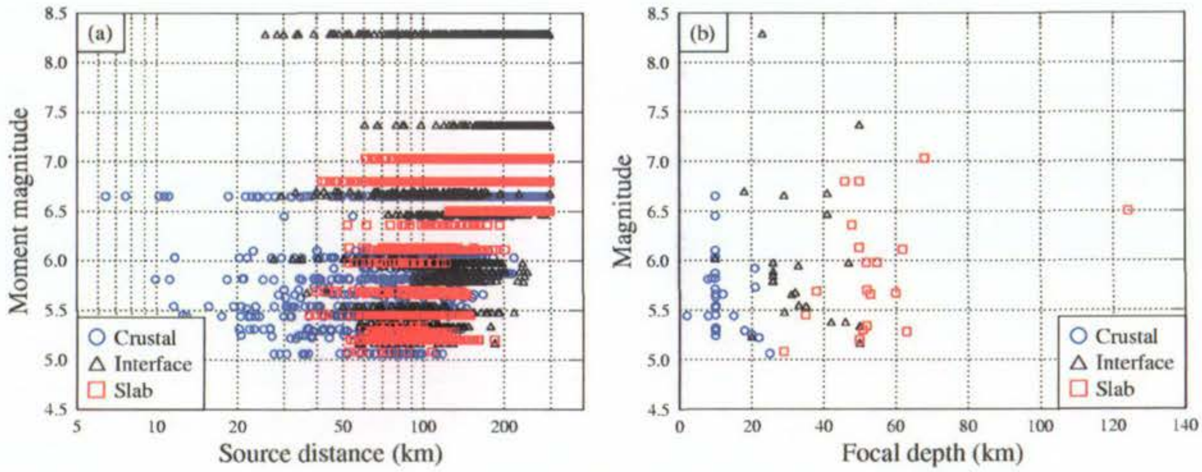

Figure 1 Data distribution with respect to magnitude, source distance and focal depth

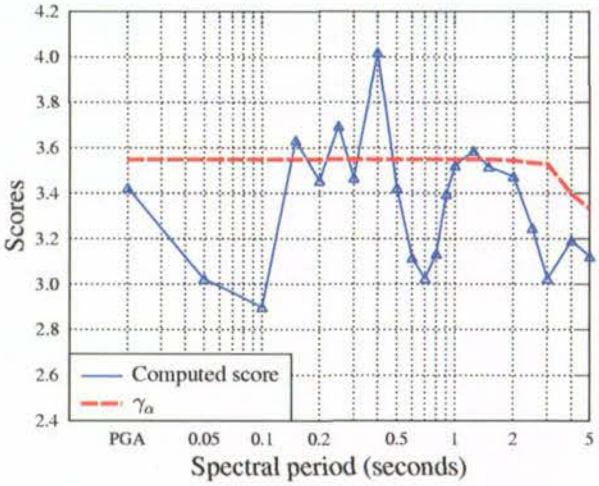

Figure 2 The computed maximum scores of the data set and the median largest theoretical scores.

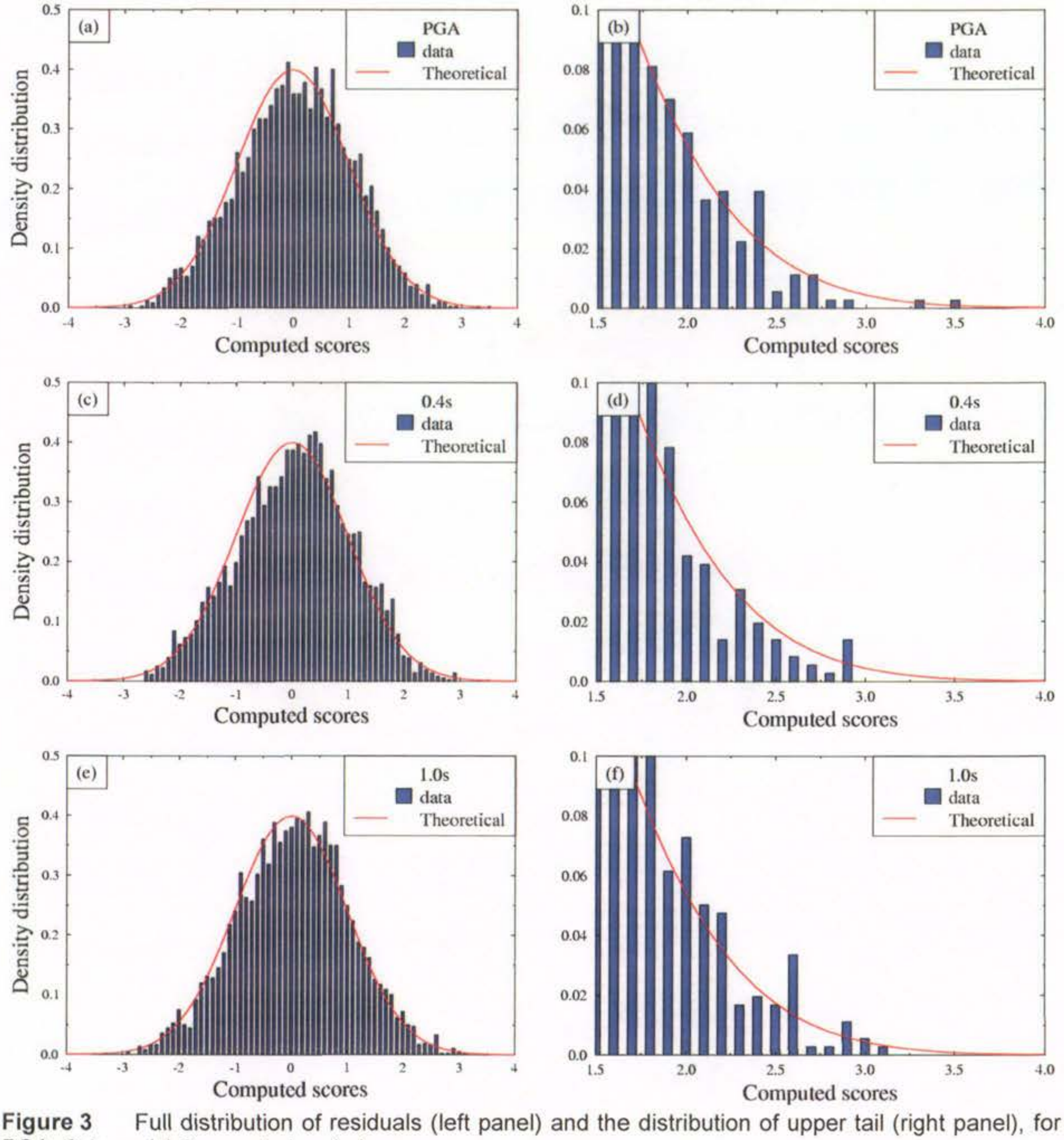

Figure 3 Full distribution of residuals (left panel) and the distribution of upper tail (right panel), for PGA, 0.4s and 1.0s spectral periods

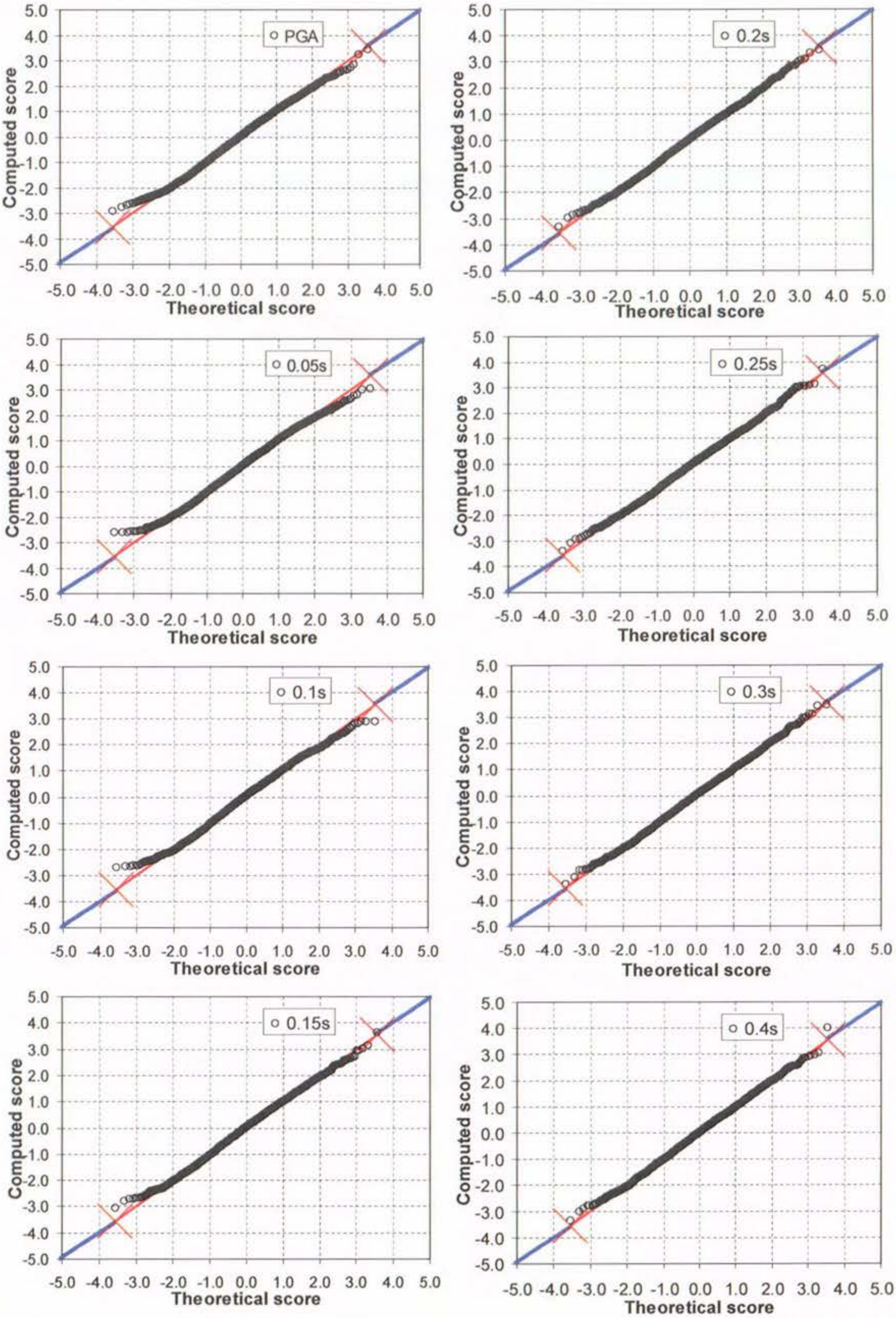

Figure 4a Probability plots for PGA and 0.05-0.4 s period

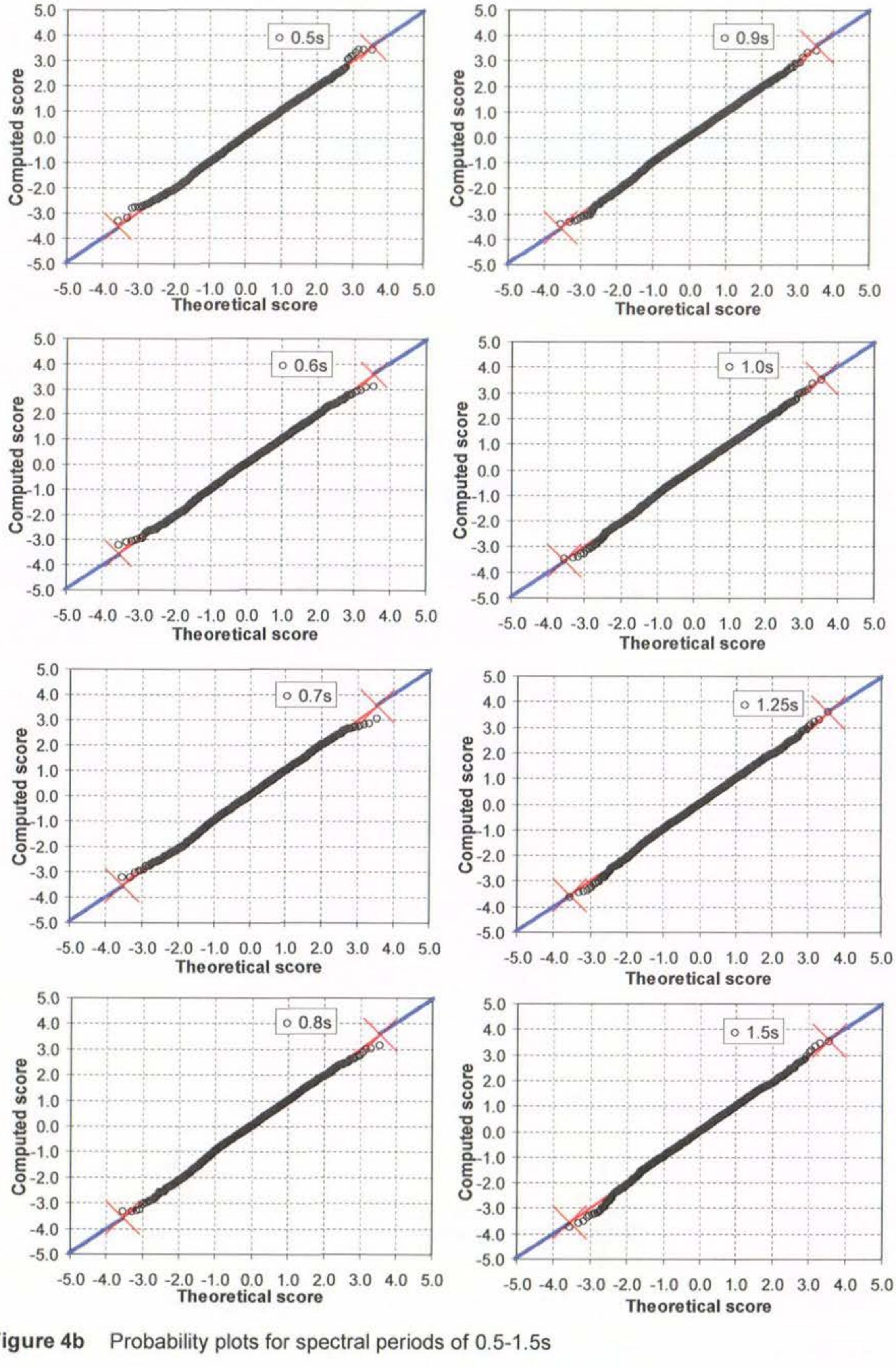

Figure 4b Probability plots for spectral periods of 0.5-1.5s

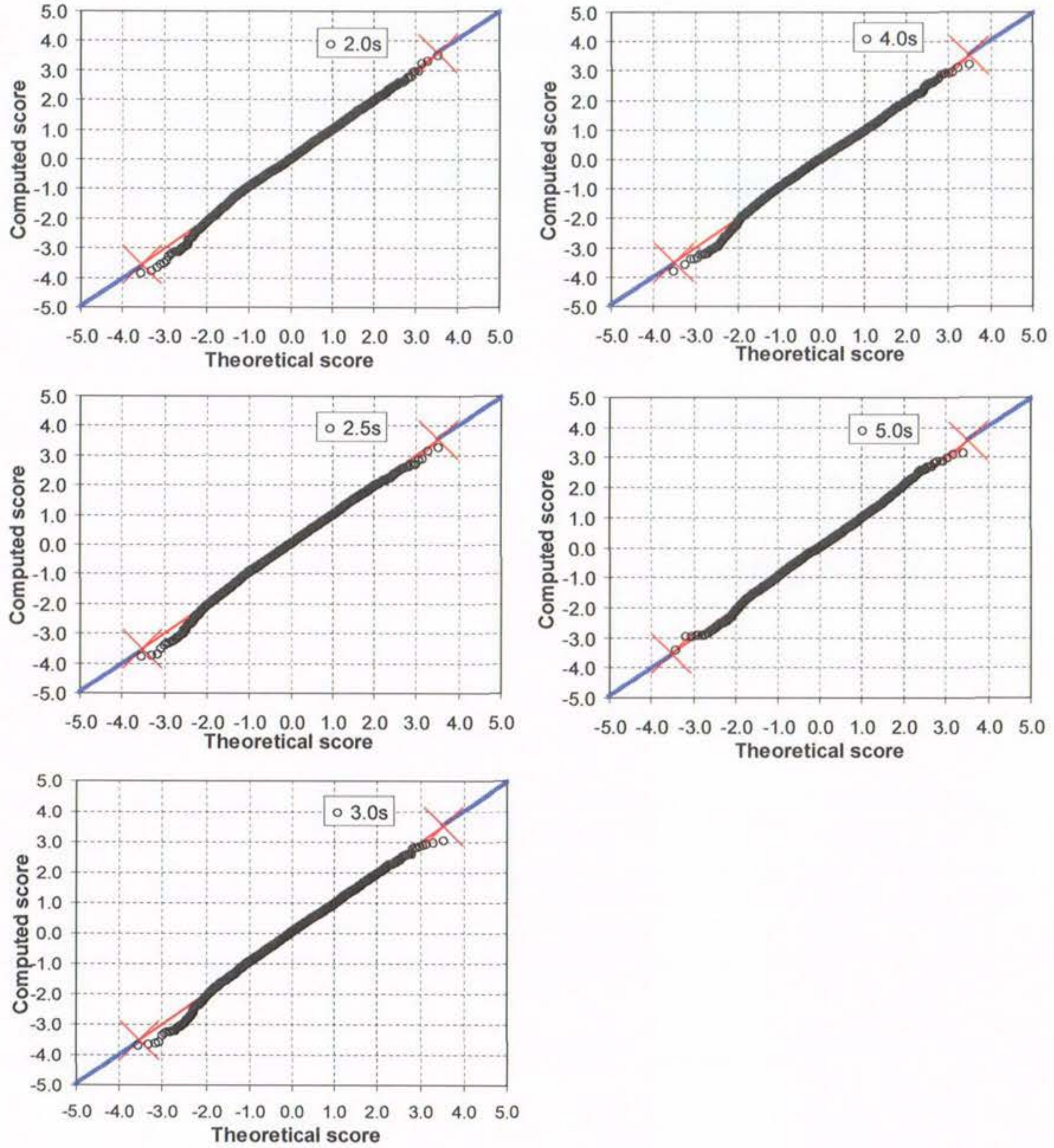

Figure 4c Probability plots for spectral periods of 2.0-5.0s

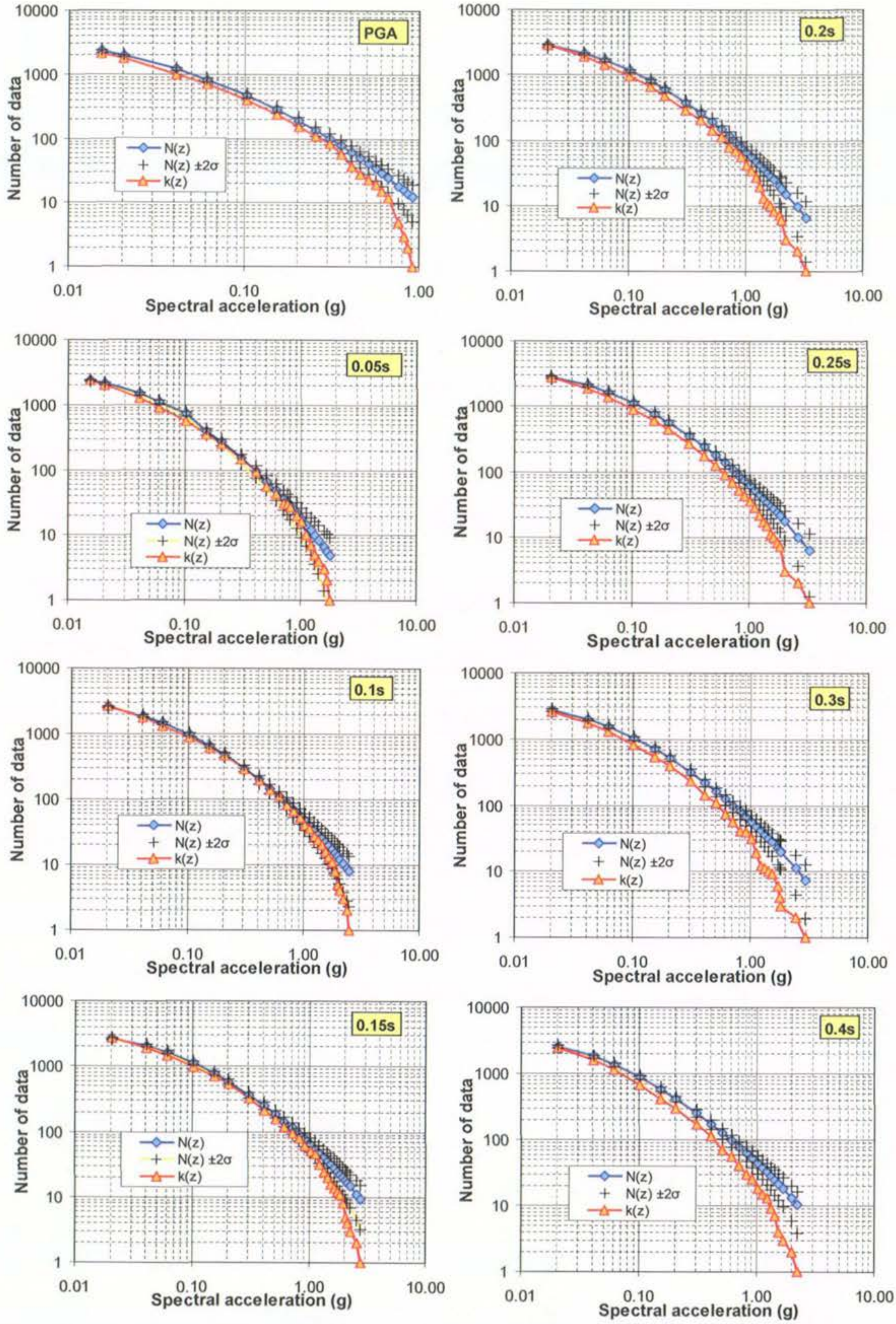

Figure 5a The expected and the actual numbers of records exceeding a given spectral acceleration for PGA, 0.05s, 0.1s, 0.15s, 0.2s, 0.25s, 0.3s and 0.4s spectral periods

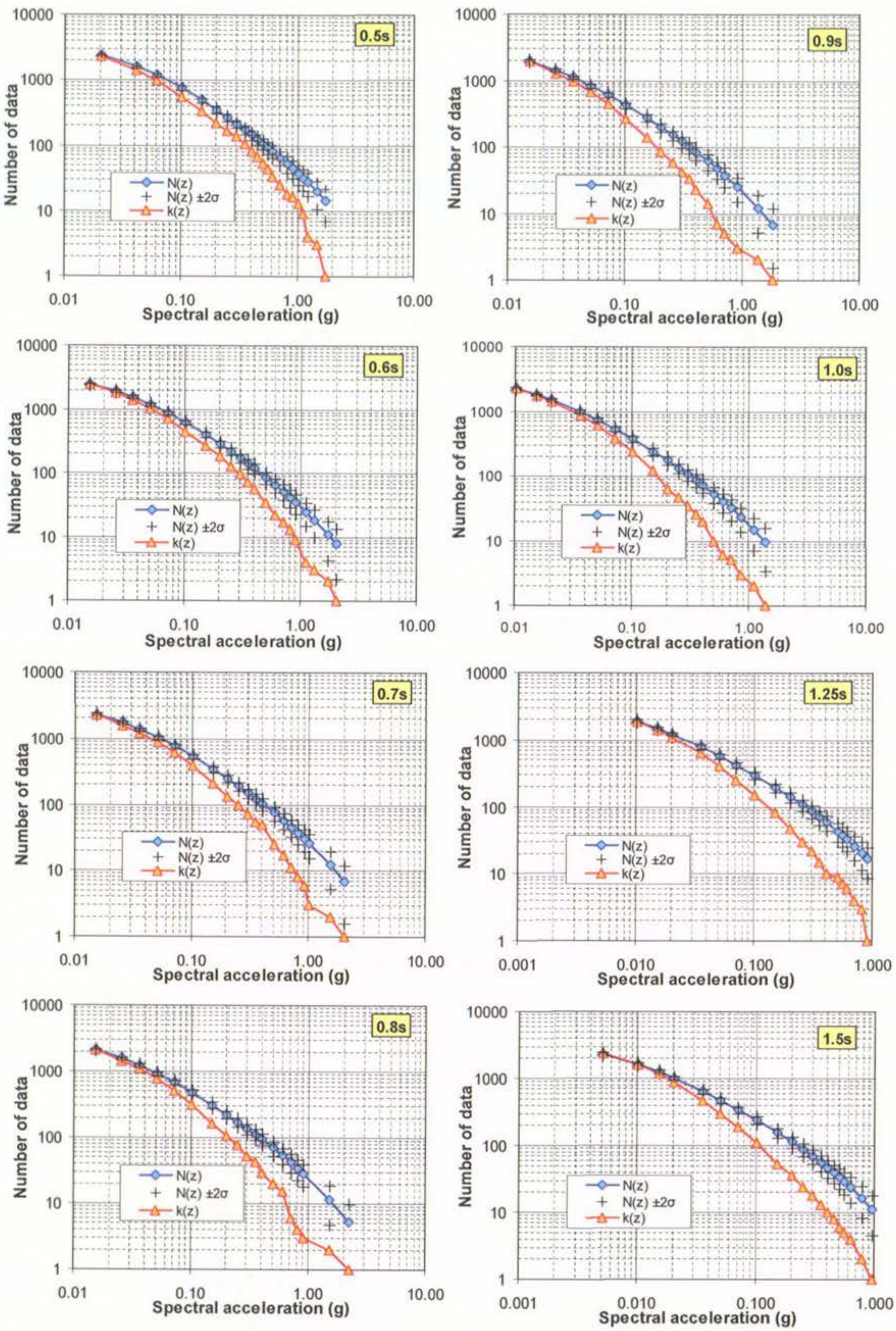

Figure 5b The expected and the actual numbers of records exceeding a given spectral acceleration for 0.5s, 0.6s, 0.7s, 0.8s, 0.9s, 1.0s, 1.25 and 1.5s spectral periods

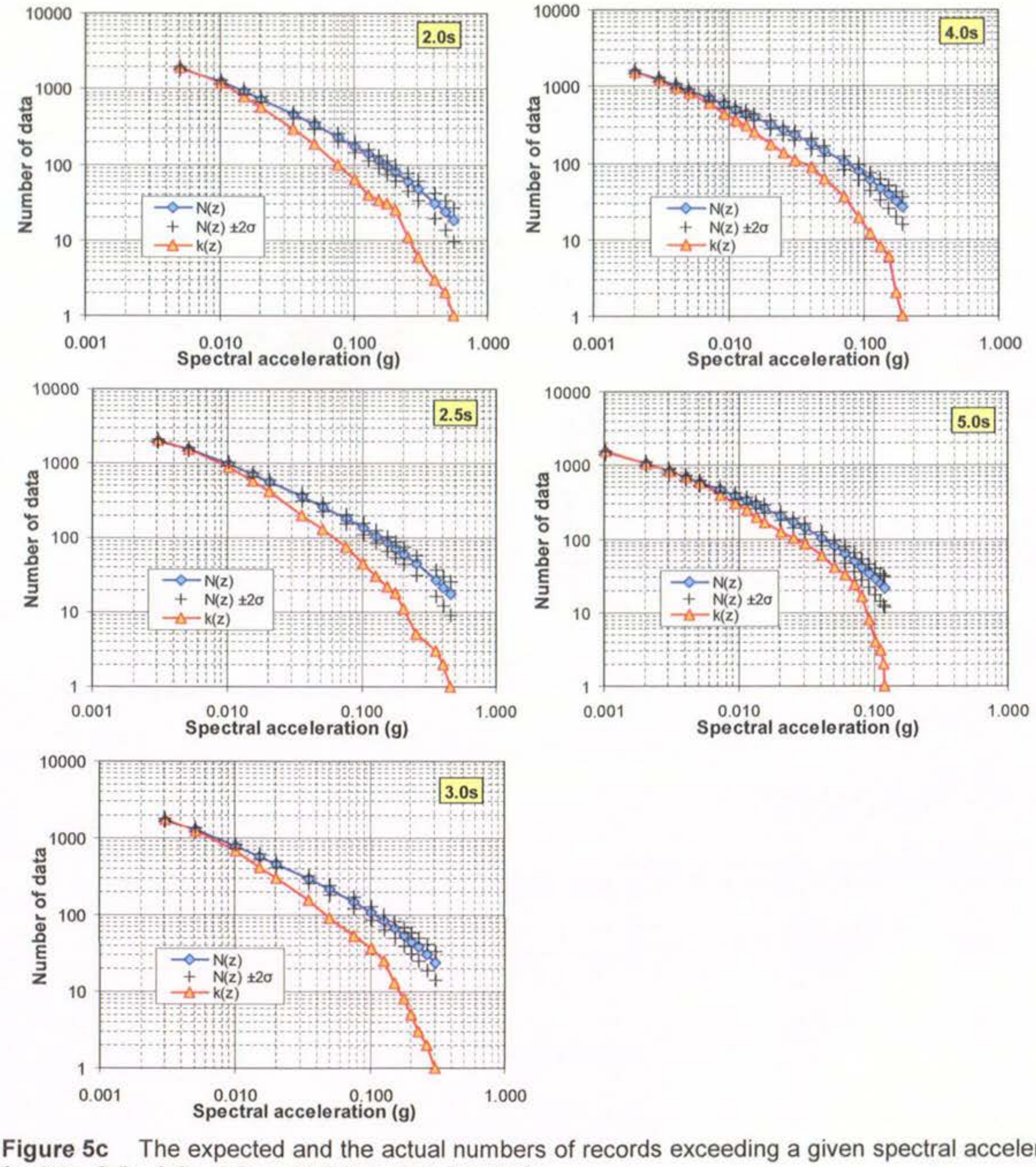

Figure 5c The expected and the actual numbers of records exceeding a given spectral acceleration for 2.0s, 2.5s, 3.0s, 4.0s, and 5.0s spectral periods

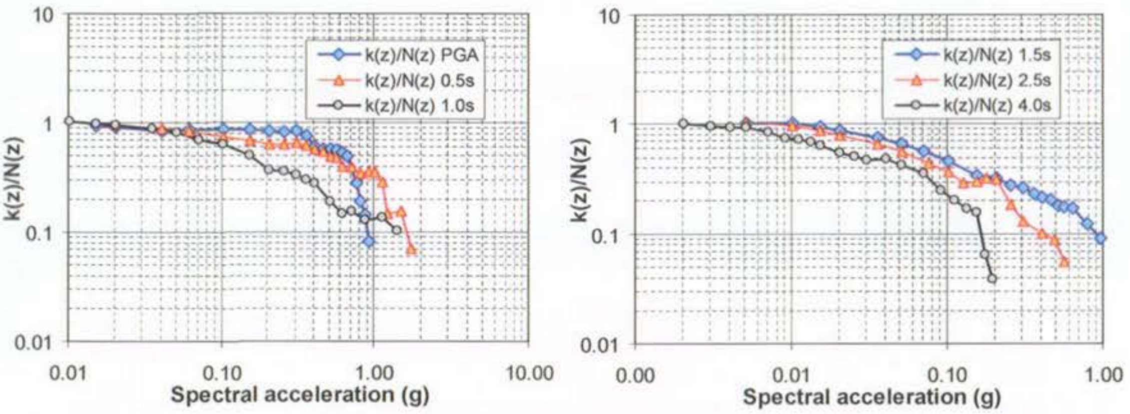

Figure 6 The ratio of the actual number and the expected number of exceedances